Aircraft Trajectory Optimization for European Flights

Assessment of the trajectory variability considering a trade-off between operating costs and climate impact

M. Blom

Delft University of Technology

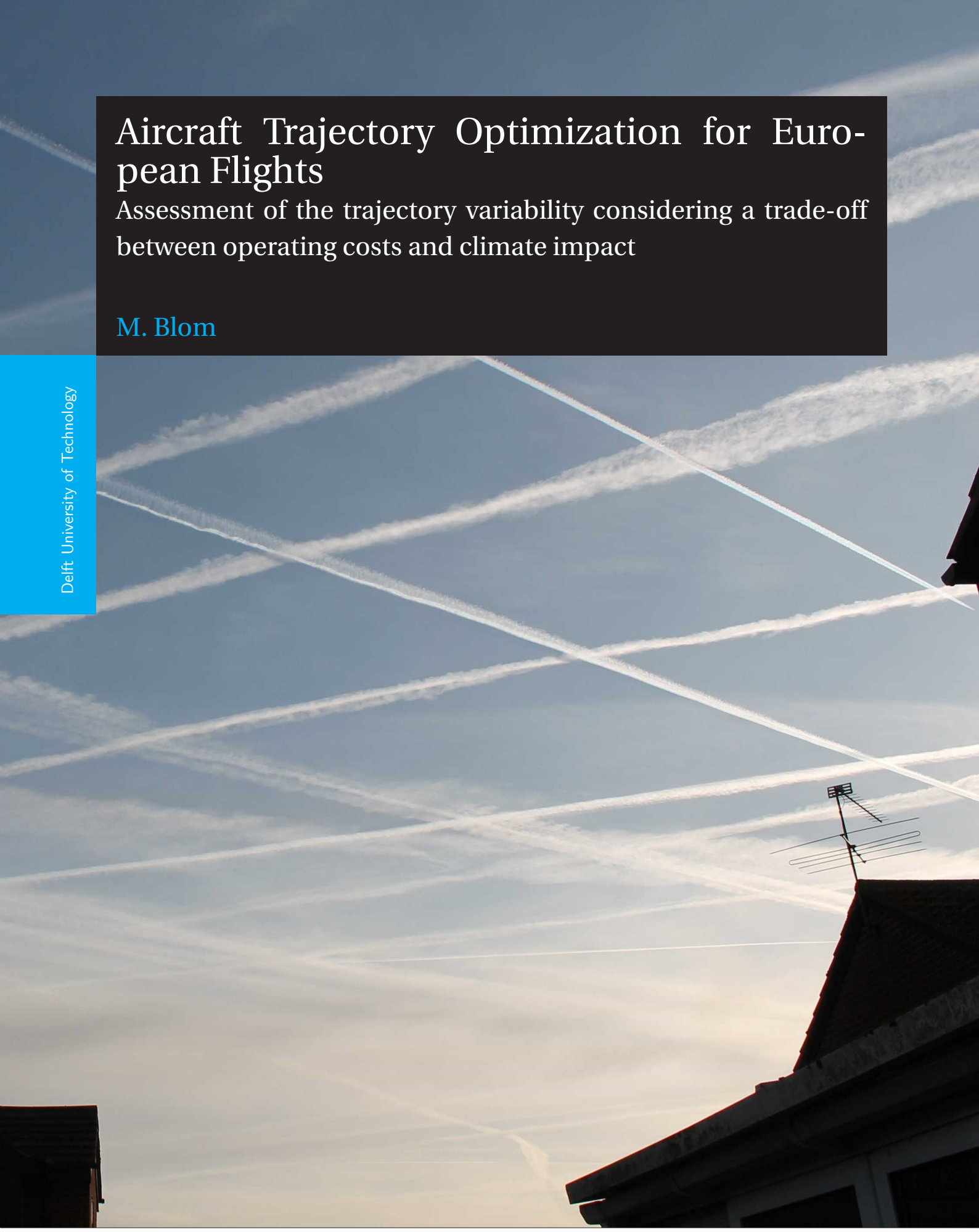

TU Delft Delft University of Technology

Challenge the future

Aircraft Trajectory Optimization for European Flights

Assessment of the trajectory variability considering a trade-off between operating costs and climate impact

To obtain the degree of Master of Science
at the Delft University of Technology,
to be defended publicly on Tuesday November 6, 2018 at 9:00.

Author:

Name	Surname	Email	Student ID
Martijn	Blom	M.blom-2@student.tudelft.nl	4166809

Thesis Committee:

Prof. Dr. V Grewe	TU Delft (ANCE), DLR
Dr. Ir. G. La Rocca	TU Delft (FPP)
Dr. Ir. B. Lopes dos Santos	TU Delft (ATO)

Project duration: December 15 2017 - November 6, 2018

An electronic version of this thesis is available at `http://repository.tudelft.nl`
Cover image by WMO (`https://cloudatlas.wmo.int/aircraft-condensation-trails.html`)

Abstract

Climate change is an ongoing topic of discussion as anthropogenic global warming is continuing to affect the temperature of the atmosphere of the earth. Aviation contributed to approximately 4.9% of the total anthropogenic global warming in 2005 and is expected to grow even further in the coming years. The aircraft industry is growing each year and although the fuel consumption per kilometer is reducing, the growth of the aircraft industry is exceeding the reduced fuel consumption. In order to reduce the climate impact induced by the aircraft industry, several mitigation methods must be applied. As an example, current engine technologies can be improved to reduce the emissions. However, the current study which investigates how aircraft trajectories can be altered to reduce the overall climate impact does not require any technological changes. This study examines the variability between cost optimized and climate optimized flight trajectories to establish how the climate impact reduction affects the operating costs and vice versa.

To evaluate the climate impact of air traffic, a model called the EMAC model is used, which originates from the ATM4E project. It uses a climate-chemistry model to simulate the earth its atmosphere and sub-models to study aircraft trajectories with their corresponding emissions. Previous models were only able to model several weather situations but the EMAC model allows for rapid generation of weather data using algorithmic climate change functions and actual meteorological data. This project models an Airbus A330-300 using two General Electric CF6 engines as reference aircraft and analyzes 85 flights in the European airspace. The analysis is done for 182 days which resembles six months, starting on January 1^{st} until June 30^{th} 2016. Three different aircraft routes are examined which include great circle routes which features the shortest trajectory between two points on a sphere. Secondly, all flights are optimized to reduce the operational costs and finally, the flights trajectories are optimized to reduce the climate impact. The three different types of trajectories are compared in this research.

During the project, the cost and climate optimized flights are analyzed to gain an insight on the optimization performance of the model. Furthermore, a general analysis, a seasonal analysis and a comparison between four flight directions was done, comparing the great circle, cost optimized and climate optimized flights.

The results that were obtained from the simulation of the EMAC model showed that in 57 out 85 days, the climate impact of the climate optimized flights is higher than the climate impact of the same cost optimized flights. This showed that the model is not performing as intended. Similarly, there are flights which are climate optimized which have lower operating costs than their equivalent cost optimized flights. However, on a daily average, the operating costs of the cost optimized flights are exclusively lower.

The results of the general analysis show that the climate optimized routes have an increased flight length and therefore an increased fuel consumption, but on average have a lower climate impact because they avoid climate sensitive regions. The season does not significantly affect the climate impact of the trajectories, but the operating costs of the climate optimized flights are largely reduced during the summer season because the aircraft fly higher which results in a reduction of the fuel consumption. The climate impact and operating costs of the flights in each direction are mainly affected by the wind

speed and direction. The main wind direction (jet stream) is east which benefits the eastbound flights and obstructs the westbound flights. Overall, the results of this study show promising trends which can be further improved if the efficiency of the model to find a global optimum is increased.

The future of aviation is dependent on finding sustainable solutions to reduce climate impact. The results presented in this thesis show some promising alternative routes that reduce the climate impact of aircraft. However, additional research is required within the coming years to establish a Pareto front to determine an optimal trade-off between operating costs and climate impact.

Preface

To complete my master and obtain my MSc degree in Aerospace Engineering at the TU Delft, this master thesis is presented as a finalization of this degree. I followed the Flight Performance and Propulsion master track and specialized in sustainable aviation at the Aircraft Noise and Climate Effects (ANCE) department. This thesis includes background information, a literature study and a core study of the effects of trajectory optimization towards reducing climate impact and/or operating costs.

I am interested in reducing the climate impact of aviation because I care about the environment and aim to eventually transform aviation such that it is driven by sustainable developments. Therefore, I have decided to extend my enthusiasm for aircraft and sustainability and start my career as a consultant/engineer in sustainable aviation at the Netherlands Aerospace Centre (NLR). I am looking forward to apply the knowledge I have obtained during this thesis.

I would like to thank my two supervisors (Prof. Dr. V. Grewe and Dr. F. Yin) for guiding me through my thesis but also giving me the freedom to do research on the topics that I thought would be interesting or could potentially lead to breakthroughs in trajectory optimization. I would also like to thank my family and girlfriend for hearing my out about my struggles during my thesis and to motivate me to come up with creative solutions to compare and analyze the simulation data.

Contents

List of Figures

List of Tables

Nomenclature

Acronyms	Explanation
AGWP	Absolute Global Warming Potential
AGTP	Absolute Global Temperature change Potential
ATM	Air Traffic Management
ATM4E	Air Traffic Management for Environment
ATR	Average Temperature Response
BADA	Base Aircraft DAta
CCF	Climate Cost/Change Function
C_{cli}	Climate cost
C_{eco}	Economic cost
CIC	Contrail Induced Cirrus
CPC	Contrail Potential Coverage
DLR	German Aerospace Center (Deutsches Zentrum für Luft- und Raumfahrt)
ECF	Environmental Change Function
ECHAM	European Centre Hamburg general circulation model
EMAC	ECHAM5/MESSy Atmospheric Chemistry
GA	Genetic Algorithm
IR	InfraRed
KS	Kolmogorov-Smirnov
MESSy	Modular Earth Submodel System
REACT4C	Reducing Emissions from Aviation by Changing Trajectories for the benefit of Climate
RF	Radiative Forcing
SESAR	Single European Sky ATM Research
UV	UltraViolet

1 Introduction

Climate change is an ongoing topic of discussion as anthropogenic global warming is continuing to affect the temperature of the atmosphere of the earth. Aviation contributed to approximately 4.9% of the total anthropogenic global warming in 2005 and is expected to grow even further in the coming years (Lee et al., 2009). Air transport is growing faster than motor transport with an annual increase of about 5% each year and have a stronger influence on the radiative forcing (RF) budget of the earth. Aircraft change the chemical composition of the atmosphere which alters the radiative forcing of incoming and outgoing radiation and therefore the equilibrium temperature is adjusted.

1.1 Background Information

As the car industry is trying to move more towards electric vehicles, for the aircraft industry it is more difficult to follow these trends. However, the aircraft industry can use different measures to mitigate its climate impact. Trajectory optimization has been an important tool to reduce the travel time and operating cost. Over the past decades, it has developed towards more advanced methods up to a point where it is now possible to navigate precisely over the entire world and use weather conditions to optimize the trajectory.

Mitigation can be done in two ways, by a logistical or a technological measure. A technological measure involves reducing the aircraft weight to reduce fuel consumption, improve engine technology or improve fuel quality. Logistical mitigation involves the volume of fuel used as it decreases the number of greenhouse gasses emitted (Irvine et al., 2013). However, not only the volume of greenhouse gasses emitted but also the geographical location, season and other atmospheric parameters have an effect on the radiative forcing of the emitted products. The location where CO_2 is emitted is of less significant value since CO_2 spreads through the atmosphere rapidly. Although, there is some dependence between day and night which is explained by Lim et al. (2017). The impact of other species such as NO_x and water vapour are more location dependent.

There are several ways in which global warming due to aircraft can be mitigated. The three options that are standing out the most are:

- Reduce the number of operating aircraft. For instance, change short flights to more environmentally friendly ways of transport, like electric vehicles or eventually the Hyperloop.
- Reduce emission of greenhouse gasses by the aircraft engine. This can be done by making the engine more efficient or by burning sustainable alternative types of fuel. This will result in less radiative forcing and hence less temperature change.
- Rerouting aircraft to avoid climate sensitive regions such as humid cold regions where cirrus cloud formation due to aircraft can result in global warming.

To keep the economy going, the first option is not yet viable and is more of a political debate. The technological mitigation strategy is a viable option but the latter option has the advantage that it requires the current technology and is therefore cheaper since it does not require any physical changes. On the other hand, the computational effort of doing trajectory optimization can also be expensive.

Ultimately, however, technological mitigation is required to improve the climate impact even more.

Something that should be kept in mind is that active flight planning (trajectory planning during the flight) will require the aircraft to take additional fuel on board because the aircraft should be able to extend its trajectory to avoid climate sensitive regions. This increases the take-off weight of the aircraft and will increase the fuel consumption and therefore increase the emissions during the flight.

1.2 Research Question

The objective of this thesis is to find out how trajectory optimization towards reducing climate impact and operating costs of aircraft, changes the aircraft trajectories. This is done by using a global atmospheric model with a trajectory optimization sub-model. The optimization will be done using two optimization variables (climate impact and direct operating cost) using a weighting factor which can be varied over an interval ([0,1]) to change the importance of the two optimization variables.

The research question for this project is the following: *How does flight trajectory optimization of European flights affect climate change and direct operating costs and what is the variability of these flight trajectories?* It is important to not only optimize towards direct operating or climate costs but to find an optimum where the sum of both can be optimized, or to create a Pareto front which can be used to see how optimization towards one of the objective functions affects the other. However, this is not in the scope of this thesis and will require additional research.

Besides the main research question, there are some sub-questions that need to be answered in order to get a complete and accurate understanding of the possibilities for trajectory optimization inside the European airspace. The first sub-question reads: *How is the optimization model minimizing the objective function and is the minimization of this objective function always achieved?* Another sub-question is: *How does the season affect the optimized flight trajectories?* The final sub-question is: *How does the flight direction affect the optimized flight trajectories?* In contrast to trans-Atlantic flights where the dominant flight direction is either east or west, flights in the European airspace operate in the whole directional domain which makes it more difficult to compare trajectories in different directions. The EMAC model that is used during the ATM4E project is also used for the simulation of this thesis.

1.3 Relevance of the Research

Since the trans-Atlantic region has been investigated extensively, it is also crucial that the aircraft trajectories for European flights are optimized to further reduce climate impact and allow for policy changes towards reducing global warming. The research question is relevant because there is no research done which examines the variability of flights in the European airspace to this extend. Previous research has grasped upon evaluating the variability of flight trajectories inside the European airspace. However there are no existing studies which evaluate six months including different weather systems on each individual day. Furthermore, for the first time, flight directions and a seasonal effects are evaluated between 85 different airport pairs.

The strategy of this master's thesis is to use existing aircraft simulation technologies to analyze the flight trajectories in the European airspace for each optimization strategy. Furthermore, analysis of

the results allows for the verification of the existing simulation model. The results presented in this thesis allow for a better understanding of the preferred flight trajectories in the European airspace and will determine whether or not there are significant trends present in the general flight paths, but also the flight direction and season. Finally, the trajectory variability results will be used to determine which atmospheric parameters influence the flight trajectories.

2 Literature Review

To investigate the impact of greenhouse gas emissions of aircraft, the International Civil Aviation Organization (ICAO) assessed the situation of greenhouse gasses in 1996. The rapid growth in the aircraft industry required policy intervention. The report by Penner et al. (1999) describes an unbiased accurate state of knowledge of gasses emitted by aircraft. The report states that aircraft affect the composition of the lower stratosphere and the upper troposphere by altering the concentration of CO_2, CH_4, H_2O and O_3, and trigger the formation of contrails and cirrus clouds. All of these gasses contribute to climate change.

This chapter describes the properties of the atmosphere around the earth and shows how the climate changes. The properties of the atmosphere strongly determine the trajectory of the aircraft and therefore, it is important to know why and how the trajectories are altered due to these atmospheric properties. It also describes previous research on trajectory optimization where the main focus is on the trans-Atlantic and European airspace.

2.1 Radiative Forcing

Radiative forcing is the difference between the radiation absorbed by the earth (coming from the sun and to lesser extend other stars and light emitting sources) and the outgoing radiation from the earth. If the absorbed radiation from the sun is more than the outgoing radiation, there is a radiative imbalance resulting in a temperature increase of the earth and its atmosphere. This is called positive radiative forcing (Houghton, 1994). It is usually measured at the top of the atmosphere as the amount of watt per square meter.

Radiative forcing can be caused by several factors, one of which is a change in solar flux, increasing the incoming radiation onto the earth. Anthropogenic radiative forcing is a another factor resulting in positive radiative forcing. This is an increasing issue as it results in global temperature rise which can destroy the earth its biota.

Anthropogenic Radiative forcing is caused by both CO_2 and non-CO_2 emissions. Globally, CO_2 emissions have the largest impact on the global climate change. However, in air transport, NO_x and water vapor emissions also play an important role. Although aircraft are becoming more fuel efficient, the growth in air transport is most likely to increase faster, resulting in an increasing positive radiative forcing due to air transport.

2.2 Effects of Climate Change

Temperature rise can give a positive feedback. An example of positive feedback is that an increased temperature results in melting of ice which reduces the albedo (reflectivity of radiation) of the earth. This increases the temperature of the earth even more, thawing more ice. This will increase the sea level bringing potential harm to countries with a low average land altitude. Melting of ice also releases methane gasses and carbon dioxide which is stored in the permafrost. The greenhouse gasses increase

the atmospheric temperature (Simons, 2015).

Another example of positive feedback is that due to temperature rise, the oceans warm up which allow them to absorb less carbon dioxide and hence more carbon dioxide is released into the atmosphere resulting in a temperature rise (Simons, 2015).

Temperature increase can also give a negative feedback. An increase of water vapor in the atmosphere develops more clouds which increases the albedo of the atmosphere, reflecting more radiation from the sun.

2.3 Atmospheric Dynamics

Vorticity in the atmosphere is a clockwise or counterclockwise rotation of air and is caused by a change in the direction or magnitude of the wind speed. Vorticity allows for mixing and spreading of gasses. It is produced by shear, curvature and the Coriolis force. The shear is a result of a change in magnitude of the wind speed while there exists a curvature when the wind changes direction. Finally, the Coriolis force which is strongest at the poles and weakest at the equator changes the wind speed flowing from and towards the poles where the wind flow is increased going towards the poles (Haby, 2001).

An aircraft creates a vortex at the wing tip which catches the the gasses coming from the engine exhaust. The way the vortex behaves and the properties of the atmosphere determine the contrail depth and the ice crystal loss. This is mostly dependent on the vertical wind shear. Vorticity usually results in a descend of particles which is accompanied by an increase in temperature and therefore a lower chance to form contrails (Grewe, 2015).

Another form of atmospheric dynamics is the circulation of air. There are three cells of circulating air transport on each hemisphere resulting in trade winds. These cells are called the Hadley cell, Ferrel cell and polar cell and are shown in figure 2.1 (Mulder, 2015). The Hadley cell is the circulation of air close to the equator, where air moves up at the equator, transports towards the poles in the upper troposphere, moves down at the sub-tropics and flows back to the equator at sea level (Mitas and Clement, 2005). The other two cells also have a circular pattern resulting in a pressure system over the earth. There is a low pressure system at the equator and a high pressure at the surface of the poles and the subtropics.

The difference in high and low pressure results in trade winds at the earth its surface and jet streams at the top of the circulation pattern. In the northern hemisphere, these pressure systems will result in trade winds from the north-east close to the equator and trade winds from the south-west further away from the equator (northern Europe). The main jet streams on the northern hemisphere called the westerlies (wind from west to east) usually occur in the stratosphere, are very large in volume and can reach speeds up to 500 km/hr in the winter (Mulder, 2015). These wind speeds can have a large impact on the aircraft emission volume and distribution.

It is found that due to greenhouse gas global warming, the Hadley cell is expanding towards the poles. Due to a larger Hadley cell, the warm air rising from the equator warms a larger part of the northern hemisphere. This has resulted in increased global warming in the subtropics and minimized global

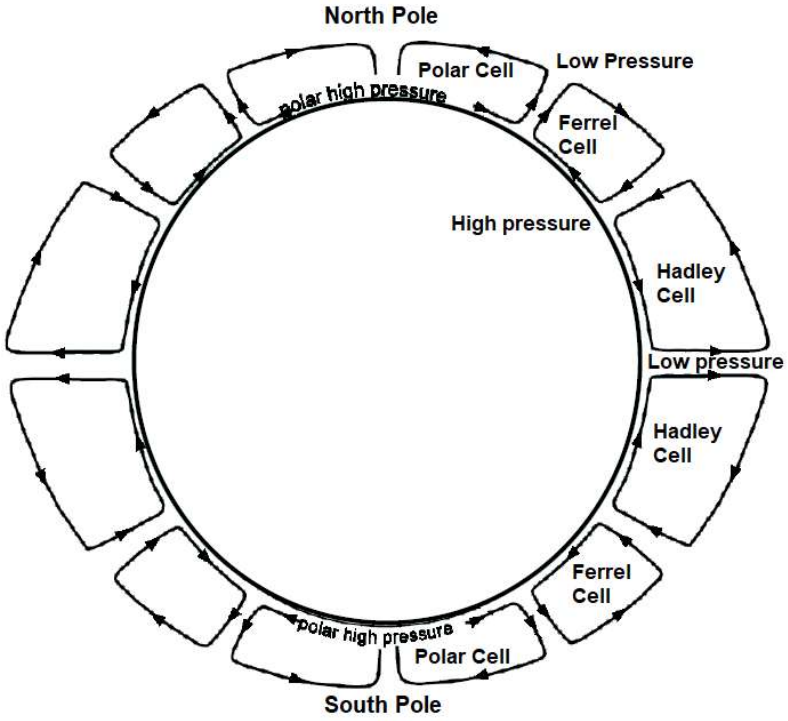

Figure 2.1: Circulation of air on each hemisphere results in high and low pressure areas. Adopted from Mulder (2015)

warming at the equator (Lu et al., 2007). Since the Hadley cell is expanding, it could influence the climate impact of the flights which cover the southern part of Europe.

2.4 Different Climate Metrics

Climate impact can be measured qualitatively by climate scores. This is done by giving scores according to environmental, social and governmental impact (Dupré et al., 2016). It can also be measured quantitatively, for instance, by using the global warming potential (GWP) which was introduced to compare the importance of different greenhouse gasses and their effect on global warming. The lifetime of the greenhouse gas is hereby also taken into account. It is the ratio of the time integral of the radiative forcing by a pulse emission of a unit mass compared to the emission of one kilogram of carbon dioxide (Mulder, 2015).

The global warming potential shows that the warming potential of NO_x is 21 times higher on average than that of carbon dioxide, where in the tropopause and the lower layer of the stratosphere NO_x may even have a global warming potential of 250 (Mulder, 2015).

The average temperature response (ATR) after a certain number of years is used to show the impact

of the emission of gasses on the future. For instance, the ATR20 is a measurement of the average temperature response twenty years after a certain emission. The temperature change can be sensed in contrast to radiative forcing. During this thesis, the ATR20 climate metric will be used. Both he ATR and GWP are computed based on the radiative forcing.

2.5 Aircraft Emissions

In order to determine the effect aircraft have on the environment, the emitted species coming from the engine exhaust need to be evaluated. The emissions from the aircraft engine will be divided into three different categories. The first category consists of the CO_2 emissions which directly affect the climate. The second category is NO_x which does not contribute to climate change by itself but interacts with other atmospheric gasses resulting in the formation of ozone and depletion of methane. Finally, the third category is water vapor which is a direct greenhouse gas and can also result in the formation of contrails and eventually clouds. The latter category has a large contribution to the temperature rise due to emissions of aircraft. These are the three types of emissions that will be considered for the flight trajectory optimization. There are other species emitted by the aircraft exhaust as explained in section 1.1, but the uncertainty of these species is too high to do a valid analysis on these species. The impact of the species help to understand in which way the optimization takes place and what trajectory is eventually chosen to reduce the overall climate impact the most.

Figure 2.2 shows the products that are released during the combustion process of an aircraft engine using kerosene as engine fuel. During the complete combustion of kerosene, all fuel is converted to carbon dioxide, water vapour and sulphur dioxide. However, during a flight, the air to fuel mixing ratio is not always perfect which results in additional combustion products. All combustion products result in a change in the composition of the atmosphere and can directly or indirectly result in radiative forcing.

2.5.1 Carbon Dioxide Emissions

Carbon is transferred in nature through a carbon cycle over several different carbon reservoirs. This is dominantly done by carbon dioxide. Humans contribute to this cycle by breathing and exhaling carbon dioxide. Since the beginning of the industrial revolution, the carbon dioxide cycle has been strongly altered. The amount of carbon dioxide extracted from ocean sedimentation is partly absorbed by the ocean and the atmosphere (Houghton, 1994).

CO_2 emissions can sustain for many years and therefore the emitting CO_2 molecules now, will have an impact on the climate for a long time in the future. A lifetime of approximately 100 years is usually referred to for guidance as there is short-lived carbon dioxide which sustains only for a couple of months or years and long-lived carbon dioxide molecules that remain for centuries.

In 2015, the concentration of carbon dioxide in the atmosphere was approximately 400 ppmv and yearly about 5 Giga ton of carbon is emitted into the atmosphere which adds approximately 2.3 ppmv each year. In 2050 this would result in a concentration of 480 ppmv. Such a concentration will have a radiative forcing response to increase the temperature by 0.8 °C. It is expected that with the current emitting pattern, fossil fuels will run out in about 100 years (500Gt remaining). This will

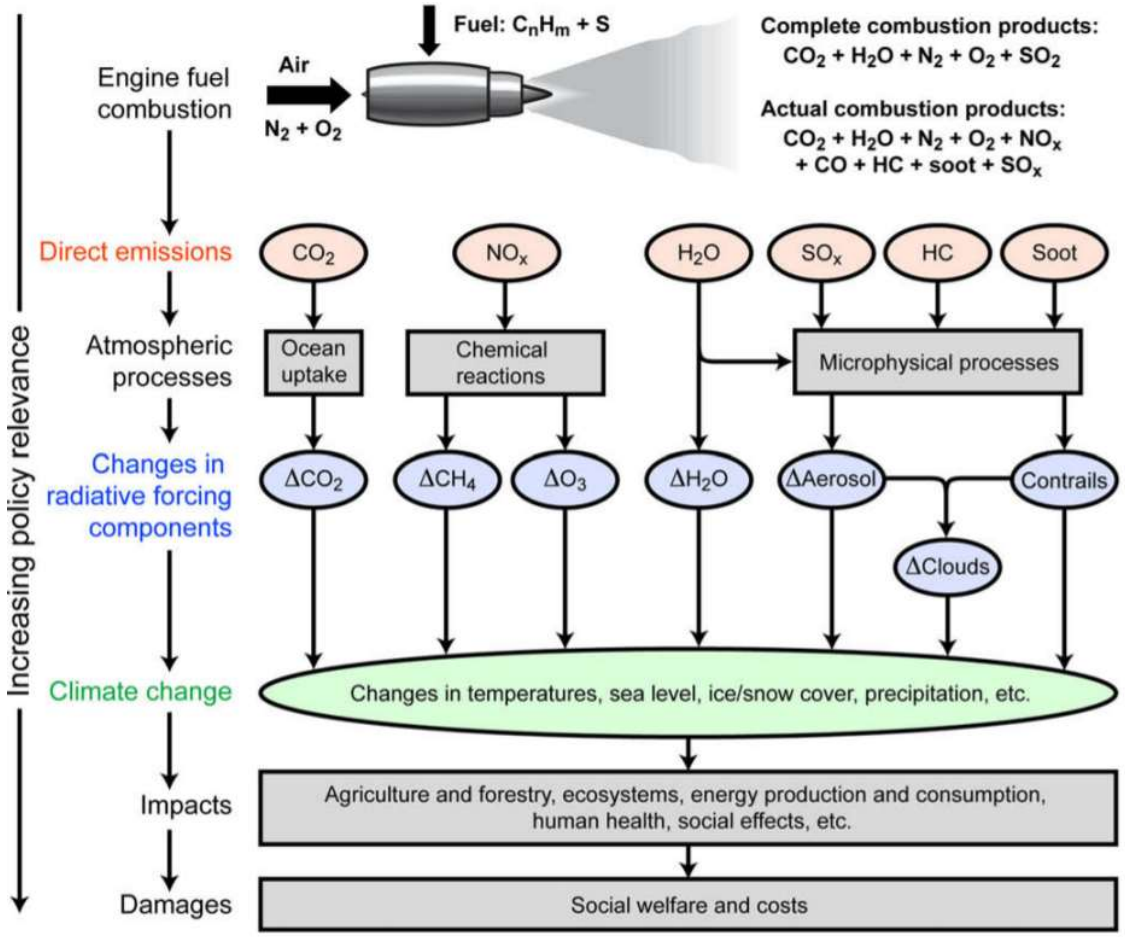

Figure 2.2: Engine combustion products and the impact of the combustion products on the atmosphere and climate. The climate impact results in ecosystem deprivation and human welfare damage. Figure from Lee et al. (2009)

produce a temperature increase of almost 2 °C with respect to 2015 (Simons, 2015).

Even if no more carbon dioxide will be emitted from this point onward, the concentration in the atmosphere is of such large volume that for the coming thirty years, the temperature will increase by about 1.4 °C due to the long lifetime of carbon dioxide in the atmosphere. after thirty years, the temperature will slowly start to decay towards its initial state.

2.5.2 Nitrogen Oxide Emissions

Only approximately one percent of the NO_x emission originate from aviation while most of the emissions come from lightning and burning surface fossil fuels (Berntsen and Isaken, 2016). However, only lightning and aviation change the natural level of NO_x in the upper troposphere and the lower stratosphere.

Nitrogen oxides in itself are not responsible for climate change but nitrogen dioxide exposure is associated with health effects, so emissions of nitrogen dioxide at low altitude can be harmful to human welfare (United States Environmental Protection Agency, 2014). In the presence of sunlight, Nitrogen oxides can form ozone which is a greenhouse gas, warming up the atmosphere. Furthermore, Nitrogen oxides react with hydroperoxyl (HO_2) to form the hydroxyl radical (OH) which is highly reactive (Grewe, 2015). Ozone itself also causes a chemical reaction in the presence of sunlight to form an oxygen atom which reacts with water to form hydroxyl. Hydroxyl reacts with methane which results in depletion of methane (greenhouse gas) and a corresponding temperature decrease of the atmosphere.

Figure 2.3 shows the reaction process of ozone formation and methane depletion through the reaction between HO_x and NO_x. The figure is adapted from Grewe (2018). What is important to notice is that methane is necessary for the formation of the HO_2 and if there is more NO_x present in the atmosphere, the reaction is increased requiring more methane. The reaction to form the HO_2 molecule loosens the oxygen bond and the HO_2 molecule is used to form NO_2 in a bonded cycle which in a reaction with UV light can form ozone (Grewe, 2018).

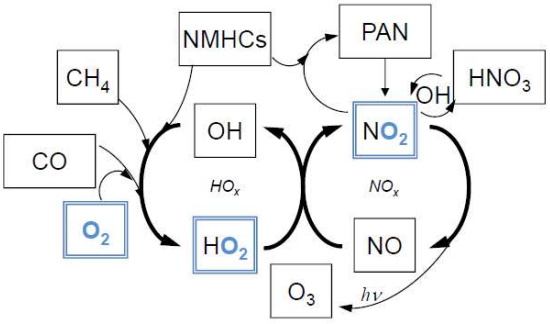

Figure 2.3: Chemistry in the troposphere to form ozone and deplete methane (Grewe, 2018)

The lifetime after a nitrogen oxide emission is usually between days and weeks, while ozone remains in the atmosphere for weeks up to a month and methane dissipates after approximately 12 years. After an impulse emission of NO_x, the chemical reaction instantly results in the formation of ozone and to some extend the depletion of methane. This usually results in a net temperature rise of the atmosphere. However, after a while (usually 5 to 15 days), the amount of ozone in the air accelerates the depletion of methane while the ozone volume does not grow as fast anymore. Therefore, for a pulse emission, the long term effects of decreased methane dominates the increase of ozone (Grewe, 2015).

NO_x is only removed from the atmosphere by rain out or if it sticks to a surface. The life time of NO_x at sea level is shorter than at higher altitude since more dry and wet deposition happens at lower altitude. Furthermore, the life time of NO_x is dependent on the season. Since there is less convection during winter time, the life time of NO_x is increased. This results in allowing for the NO_x to create more ozone (more cycles). Also, there is more creation of ozone in the tropic regions since the temperature is higher which increases the chemistry and there is more sunlight which allows for more ozone to be formed using an oxygen molecule from NO_2 (Grewe et al., 2017). Around the equator, ozone production has a warming effect which is larger than the cooling effect due to methane depletion, while close to the poles the effect of methane is dominant resulting in a small cooling effect due to NO_x emissions (Grewe, 2018).

The article written by Søvde et al. (2014) researches emission mitigation by changing the flight altitude and mainly discusses the effect of NO_x emissions. The research is part of the REACT4C project and applies chemistry transport models and two climate chemistry models. The short-lived radiative forcing caused by the formation of ozone has an average value of 19.5 mW/m^2 and the long-lived radiative forcing caused by the depletion of methane results in a total radiative forcing of approximately 5 mW/m^2 on the long term. If the altitude is increased by 2000 feet, it increases the radiative forcing by approximately 2 ± 1 mW/m^2 and an altitude decrease of 2000 feet decreases the radiative forcing by the same value (Søvde et al., 2014).

2.5.3 Water Vapor Emissions

Water vapor is emitted by aircraft but it is also increased by evaporation of ocean water. Water vapor is a greenhouse gas and will therefore increase the temperature of the atmosphere and the ocean which stimulates more evaporation of ocean water. On the other hand, Water vapor in the atmosphere can give a negative feedback as well. It extracts heat from the oceans which allows for more carbon dioxide uptake by the oceans and a decrease of the CO_2 concentration in the atmosphere.

2.5.4 Contrails and Clouds

Water vapor can also result in the formation of contrails when it is emitted from the aircraft exhaust and eventually turn into cirrus clouds. Clouds play an important role in the radiation budget of the earth. On the one hand, clouds reflect incoming radiation from the sun resulting in a negative radiative forcing. On the other hand, clouds also reflect and absorb radiation emitted by the earth which has a consequential increase in radiative forcing. During the day, depending on the geographical location and time of day, clouds can have an overall cooling effect on the earth since the incoming radiation reflected is more than the outgoing radiation absorbed. However, during the night, there is almost no incoming radiation from the sun so clouds will retain the radiation emitted by the earth. Clouds do however, reduce the amplitude of temperature variation on earth (Meerkötter et al., 1998).

Engine emissions can cause contrails behind aircraft and if these contrails result in clouds, it is called contrail induced cirrus (CIC). Contrails are formed in certain atmospheric conditions when the Schmidt–Appleman criterion is met (high humidity and low ambient temperatures of below $-38°C$ (Grewe, 2015)). This is also shown in figure 2.4. The condition where clouds are formed depends on the exhaust conditions of each engine, but on average the dashed line can be used, where the exhaust

emits high temperature moist air which is cooled down. Contrails will only be formed in the gray areas as in the top left corner natural cirrus is already present and in the bottom right corner the sky is clear.

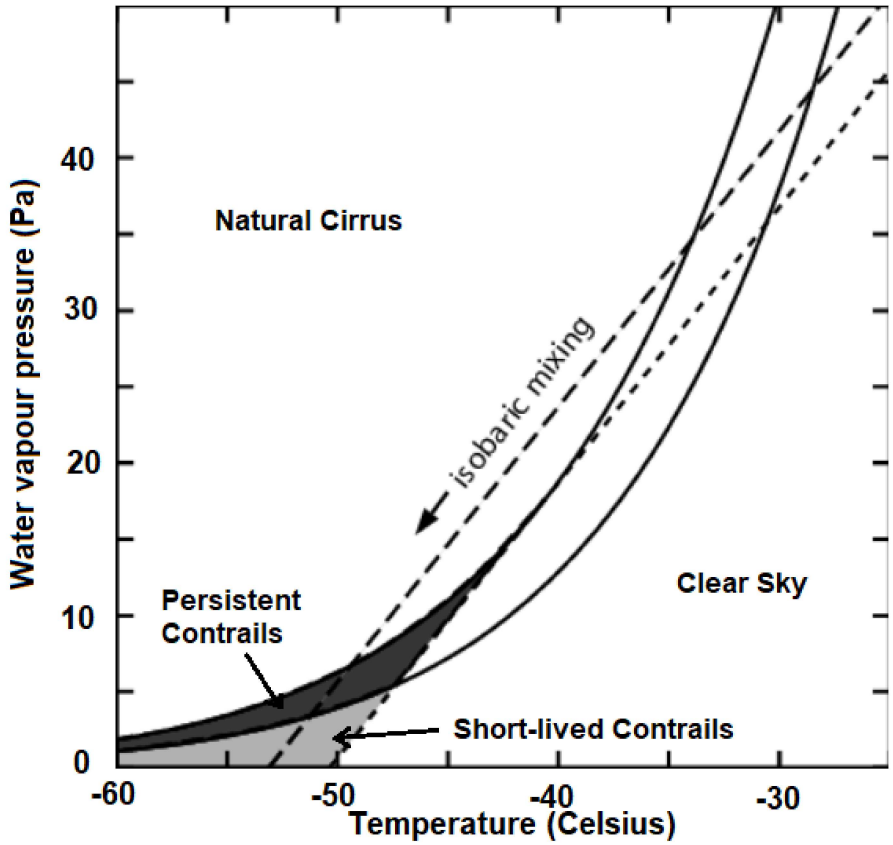

Figure 2.4: The Schmidt-Appleman criterion, where persistent (dark gray) and short-lived (light gray) contrails can be formed depending on the exhaust conditions of the aircraft engine and the atmospheric conditions. Adopted from Gierens et al. (2008)

The radiative forcing caused by cirrus clouds also depends on the ice particle size and shape, and the optical depth of the clouds. Recent research has resulted in a better understanding of the cloud formation so an estimation of the radiative forcing due to cirrus clouds is now available, further examination should allow for more accurate climate impact as a result of cirrus clouds.

Depending on the particle size, the impact of the ice particles is determined. Many small particles result in an increased life time and an increased albedo, thus reducing the radiative forcing. Increasing the mean particle size results in little cooling effect from the short waves while for long waves the radiative forcing is also positive and larger than the negative effect due to short waves. For very

small particle sizes, short waves have a stronger negative impact on the radiative forcing which can sometimes lead to a cooling of the earth its atmosphere (Grewe, 2015).

Contrails usually sustain from several minutes to hours. If they sustain for hours contrails usually turn into cirrus clouds. High Thin cirrus clouds are very strong greenhouse gasses as they are highly transparent to shortwave radiation from the sun but absorb a large part of the longwave spectrum emitted by the earth. The radiation absorbed by the clouds is emitted in all directions as longwave radiation. Low thick clouds have a negative radiative forcing effect on the atmosphere. Since these clouds are thicker, they reflect more shortwave radiation from the sun and the temperature of these clouds is almost equivalent to that of the earth and therefore the longwave radiation emitted is at the same temperature and does not greatly affect the infrared radiation emitted to space (Graham, 1999). Unfortunately, most clouds created by aircraft are high cirrus clouds.

In 2002 it was estimated that contrail induced cirrus due to air traffic results in a radiative forcing of approximately 38 mW/m^2. Furthermore, it was found that clouds formed by aircraft change natural clouds reducing their radiative forcing by 7 mW/m^2, resulting in a net positive radiative forcing of 31 mW/m^2 (Burkhardt and Kärcher, 2011).

2.6 Trajectory Analysis

Trajectory optimization has already been studied extensively but it has mainly been focusing on reducing the travel time and fuel expenses. Although reducing the fuel expenses results in less emissions, it may result in using airspace that is more vulnerable to aircraft emissions and therefore increase the radiative forcing compared to a longer less affecting route.

Changing the average flight altitude has impact on the radiative forcing and temperature response and is examined by Frömming et al. (2012). This model is not applied on a specific region but is a general case for altitude and takes latitude into account as well. The study shows that if the altitude is decreased with respect to the base case, the fuel consumption and the NO_x emissions are increased while for an increase in flight altitude the opposite happens. This is a result of the change in atmospheric composition and therefore the resulting efficiency of the aircraft engine (Frömming et al., 2012).

There is research performed on trajectory optimization on both the European and the trans-Atlantic airspace. All reports show that the great circle or the cost optimized routes are different from the routes that are optimized for climate impact. Research has also concluded that the climate impact of air traffic is highly dependent on the season, as well as the time of day when the trajectory is planned.

Most optimization algorithms use a discretized grid where the weather in each grid point is a constant value during the flight. The climate impact is computed by calculating the effect of a unit emission in each grid point and afterwards computing the total climate impact of the aircraft trajectory.

For both, European and trans-Atlantic studies, the global warming potential (most used worldwide) is used to compare the different types of emissions. All studies show that there are costs accompanied with optimization towards reducing climate impact. The studies also show that when the direct operating costs are optimized, it is accompanied by an increase in global warming potential.

For the trans-Atlantic flights it is found that wind plays an important role. For eastbound flights it is preferred to follow the jet stream, while for westbound flights it is preferred to avoid the jet stream and depending on the magnitude and tilt of the jet stream flights are redirected south or north of it.

For the two European flight trajectory optimization studies, Gardi et al. (2016) optimizes the trajectory for several objectives like cost, noise and several climate factors while Rosenow et al. (2017) optimizes for cost and contrails only.

The study performed by Lim et al. (2017), investigating a flight between Paris and Beijing, tries to minimize an objective function containing time (hrs), distance (km), CO_2 emissions (tons) and radiative forcing due to contrails (W/m^2). These climate metrics all have a corresponding weighting factor. Rosenow et al. (2017) determines its trajectory based on the ecological costs, direct operating costs and contrail costs in euros, and fuel burn in kilograms.

The REACT4C and WeCare projects use a cost model for the direct operating costs which assumes 75 cents per kilogram of fuel burned and 25 euros per minute for the cost of the crew. Furthermore, the climate metric used is the average temperature response after twenty years (ATR20) to compute the radiative imbalance Grewe et al. (2017). To compute the dependency of the flight altitude, Frömming et al. (2012) uses the radiative forcing (mW/m^2) of contrails, water vapor and ozone emissions.

3 Model Implementation

The ATM4E project is a follow-up project of the REACT4C project. It uses a climate-chemistry model to simulate the earth its atmosphere and sub-models to study aircraft trajectories with their corresponding emissions. Environmental Cost Functions (ECFs) are used to find optimized trajectories (SESAR Joint Undertaking, 2017).

This research originates from the ATM4E project which aims to examine if it is possible to assess air traffic management operations to be optimized towards reducing environmental impact of air traffic. The project started in May of 2016 and focuses on civil transport in the European airspace. The project uses existing technologies from the previous REACT4C project. It focuses on climate effects, air quality and noise impact of aircraft. The project is led by the DLR-institute for Atmospheric Physics. The model is used to analyze the effect of present impacts on the future (SESAR Joint Undertaking, 2017).

The model that is used during the projects is called the EMAC model which is short for ECHAM5/MESSy Atmospheric Chemistry model. The ECHAM5 model is a general circulation model meaning that it is a mathematical model to simulate the atmosphere of the earth. The modular earth sub-model system (MESSy) software provides a framework of earth system models. It currently consists of approximately 60 sub-models and is a collaborating project between multiple institutes. The software is "bottom-up" which means that the software uses generalized interfaces for the coupling of components. MESSy has achieved to design a flexible tool by using modules which allow it to be used by a large community in a wide variety of research fields (Joeckel, 2018).

The model that was used during the REACT4C project is less sophisticated than the model used for the ATM4E project because during the REACT4C project, only eight weather situations could be modelled while the model for the ATM4E project uses algorithmic climate cost functions to model the weather for an entire year. In both models, the weather situation is selected and using the EMAC model, climate cost functions are computed. For the ATM4E project, also environmental change functions (ECFs) are used for which actual meteorological data is required (Matthes, 16 b).

The environmental change functions link the ATM4E project to the REACT4C project by using the meteorological data generated during the REACT4C project. Together with the climate cost functions generated by the ATM4E project, the computational effort is reduced and additional environmental impact is generated such as air quality and noise impact. The ECFs are used to simulate air traffic at any possible day and are not restricted to the selected weather patterns of the REACT4C project (Matthes et al., 16 a).

The work flow of the models used for the REACT4C and ATM4E projects are schematically shown in figure 3.1. Climate change functions (CCFs) are computed using unit emissions released into the atmosphere. The emissions alter the chemical composition of the atmosphere, resulting in a radiative imbalance. The radiative imbalance is used to estimate the climate impact for a chosen time frame. The EMAC model allows for algorithmic CCFs to simulate air traffic for an entire year taking many different weather situations into account and therefore the entire spectrum is analyzed. The ATM4E project uses actual available weather data, which is related to the existing climate cost functions to

generate new climate cost functions rapidly. Pre-calculated algorithms are used which reduces the computational effort (Matthes et al., 2017). The species that are examined in this thesis are, carbon dioxide, nitrogen oxides and water vapor. Similar to the REACT4C project, the climate metric used for the ATM4E project is the ATR20 metric (SESAR Joint Undertaking, 2017).

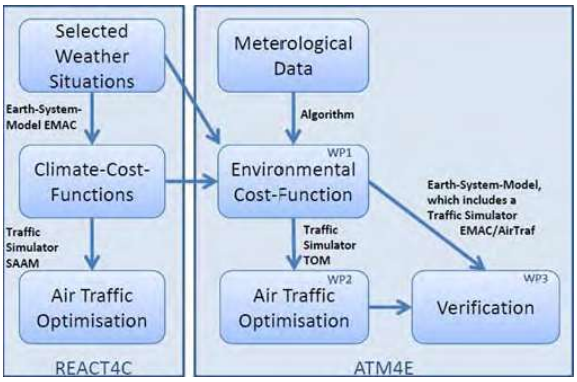

Figure 3.1: Work flow of the REACT4C and ATM4E Project (Matthes et al., 2017)

The AirTraf model is a simplified global air-traffic simulation model that is used to simulate and optimize trajectories of each flight that is chosen within a time frame. The aviation and engine data that is used to simulate the air traffic is obtained using base of aircraft data (BADA). The EMAC model provides meteorological data to AirTraf which is used to plan the trajectories, and simulate the fuel flows and emissions. AirTraf assumes that the earth is spherical with a radius of 6371 km. The emissions of the aircraft are interpolated towards the nearest grid point (longitude, latitude and altitude) of the model. The grid consists of a "horizontal quadratic Gaussian grid in latitude and longitude" (Yamashita et al., 2015). The fuel and aircraft weights are accurately calculated using a backward approach after the trajectory is established. The empty weight including the payload and 3% additional fuel are used as the weight for the final waypoint. From this point a backward calculation is used to estimate the fuel at the beginning of the flight (Yamashita et al., 2016). For this study, conflicts between aircraft trajectories are not taken into account. Only the cruise component of the flight is considered, so no take off and landing are taken into account for the trajectory optimization (Yamashita et al., 2015).

In the model, one aircraft type will be used to model all European flights. This is the Airbus A330-300 using two General Electric CF6 engines. The emissions coming from the engine are calculated for the cruise condition and will be incorporated into the model. 5D Data-sets are used where the first three dimensions indicate the geographical location and altitude, the fourth dimension indicates the time of the emission and the fifth dimension indicates the type of emissions (NO_x, CO_2 or H_2O) (Grewe et al., 2017).

The main objective of the ATM4E program can be divided into four different sub-objectives. The first sub-objective is to "establish a multi-dimensional environmental change function concept" (SESAR Joint Undertaking, 2017) for air quality, noise and climate impact. The second objective of the pro-

gram is to plan flight trajectories in the European airspace avoiding climate sensitive regions that were established by the first objective. Thirdly, optimized routes will be examined to prove the potential of trajectory optimization and finally, recommendations about the implementation will be given working together with everyone associated to aviation (SESAR Joint Undertaking, 2017).

Rosanka (2017) explains that it is difficult to verify the model of the REACT4C project since it is impossible to exactly trace emissions for several months in the atmosphere. However, the model is compared to previous results from other studies to examine whether the results are comparable. The other studies are different in their modelling approach, so comparison between the models is difficult. Rosanka (2017) describes that the weather pattern that has been used during the REACT4C project, mainly demonstrates differences between seasons and that within the season, the differences are small. The ECHAM5 part of the model has been verified extensively. However, Grewe et al. (2017) found that the model still underestimates regional differences for particular weather conditions.

The EMAC model uses the cruise component of the flight for each of the chosen trajectories. The analysis in this thesis is done for 182 days starting from the first of January 2016 until the 30^{th} of June 2016. This results in six months of data and 182 different weather patterns. Each day is analyzed for three different types of trajectories whose characteristics are explained in the following sections.

3.1 Optimization Strategies

The optimization strategies all aim at minimizing a certain objective function. The three different optimization strategies result in a great circle, climate optimized and a cost optimized trajectory for each airport pair.

A great circle trajectory is the shortest route between two points on a sphere. The great circle flights have a constant altitude and Mach number during the entirety of the flight. Comparing this trajectory with any other trajectory shows how far the other trajectory is deviated from the shortest route.

Optimization towards climate impact often results in a different trajectory than the great circle trajectory. The trajectory starts at a predefined location and altitude but rather than staying at the same altitude and travelling the shortest distance, it optimizes to find a trajectory which minimizes the temperature increase due to the traveled flight path. The temperature change is measured as the average temperature response after twenty years (ATR20). This is calculated for every single flight and summed-up to find the average temperature response on that day.

Optimizing towards operating costs again often results in a different trajectory than the great circle and the climate optimized trajectory. This trajectory starts at the same predefined location and altitude and also has to return to a predefined final location and altitude. Other than that, the aircraft is free to move between an lower and upper boundary of the simulated atmospheric domain. The route is found by reducing the operating costs which are a function of the flight time and the amount of fuel used.

3.2 Trajectory Optimization Process

The EMAC model is used to analyze three different trajectories for each day. The great circle trajectory is simply the shortest distance between start and end of the trajectory while the altitude is kept constant. This trajectory does not require any optimization since the trajectory is not dependent on any variable other than the initial and final point. For the cost and climate optimized flights, the trajectories are optimized according to their objectives.

The algorithm aims at finding a minimum climate impact for the climate optimized flights, while for the cost optimized flights, the aim is to find the lowest operating costs. Although the optimization for cost and climate optimum are simulated separately, during the same simulation day, the atmospheric properties are the same for the climate and cost optimized flights. However, the atmospheric properties are not constant during the day, but reflects an actual weather system.

The trajectory optimization towards reducing climate impact is done using a trajectory optimization module (TOM) which uses the ECFs in combination with an earth system model which includes the AirTraf model as a sub-model (Matthes et al., 16 a). By rerouting aircraft trajectories horizontally and vertically, the impact of air traffic can be reduced. AirTraf contains a module that is used for the optimization of the trajectories and is "parallelized using a message passing interface (MPI) based on a distributed memory approach" (Yamashita et al., 2015). The aircraft routes are distributed evenly so every core has a similar work load. The flowchart of the AirTraf sub-model is given in figure 3.2.

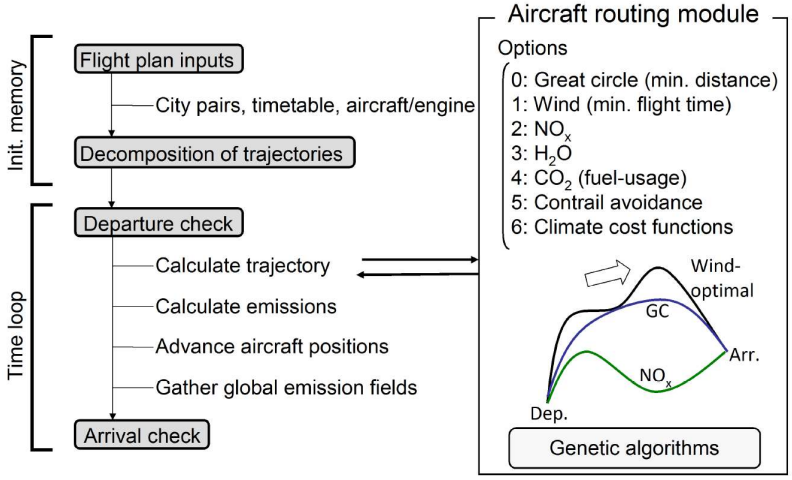

Figure 3.2: Flow chart of the AirTraf sub-model. Adopted from Yamashita et al. (2015)

The AirTraf model uses a flight plan as input for the time and origin of the flights. As soon as the departure time is reached, the flight status changes to "in-flight". The trajectory can be optimized towards many different objective functions which are shown in figure 3.2 on the right. The current version of the AirTraf sub-model also allows for the trajectory calculation of several different cost optimization types. The chosen objective function results in a "single objective minimization opti-

mization problem" (Yamashita et al., 2015) which is solved by a genetic algorithm (GA). Genetic algorithms are commonly used to solve complex optimization problems. The basic idea of a genetic algorithm is to change the input to create a better output (Jain, 2017). The algorithm is based on a evolution theory. An initial population randomly generated eventually evolves into a converged superior species. Genetic algorithms are useful for AirTraf because it consists of several types of functions which the GA is able to work with. However, genetic algorithms are computationally expensive in finding an optimal solution (Yamashita et al., 2015).

The atmosphere around the earth is modelled by the EMAC model and its properties are given for a discrete number of data points. The atmospheric properties are modelled in lateral and longitudinal direction, and altitude. The model contains evenly distributed points including 64 latitude points with a spacing of 2.8 degrees, 128 longitude points with a spacing of 2.8 degrees and 31 flight levels. Each flight level corresponds to a certain pressure level where the first flight level represents the top of the atmosphere (1000 Pa which corresponds to an altitude of approximately 32 km) and the 31^{st} flight level represents the pressure at sea level.

To find the point of minimum climate impact for the climate optimized trajectories, the algorithm is required to find a minimum value in a complex system. To reduce the computational effort, a number of points is chosen in the genetic algorithm, which are analyzed for their impact. Each point is optimized for latitude, longitude and altitude. Several iterations of the algorithm are performed in which points are selected which potentially can result in a global minimum. However, to reduce the computational effort, the limited number of iterations may result in a trajectory which is not actually a global minimum. This may result in a trajectory which is not fully optimized. If the number of iterations would be increased, the global minimum would be achieved. If for a certain trajectory, the cost and climate optimized trajectories lie on the same path, it is possible that after the final iteration, the cost optimized trajectory is found (which is less complex), while the climate optimized trajectory has not been found due to the complexity of the optimization process. Since the two trajectories would be on the same path, the climate impact of the cost optimized trajectories can be lower than the climate impact of the climate optimized trajectories. Section 4 discusses a number of examples where the optimization does not result in a global minimum.

3.2.1 Minimization Function

Optimization to find a global minimum requires an objective function. The objective function is presented in equation 1 which is a function of the climate and economic costs. The climate costs are equivalent to the average temperature response over a time horizon of 20 years (ATR20) of all emitted species and is measured in degrees Kelvin. The economic costs are computed using the flight time and the fuel consumption over the chosen time domain and is measured in dollars. To be able to compare the costs, a climate-cost parameter (k), shown in equation 2 is used. This parameter translates the temperature change to a cost function. Both equations are adopted from Verbist (2016).

$$f_{obj} = \alpha \cdot k \cdot C_{cli} + (1 - \alpha) \cdot C_{eco} \tag{1}$$

$$k = \frac{C_{eco,clim\_opt} - C_{eco,cost\_opt}}{C_{cli,clim\_opt} - C_{cli,cost\_opt}} \tag{2}$$

The alpha symbol represents the weighting factor. Depending on the objective of the minimization, the alpha value can be modified. A weighting factor of zero results in trajectories which are fully cost optimized while a weighting factor of one results in trajectories which only take the climate impact into account. The weighting factor can obtain any value between zero and one and as such the weight of the cost and climate can be changed to analyze several different combinations of cost and climate impact. The different optimization results (different alpha values) can be used to create a Pareto front which shows the climate costs as a function of the economic costs.

4 Model Verification

Simulations using optimization techniques that aim to find a global minimum are sometimes restricted by their complexity or computational effort. Therefore, it is often difficult to find a global minimum within a certain time frame. This section discusses the results of the optimization towards reaching a global minimum for the cost and climate optimized trajectories.

After the optimization of the cost and climate optimized trajectories it turned out that the cost optimized trajectories sometimes have increased operating costs compared to the climate optimized trajectories. However, during the analysis of the climate impact of both cost and climate optimized trajectories, it turned out that the cost optimized trajectories are quite often more climate efficient than the climate optimized flights. The difference in average climate impact between the climate and cost optimized trajectories is shown in figure 4.1.

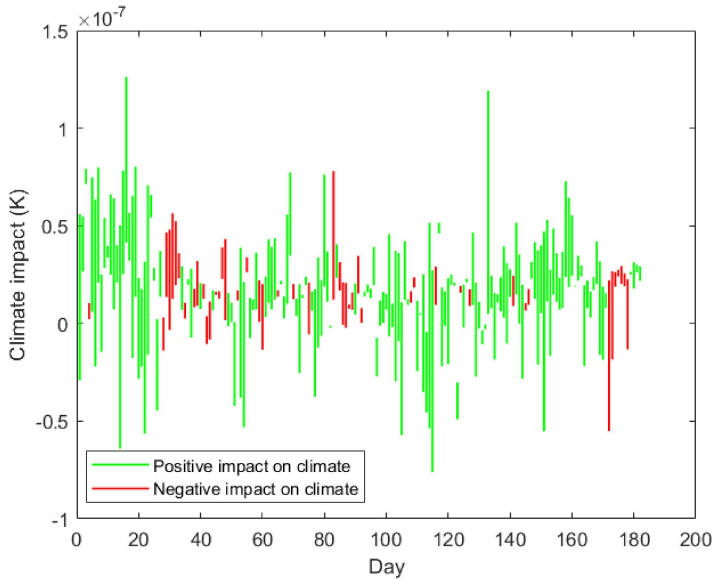

Figure 4.1: Difference in climate impact between the cost and climate optimized trajectories for a period between January 1^{st} and June 30^{th} 2016

Figure 4.1 shows red and green lines of different sizes for each simulation day. A red line indicates that ATR20 of the climate optimized trajectories is higher than the ATR20 of the cost optimized trajectories on that particular day. A green line indicates that the ATR20 of the climate optimized trajectories is lower than the ATR20 of the cost optimized trajectories on that day. The length of the lines indicate the difference between the impact of the cost and climate optimized trajectories. So a green line which is located below zero means that the climate impact of both trajectories is below zero but the climate optimized flights have a more negative value. The climate impact of a single day

is calculated as the sum of the climate impact of each trajectory on that day.

Figure 4.1 shows 47 days with a negative climate impact and 135 days in which the climate impact is positive. This means that for at least 47 days the algorithm was not able to find a climate optimized trajectory which resembles a global minimum. To find out if it is possible that the simulation is random (which means that on average halve of the time it results in a positive impact and halve of the time in a negative impact) a statistical test will be performed that tests whether the impact on the climate can come from a uniform distribution. In this case a negative impact on the climate is denoted by a value of one and a positive impact by a value of two. A variable with 182 values is constructed and compared to a data set containing 182 random variables drawn from a uniform distribution. The test that will be used for the analysis is the two-sample Kolmogorov-Smirnov (KS) test. This test compares two data sets and follows a null-hypothesis that the two data sets have the same distribution. The KS method rejects the null-hypothesis (probability is $1.63 * 10^{-9}$) and therefore concludes that the impact on the climate is not uniformly distributed. This means that the simulation is not random but actually aims at optimizing the climate optimized trajectories towards reducing the climate impact.

A similar figure showing the difference in operating costs is illustrated in figure 4.2. A green line is displayed when the operational costs of the cost optimized trajectories is lower than the operational costs of the climate optimized trajectories on that day. The figure only shows green lines which means that the optimization towards reducing the operational costs does not fail on a daily average. The length of the lines shows the difference in operating costs.

4.1 Negative Climate Impact

Some of the red lines shown in figure 4.1 are very small which means that the climate impact of the cost and climate optimized trajectories is close together. To find out what causes the deviation in the results, three days with a high negative impact will be analyzed to find out which species and flights cause the negative impact. The three days with the highest negative difference are days 30, 83 and 172.

Day 30 corresponds to January 30^{th} of 2016. The total climate impact of every flight is analyzed and shown in figure 4.3. It shows that the majority of the flights have a negative impact on the climate which means that the cost optimized trajectories have a lower ATR20 than to the climate optimized trajectories. For this day, approximately 86% of the flights have a negative impact on the climate. Similar analysis for days 83 (March 23^{th}) and 172 (June 20^{th}) result in a negative impact of 75% and 95% respectively. Appendix A shows the difference in climate impact between the cost and climate optimized trajectories of days 83 and 172 in figures A.1 and A.2 respectively.

Next, it is important to establish which type of emissions cause the deviation of the climate impact of the flights. To find the most polluting type of emission, the three most impactful climate optimized flights will be considered. From figure 4.3 it follows that flight numbers 5, 27 and 80 have the largest negative climate impact. The impact of every species for the three selected flights is shown in figure 4.4. The figure shows a bar diagram containing the difference in the ATR20 between the climate and cost optimized trajectory species. It shows that for each of the three days, the contrail potential coverage results in the largest discrepancy between the climate and cost optimized trajectories. In

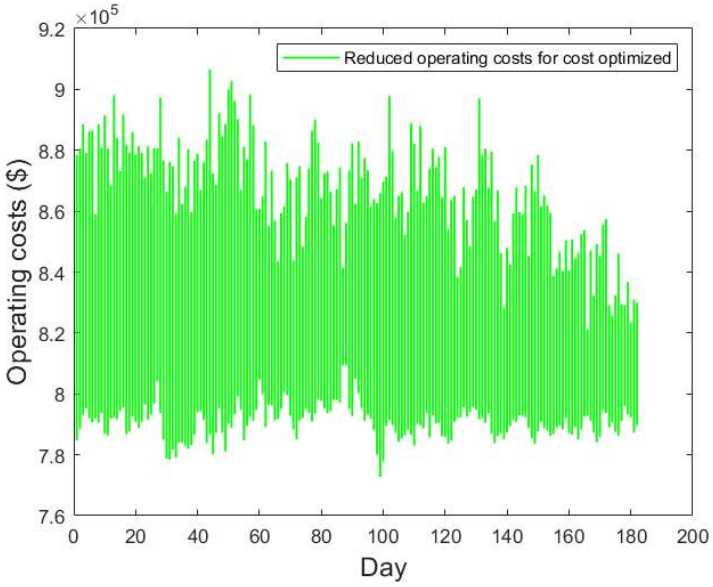

Figure 4.2: Difference in operating costs between the cost and climate optimized trajectories for a period between January 1^{st} and June 30^{th} 2016

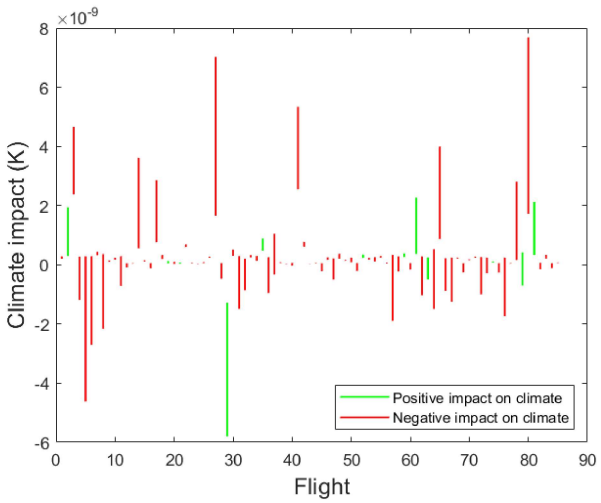

Figure 4.3: Difference in climate impact between each cost and climate optimized trajectory on January 30^{th}

general, it is found that if there is a large discrepancy between the impact of the climate and cost

optimized flights, it is a result of the discrepancy between the contrail potential coverage of both optimized flights.

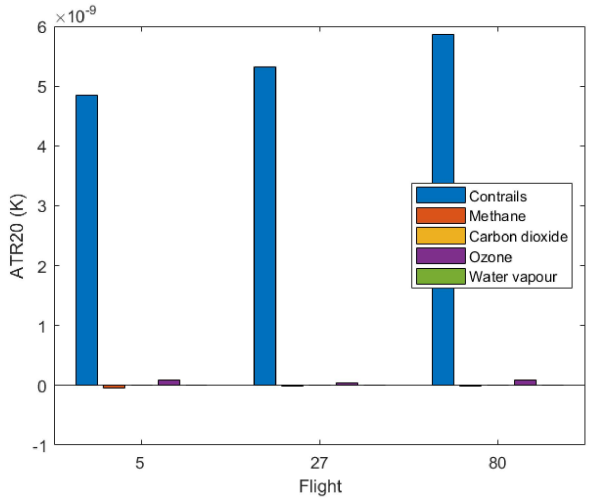

Figure 4.4: Difference in climate impact between each species of the three most impactful cost and climate optimized trajectories on January 30^{th}

The great circle, climate optimized and cost optimized trajectories of the three most impactful days are shown in figure 4.5. The three flights shown in figure 4.5 are all flying in a western direction and the flights are located in central Europe. Flight number five is located most east and covers a trajectory between Baku (Azerbaijan) and Istanbul (Turkey). Flight number 27 is located most west and covers a trajectory between Vienna (Austria) and Barcelona (Spain). The final flight is located most centrally and covers a trajectory between Istanbul (Turkey) and Paris (France). The other simulated days with a highly negative climate impact show that trajectories between different cities are responsible for the highly negative climate impact. The trajectories are shown in figures A.3 and A.4 in Appendix A.

It is found that flights headed in a western direction are often causing the highest negative impact. To give an example, out of the nine routes analyzed (spread out over three days), eight flights were headed in a western direction. To find out if this is coincidental, the three most impactful flights in a negative way of all days which have an overall negative climate impact (all red lines in figure 4.1) will be analyzed. There are 47 days with a negative climate impact which results in 141 flights which will be analyzed for their flight direction. The manner in which the flight direction is determined is explained in chapter 5. If it is coincidental that many of the most badly optimized trajectories are flying in a western direction, the flights should follow a uniform distribution evenly divided over four flight directions.

Grouping the flights by their flight direction can give a better understanding of the actual distribution

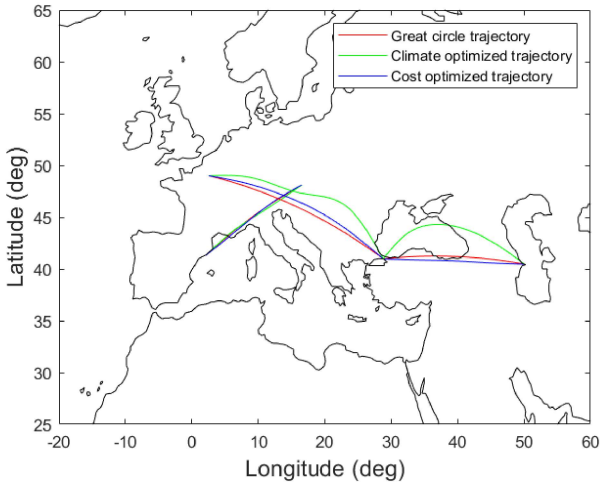

Figure 4.5: Three most impactful trajectories with negative climate impact on January 30^{th}

Table 4.1: Number of badly optimized flights in each flight direction

	Flights	**Percentage (%)**
East	33	23.4
North	20	14.2
West	78	55.3
South	10	7.1

of the most impactful flights. This results in a deviation from a uniform distribution given in table 4.1. It is represented by both, the number of flights and the percentage of all flights.

To find out if the most impactful flights can actually follow a uniform distribution, they can be compared to a uniform distribution. A data set containing 141 random values drawn from a uniform distribution will be compared a thousand times to the data set containing the most impactful flights. The deviation from the uniform distribution will be proven by means of a statistical test. The test which applies to these two data sets is the two-sample Kolmogorov-Smirnov (KS) test. The statistical test is used to analyze whether two data sets have the same distribution. If the data shown in figure 4.1 does not follow a uniform distribution, the null-hypothesis of the KS test is violated. Comparison of the most impactful flights with the uniformly distributed data set results in a deviation from a uniform distribution. However, there are more flights which fly in a eastern or western direction, than flights flying in either a northern or southern direction. Therefore, it is more likely that a flight is going towards the east or west is highly impactful. This has to be accounted for in the KS test which reduces the difference between the westbound flights and the flights in the other directions and also reduces the strength of the KS test because the number of data points is reduced. The reduced data set does not violate the null-hypothesis (probability >0.05) and therefore, it can not be concluded that the western or any other direction of flight is more responsible for a negative climate impact.

The contrail potential coverage has a climate impact on the trajectories which is illustrated by figures 4.6 and 4.7. Figure 4.6 shows the great circle and climate optimized flights, while figure 4.7 shows the great circle and cost optimized flights. The first trajectory shown on the left corresponds with flight number five and the trajectory on the right corresponds to flight number 80. The average flight altitude is chosen as the altitude and the corresponding flight level is calculated and used to show the contrail potential coverage at that level.

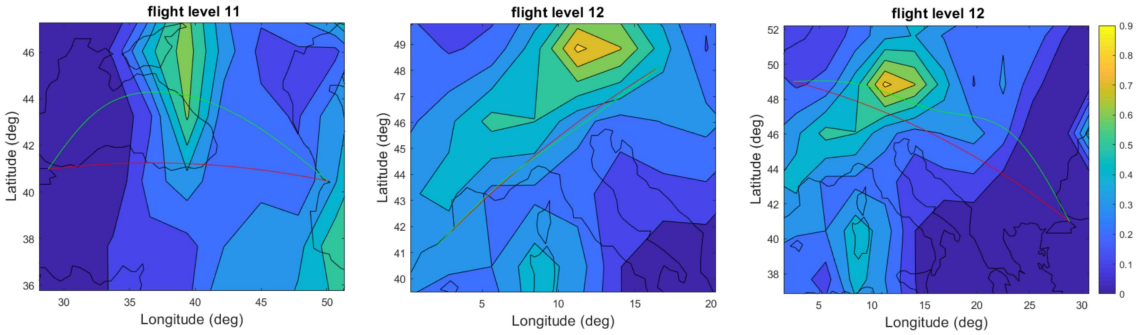

Figure 4.6: Average contrail potential coverage of three most impactful climate optimized trajectories (5, 27, 80) with negative climate impact on January 30^{th}

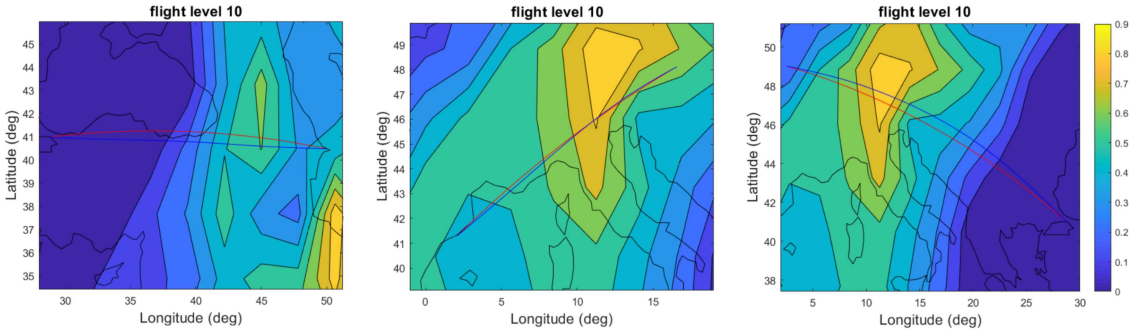

Figure 4.7: Average contrail potential coverage of three most impactful cost optimized trajectories (5, 27, 80) with negative climate impact on January 30^{th}

Looking at figures 4.6 and 4.7, it does not become apparent that the contrail potential coverage of climate optimized flights is larger than that of the cost optimized trajectories. However, the climate optimized trajectories are often directed more towards climate sensitive regions which increases the climate impact of the trajectories. For instance, it would be expected that trajectory one in figure 4.6 has a southbound offset from the great circle trajectory but instead it is located entirely north of the great circle trajectory.

The figures that contain the contrail potential coverage show an average contrail potential coverage over the past 24 hours. Since contrail potential coverage is highly volatile, it has the tendency to change quickly over a short period of time. For this reason, it is possible that the contrail potential coverage is higher for the climate optimized trajectory while it does not show in figures 4.6 and 4.7.

4.2 Positive Climate Impact

Similar to the days with a high negative impact, the day with the largest positive impact will be analyzed as well to get a better understanding as to how or why the global minimum is achieved (or at least a better climate optimized trajectory than the cost optimized trajectory) on those days. The day with the largest positive climate impact is day 133. Just like the days which have a high negative climate impact, the positive days are spread out over the analysis domain. Therefore, whether or not the model is able to find a global minimum is not strongly affected by the season.

Similar to figure 4.4, the day with the highest positive climate impact can also be captured which is shown in figure 4.8. The highest positive climate impact is achieved on May 12^{th} 2016. The figure shows some flights with a negative climate impact (red line) meaning that the optimization towards climate impact reduction did not find a global optimum for all flights.

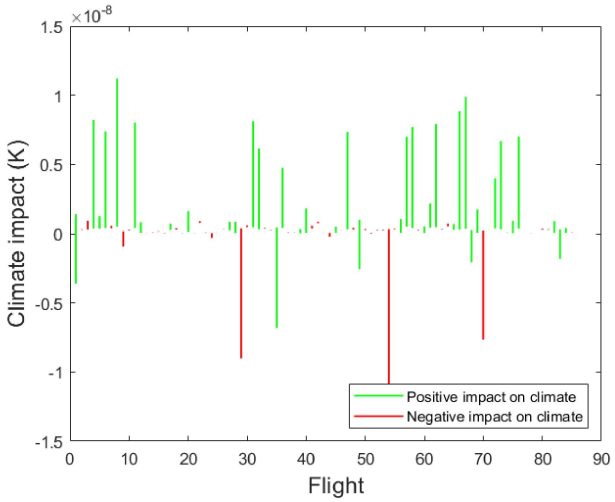

Figure 4.8: Difference in climate impact between each cost and climate optimized trajectory on May 12^{th}

The days with the highest negative climate impact showed that it was always the difference in contrail potential coverage between the two flight types that resulted in a large difference between climate impact of the cost and climate optimized trajectories. January 30^{th} shows that the negative climate impact also obtains values larger than zero (red line above zero), meaning that the contrail potential coverage of the climate optimized trajectories is above zero. For May 12^{th}, the climate impact of

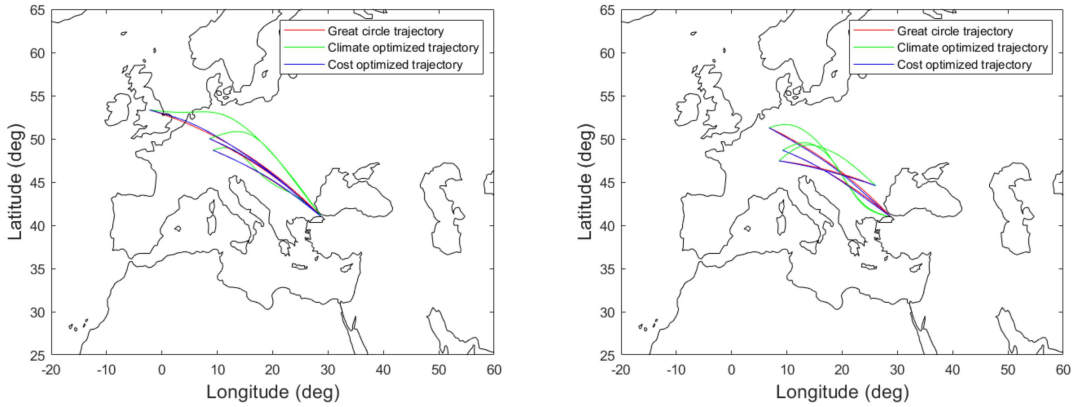

(a) Positive impact on climate **(b)** Negative impact on climate

Figure 4.9: Flight locations of the flights with the most positive and negative climate impact

the climate optimized trajectories never obtained a value above zero. The red lines shown in figure 4.8 are only a result of the other emitted species which result in a small negative climate impact, or because the contrail potential coverage of the cost optimized trajectories has a sequential reduction of the atmospheric temperature.

The most impactful trajectories shown in figure 4.8 are flight numbers 8, 66 and 67 (highest positive impact), and flight numbers 29, 54 and 70 (highest negative impact). All climate optimized flights have a zero contrail climate impact and the sign of the impact is determined by the contrail potential coverage of the cost optimized flights. Furthermore, the three flights with the highest positive climate impact are all flying eastbound while the three flights with the highest negative climate impact all have a westbound flight direction. All flights are located in the central part of Europe as shown in figure 4.9.

The contributions of each individual species for both, the flights with the highest positive and negative climate impact are shown in figure 4.10 and confirms the dominance of the contrail potential coverage on the overall climate impact. The figure also shows that when the contrail potential coverage is disregarded, the climate impact of the cost optimized trajectories is almost always less (84 out of 85 flights) than that of the climate optimized trajectories. This is a result of the additional fuel consumption due to the extended flight distance of the climate optimized flights. However, this means that the optimization module most likely, strictly aims at optimizing the climate impact of the contrail potential coverage. Since the contrail potential coverage of quite some cost optimized flights is also zero, the overall climate impact of the climate optimized flights is larger.

All positive green lines shown in figure 4.8, show that there are contrails produced by the cost optimized flights which have a temperature increase as a result. However, the negative red lines shown in the same figure and in figure 4.4 show that the cost optimized flights are able to use the production of contrails to their advantage by reducing the average atmospheric temperature. This is coincidental, because the trajectories are not optimized to avoid contrails or use contrails to their advantage. How-

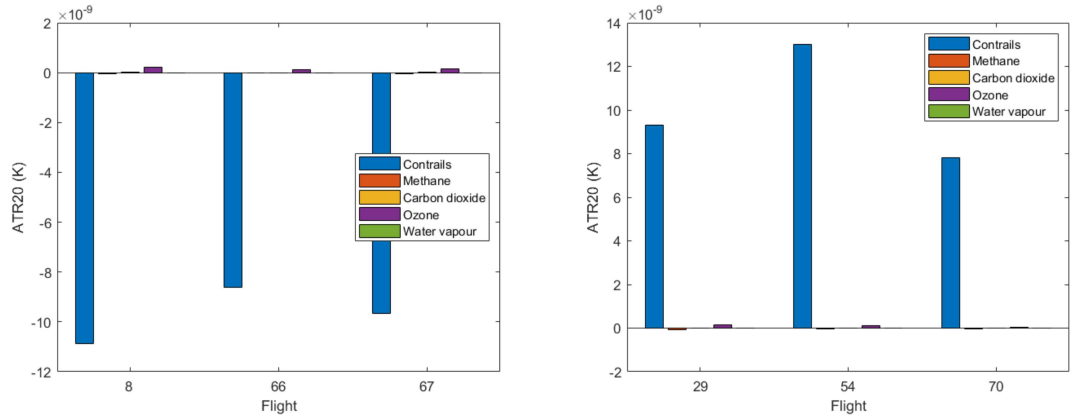

(a) Positive impact on climate **(b)** Negative impact on climate

Figure 4.10: Difference in climate impact between each species of the cost and climate optimized trajectory on May 12^{th}

ever, the climate optimized flights often are not able to fly a trajectory which has a similar climate impact or less.

4.3 Analysis of Single Flights

The flights can also be analyzed over a period of time which may give an insight on certain flights which have a more negative overall climate impact. Figure 4.11 shows the average difference in climate impact between each cost and climate optimized trajectory during the analysis period of six months. The figure shows that there are six trajectories which on average contribute to a negative climate impact. Five of these trajectories have a relatively small negative impact while flight number 42 has a fairly high negative impact. Flight number 42 is a flight between Trondheim (Norway) and Gran Canaria (Spain) which is considered as a southern flight. This flight is also responsible for a negative climate impact on the 23^{th} of March which is shown in figure A.3 in appendix A. The main reason for the negative climate impact of the route is caused by contrail potential coverage, which on average results in a high negative impact on the climate for the climate optimized flight, while for the cost optimized trajectory, the climate impact is also positive but has a lower magnitude.

The high negative climate impact of flight 42 can be explained by the geographical location of the flight. The flight has its starting point just south of the boundary between the Hadley and the Ferrel Cell. This is an area where there is a downward motion of the air. It is possible that the simulation model has trouble modelling the climate impact of each species in this area, which does not allow the simulation model to converge to a global optimum within the maximum number of iterations. Analysis of the climate impact during the flight shows that on average, the part of the flight around the boundary of the two cells has more influence on the difference between the cost and climate optimized climate impact. A similar flight (flying in opposite direction) from Stockholm (Sweden)

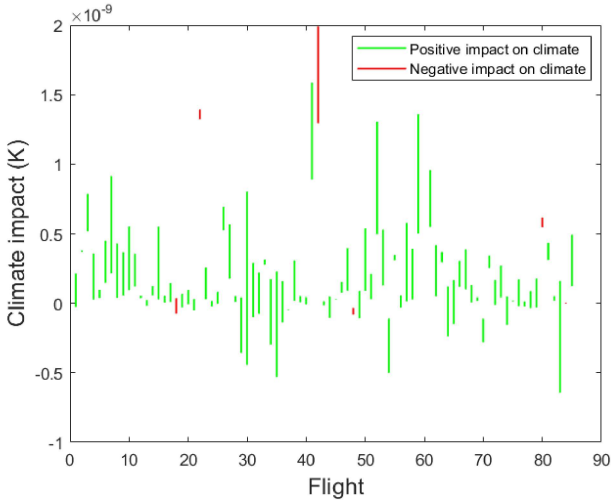

Figure 4.11: Difference in average climate impact between the cost and climate optimized trajectories over a period of six months

to Gran Canaria (Spain) also often fails to find a global optimum, which amplifies the hypothesis of atmospheric dynamics playing a role. It can also be illustrated by figure 4.12.

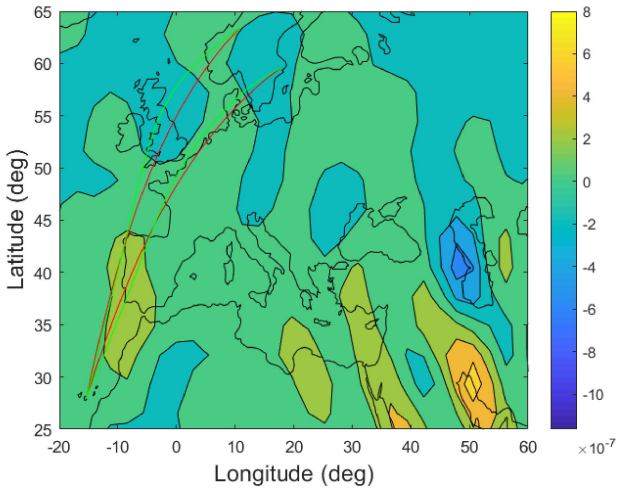

Figure 4.12: The average vertical wind speed (m/s) at an altitude of approximately eleven kilometers

Figure 4.12 shows the average vertical wind speed over a period of six months where there is a devia-

tion from zero along the two flight paths in a region covering Portugal and further south. This could possibly explain the failure of the model to find a global minimum. There are more regions which show vertical wind speed, but there are not many flights operating in these regions.

Not only the trajectories with a high negative climate impact can give an insight in the optimization procedure, but also the trajectories with a high positive climate impact can be useful. Therefore, the trajectory with the highest average positive climate impact will be evaluated. The flight with the highest positive climate impact is flight number 30. It is a flight originating from Gran Canaria (Spain) flying to Stockholm (Sweden).

It is interesting to notice that the flight with highest negative climate impact is similar to the flight with the highest positive climate impact. Furthermore, a flight which also often results in a negative climate impact is the same flight but in opposite direction as the flight with the highest positive climate impact. It is found that the climate impact of flight number 30 and 42 are dominated by a few days which either result in a large positive or a large negative climate impact.

If all flights over a period of six months are considered, there are 15470 flights which are simulated and optimized towards both cost and climate optimum. To establish how well the EMAC model optimizes the flights, the difference in climate impact and operating costs between the cost and climate optimized flights of each day are considered. This is shown in figure 4.13b. It shows the number of occurrences for each day where the climate impact of the cost optimized trajectories is lower (red line) and also each day where the operating costs of the climate optimized trajectories are lower than the operating costs of the cost optimized routes.

The values in figure 4.13a can take values up to 85 meaning that on that particular day, the climate impact of every cost optimized flight is lower than the same climate optimized flight. The figure shows that as expected, the number of occurrences where the cost optimized trajectories are not optimized correctly is significantly lower than the number of occurrences where the climate optimized trajectories are not optimized correctly. A correlation test shows that there is no correlation (probability >0.05) between the frequencies of the operating costs and climate impact on each day.

The number of occurrences where the climate optimized flights are not optimized properly are more than 57 out of 85 on average. This would suggest that more than half of the days have a higher climate impact of the climate optimized flights than of the cost optimized flights. This is, however, not the case since a large number of occurrences only have a small difference, while many of the climate optimized flights which have a lower climate impact show a large difference due to the difference in contrail potential coverage.

The maximum number of occurrences for the operating costs on a single day is twelve and the average is approximately 2. This suggests that the optimization towards reducing the operating costs is less complex than the optimization towards climate impact and therefore the number of occurrences where the optimization fails is reduced. There are 70 days for which all cost optimized flights have lower operating costs than the same climate optimized flights. Finally, there is no day where the overall operating costs of the cost optimized trajectories are higher than that of the climate optimized routes.

Figure 4.13b shows the minimum number of times the algorithm does not reach a global optimum per

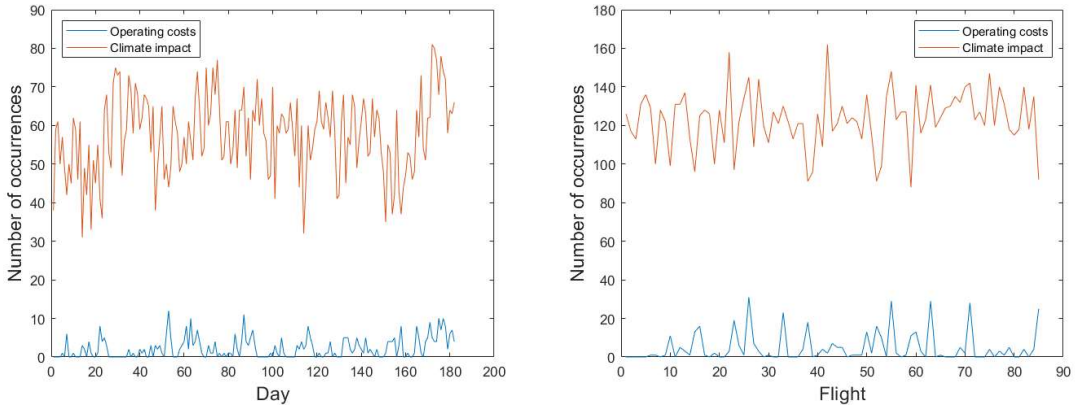

(a) Number of occurrences sorted by day

(b) Number of occurrences sorted by flight

Figure 4.13: Number of occurrences, where on the one hand the climate impact of the climate optimized trajectories is higher than the climate impact of the cost optimized trajectories and on the other hand, the number of occurrences, where the operating costs of the cost optimized trajectories are higher than the operating costs of the climate optimized trajectories (sorted by day and by flight number)

flight. This is analyzed to find out if there are certain flights for which the optimization fails more often than for other flights. A correlation test provides evidence that there is no correlation between the number of occurrences for each flight. Similar to figure 4.13a the number of occurrences where the climate optimization fails is significantly larger than the number of occurrences where the cost optimization fails. The maximum number of occurrences that can be obtained is 182 because that is the number of simulation days.

There are no salient outliers for both the operating costs and the climate impact but there are flights which show a higher frequency than other flights. The geographical locations of the flights with the highest number of occurrences are shown in figure 4.14. The flights in figures 4.14a and 4.14b occur mostly in the south-eastern part of Europe. This is in line with the results found earlier for the flight with the highest difference in climate impact between cost and climate optimum both positive and negative. Therefore, it is expected that due to weather conditions which include wind, temperature and humidity, the EMAC model is not able to converge to a global optimum within the predefined number of iterations.

On a final note, out of the 15470 flights which are analyzed, 7827 flights have a contrail potential coverage climate impact of zero for both the cost and climate optimized trajectories. However, only 516 of these flights have a lower climate impact for the climate optimized trajectories than for the cost optimized trajectories. This shows that the optimization module strictly aims at reducing the contrail potential coverage, therefore increasing the flight distance and as a result, the climate impact of the other species is increased often resulting in a larger overall climate impact.

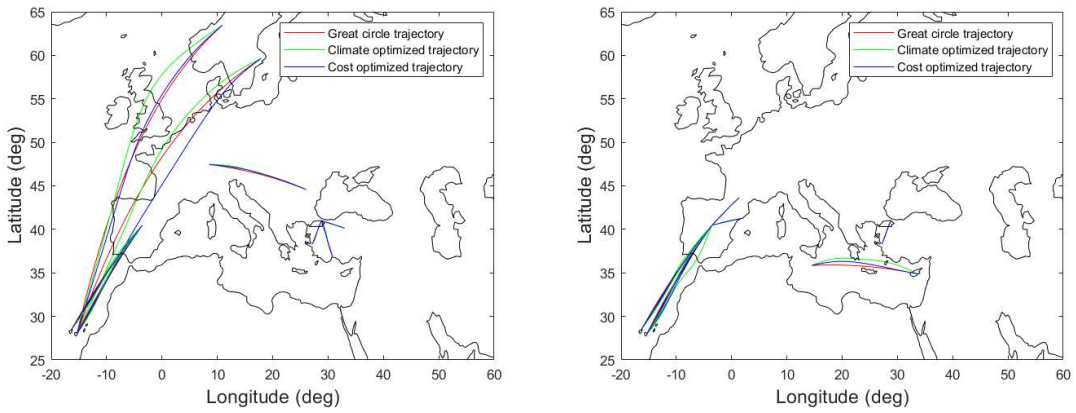

(a) Climate optimized flights **(b)** Cost optimized flights

Figure 4.14: The geographical locations of the flights with the highest failed optimization frequency

5 Analysis Description Using a Case Study

The results obtained from the EMAC model are analyzed to find the variability of the trajectories over the simulation period of six months. In the following chapter the processing and analysis of the data will be explained by means of a case study using a single city pair evaluated for three different trajectories. These trajectories are the great circle trajectory and, the climate and cost optimized trajectories.

In order to find the variability of the trajectories during the analysis, the trajectories are divided into four different groups which all define a certain flight direction (north, east, south, west). Each city pair requires the aircraft to ultimately go into a certain direction. The great circle route between two airports determines the flight direction of each flight where a flight angle of zero degrees is a flight in eastern direction and a flight angle of 180 degrees defines a flight in a western direction. This is illustrated by figure 5.1. Each flight direction takes up 90 degrees of the total 360 degrees domain. The flight departs from the red dot in the center and the arrival airport determines in which corridor the flight is placed.

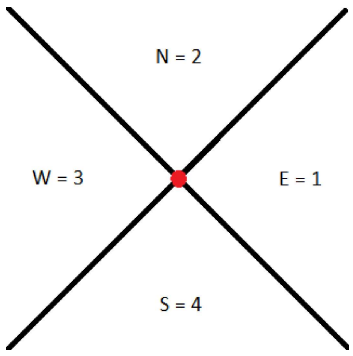

Figure 5.1: Four corridors used to split the flight trajectories into different flight directions

The trajectory of the flight that will be analyzed during the case study has a flight angle of 180.9 degrees which means that the aircraft is flying westbound. This also means that the flight is considered to be in the third group which consists of every flight between a northwestern and the southwestern flight direction.

5.1 Flight Characteristics

Figure 5.2a shows the great circle trajectory which is represented by the red line and it shows that the climate optimized and the cost optimized trajectory are both located exclusively north of the great circle trajectory. Furthermore, figure 5.2b shows the altitude of the aircraft during the flight. What becomes apparent right away, is that the initial and final altitude of the great circle trajectory is different compared to the initial and final altitude of the climate and cost optimized trajectories. Even though the initial and final altitude of the cost optimized trajectory is lower in altitude, the average altitude is of higher magnitude. For this particular trajectory, the climate optimized route

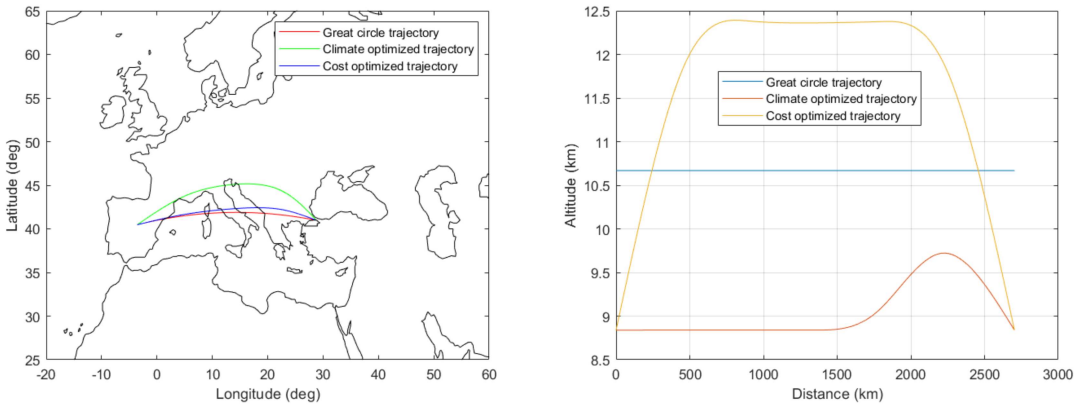

(a) Horizontal trajectory for three flight types

(b) Altitude for three flight types

Figure 5.2: Flight path and altitude for a flight between Istanbul and Madrid on January first 2016

has a lower average altitude but the altitude is different for different days.

The climate impact and fuel consumption during the flight are shown in figure 5.3. Figure 5.3a shows the average temperature response that is a result of the flight between Istanbul and Madrid. The magnitude of the average temperature response shows the climate impact of the aircraft between two consecutive measurement points (waypoints). Figure 5.3b shows the fuel used between two consecutive measurement points. The area under the curve does in this case not represent the total fuel consumption of the aircraft engines because the flight time or distance between two consecutive waypoints changes during the flight.

The average temperature response due to the flight compares rather well to the change in fuel consumption during the flight. The patterns for the climate optimized trajectory look very similar as well as for the other two trajectories. To test whether two similar series in fact show similarity, a correlation test can be performed on the data. A test which works well to detect a correlation between two series of equal length, is the linear or rank correlation. Spearman's rank correlation is a type of correlation which is non-parametric, so it does not assume any type of distribution. The correlation test returns the probability of the hypothesis being true which is a hypothesis of no correlation. The correlation test rejects the null hypothesis (probability <0.001) of no correlation between the average temperature response and the fuel consumption for all three trajectories. This means that it is almost certain that there is a correlation between the fuel consumption and the climate impact of the flight.

5.2 Trajectory Comparison

In order to find the difference between each aircraft route, the trajectories need to be compared. This is done for the horizontal flight path, altitude, climate impact and operating costs of the aircraft trajectory. The geographic coordinate system does not have an equal spacing between each degree

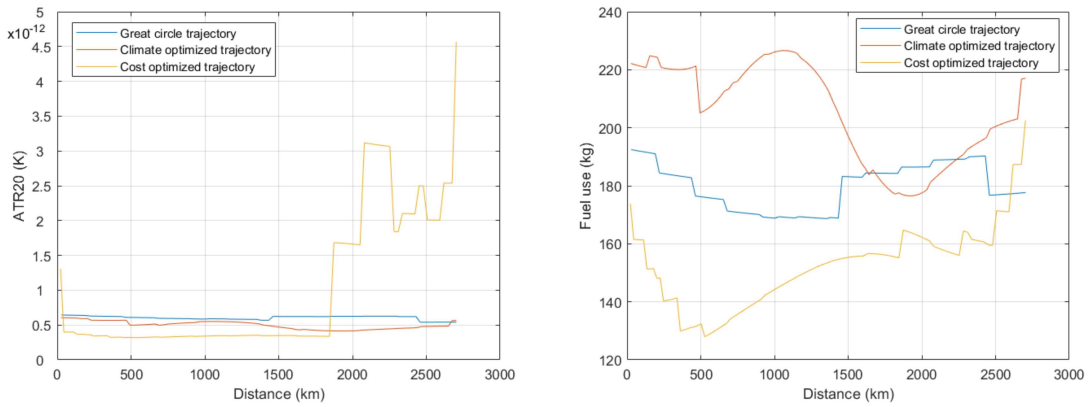

(a) Average temperature response for three flight types

(b) Fuel use for three flight types

Figure 5.3: Average temperature response and fuel use between two consecutive measurement points for a flight between Istanbul and Madrid on January first 2016

of longitude. The distance between each degree of latitude remains approximately the same. If the latitude increases which is the case when moving towards the poles, the distance between two consecutive longitude degrees decreases.

In order to be able to compare equal segments of each flight, the geographic coordinate system should be transformed to a Cartesian coordinate system where every coordinate comprises of three values which indicate the distance from that point towards the center of the earth. This coordinate system can be used to divide the great circle trajectory into equally spaced segments. To give an example of a trajectory which is split into multiple segments, figure 5.4 shows the division of segments of the flight between Istanbul and Madrid.

Figure 5.4 shows the cyan colored segments placed perpendicular to the great circle trajectory. The trajectory is divided into ten equally divided segments over the length of the great circle trajectory. Similar to the trajectory shown in figure 5.2a, the arrival airport is located at a negative x-coordinate. This is a result of Madrid being located west of the prime meridian which is located at x = 0 in the Cartesian coordinate system.

To accurately compare the three trajectories, the same segments should be compared and not every individual point. To illustrate this, as an example the climate optimized flight trajectory is rerouted very far south on the first half of the flight and closely follows the great circle trajectory on the second half of the flight. The rerouted climate optimized trajectory contains more than 50% of its points in the first half of the great circle flight. Therefore, if every individual point is examined between the two flights, two points at two completely different geographical locations may be compared. To prevent this, it is chosen to compare segments perpendicular to the great circle trajectory. The segment divisions are planes in a 3D coordinate system where every plane intersects with the center of the earth.

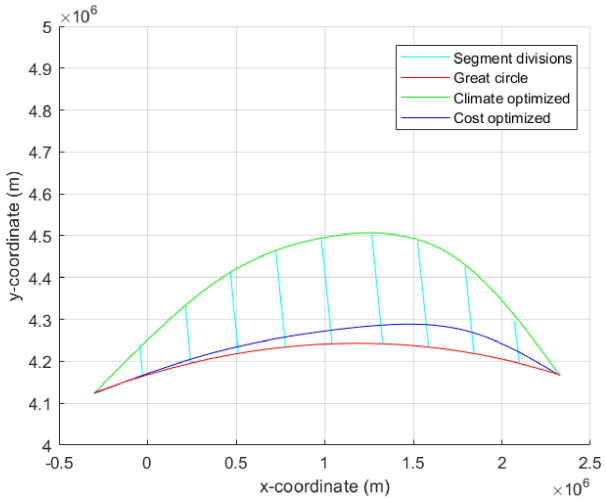

Figure 5.4: Distribution of the flight into equally spaced segments perpendicular to the great circle flight

Whenever the horizontal offset between two trajectories is compared, the offset in only one direction will be measured. For a flight in the first or third corridor (east or west) it is interesting to know the offset in a northern or southern direction. In order to be able to know the offset in a certain direction, the geographic coordinate system is required. The lateral offset of a north- or southbound flights is compared for 100 points which are equally divided between the longitudinal start and end coordinates (and lateral for the north/southbound flights) of the trajectory.

The offset of the cost and climate optimized trajectories from the great circle trajectories will be evaluated in two different fashions. The average offset shows how far on average, the trajectory is offset from the great circle trajectory. However, when the trajectory is evenly located above as below the great circle trajectory, the average offset is zero. Therefore, the absolute average offset of each trajectory will also be computed. This is the average offset at each waypoint, but independent of direction in which the trajectory is offset, the value will always be positive. This can be illustrated by an example which is shown in figure 5.5.

Figure 5.5 shows a great circle trajectory indicated by the blue line and two example trajectories. The average offset of the first optimized trajectory is zero because it has the same area under the curve above and below the great circle trajectory. The second optimized trajectory has a positive offset since the entire flight is located above the great circle trajectory. From these results, it would be concluded that the first trajectory has no offset and that the second trajectory has a positive offset. This does not represent the full pattern. Therefore, the absolute offset is also taken into account. The first optimized trajectory has a large absolute offset while the second trajectory has the same absolute offset as the average offset. The two types of offset can be used to draw conclusions without having to see a figure of each individual trajectory. For instance, the results show that the first optimized

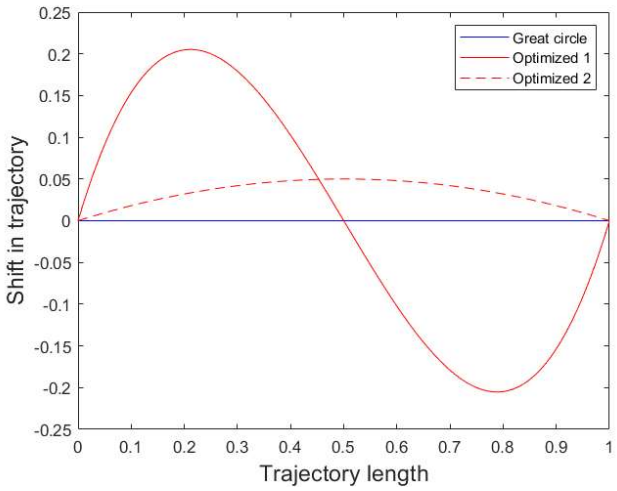

Figure 5.5: Two sample trajectories showing different offset patterns from the great circle trajectory

trajectory has a large offset which is equally located both above and below the great circle trajectory. The second trajectory has a fairly small offset, but it is always flying above the great circle trajectory.

It is important to know the flight direction to determine in which direction the offset is measured (lateral on longitudinal). Therefore, the direction of flight is considered and a positive offset is considered an offset in northern direction for flights flying in a western or eastern direction. For north- and southbound flights, offset in an eastern direction is considered positive.

For the current example, the average and absolute average offset are similar since both the climate and cost optimized trajectories are always north of the great circle trajectory. The average geographical offset can be calculated for both trajectories compared to the great circle trajectory and the results are shown in table 5.1. The table also shows the average height offset of both trajectories.

Table 5.1: Offset between the great circle, and the climate and cost optimized trajectories

	Climate optimized	**Cost optimized**
Ave. geographical offset	2.14 deg	0.30 deg
Ave. height offset	-1619.2 m	984.5 m

The average geographical offset of the climate optimized trajectory is more than the average offset of the cost optimized trajectory which resembles the flight trajectories shown in figure 5.2a. However, the average altitude of the climate optimized flights is far below the great circle flights while the altitude of the cost optimized flights is far above.

The climate impact of each trajectory is given in table 5.2. It is calculated by the summation of the

climate impact at each way point. As expected, the climate optimized trajectory results in the lowest climate impact and although the cost optimized trajectory uses the least amount of fuel as can be seen in figure 5.3b, the impact of its trajectory is the largest.

Table 5.2: Total climate impact of the three trajectory types

	Climate impact (K)
Great circle	$6.04 \cdot 10^{-10}$
Climate optimized	$4.97 \cdot 10^{-10}$
Cost optimized	$9.56 \cdot 10^{-10}$

The climate impact of the flight between Istanbul and Madrid is computed for thirty days, for every individual species and the total average temperature response, the difference in impact between the climate optimized and great circle trajectory are compared. The results of this analysis are shown in figure 5.6. In this example, the total average temperature response is sometimes negative while it would be expected to have a positive temperature response because the climate impact of the climate optimized flight is subtracted from the great circle flight. This implies that the climate impact of the great circle trajectory is sometimes smaller for the chosen time frame and airport pair. A negative ATR20 for days 2, 23 and 24 are possibly a result of the initial and final altitude difference between the two trajectories assuming that the optimization model is working correctly. However, chapter 4 already revealed that the optimization module is not always working correctly.

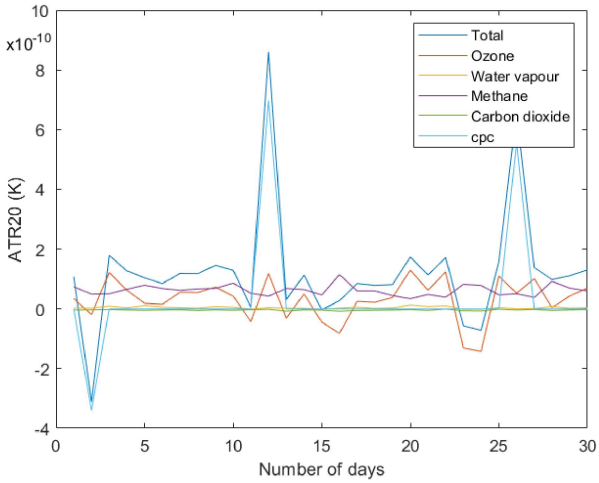

Figure 5.6: Difference between climate impact of the climate optimized trajectory compared to the great circle trajectory for thirty days

Figure 5.6 shows the total climate impact difference but also the contribution to global warming of every individual species that are emitted or react with species from the engine exhaust. The figure

shows that the total climate impact difference is dominated by the contrail potential coverage and that the difference in carbon dioxide and water vapour impact is small compared to the impact of the other species. The impact of methane is larger for the great circle trajectory and the impact of ozone depends on the day but on average is larger for the great circle trajectory as well. There are a few days with a large difference in climate impact. The difference is mainly caused by the difference in contrail potential coverage, which if used correctly, can reduce the climate impact to a large extend

Flights are also classified by the way the optimized trajectory is offset from the great circle trajectory in the horizontal plane. A trajectory can be classified into five different groups. The first group contains flights which only have positive offset. This means that a flight which is flying from east to west or from west to east, only has its offset in northern direction. Flights that fly from north to south or south to north can only have an offset in eastern direction. The second group contains flights which only have a negative offset. The third group contains flights that initially have a positive offset and cross the great circle trajectory once towards a negative offset. The fourth group is similar but initially has an offset in negative direction and crosses towards a positive offset and the fifth group contains any flight which is not in one of the first four groups. The five groups are also shown in figure 5.7. For the current example, both, the climate and cost optimized trajectories are located in the first group. The group distribution can give an insight in the flight pattern compared to the great circle trajectory.

The example flight for which the climate impact is measured for thirty days can also be classified for every day to find out if there are any trends in the offset pattern. The results of the analysis are shown in figure 5.8a. The figure shows that approximately 53 percent of the flights is situated in group one, which means that 53 percent of the flights is solely going north of the great circle trajectory. The other groups only contain up to a maximum of about 17 percent of the flights. From these results it can be noted that the climate optimized trajectory is dominantly located north of the great circle trajectory. The classification of the cost optimized trajectories displayed in figure 5.8b, shows an even more evident result where sixty percent of the flights is located in group one. Almost two third of the flights, fly north of the great circle trajectory. This indicates that there is a discernible pattern present. However, this study aims at finding patterns generalized for a flight direction so this result alone will not be used to draw conclusions. The results for all flight paths traveling in the same flight corridor will be discussed in chapter 6.

5.3 Influence of Atmospheric Properties on the Trajectory

After establishing the offset, it is required to find out what causes the optimized trajectories to fly a different route compared to the great circle trajectories. Influencing parameters include wind, air temperature, humidity which increases the potential contrail coverage and pressure at each altitude and geographical location.

To illustrate the effect of an atmospheric property on the climate optimized trajectory, the effect of the average atmospheric temperature on the average flight altitude is shown in figure 5.9. The linear trend in the data series is demonstrated by the yellow line and shows that there potentially is a positive trend between the altitude and temperature. This can also be tested by a correlation test. The correlation test shows a probability of no correlation which is smaller than 0.1%. This means that there is a high chance of correlation between the flight altitude and the atmospheric temperature.

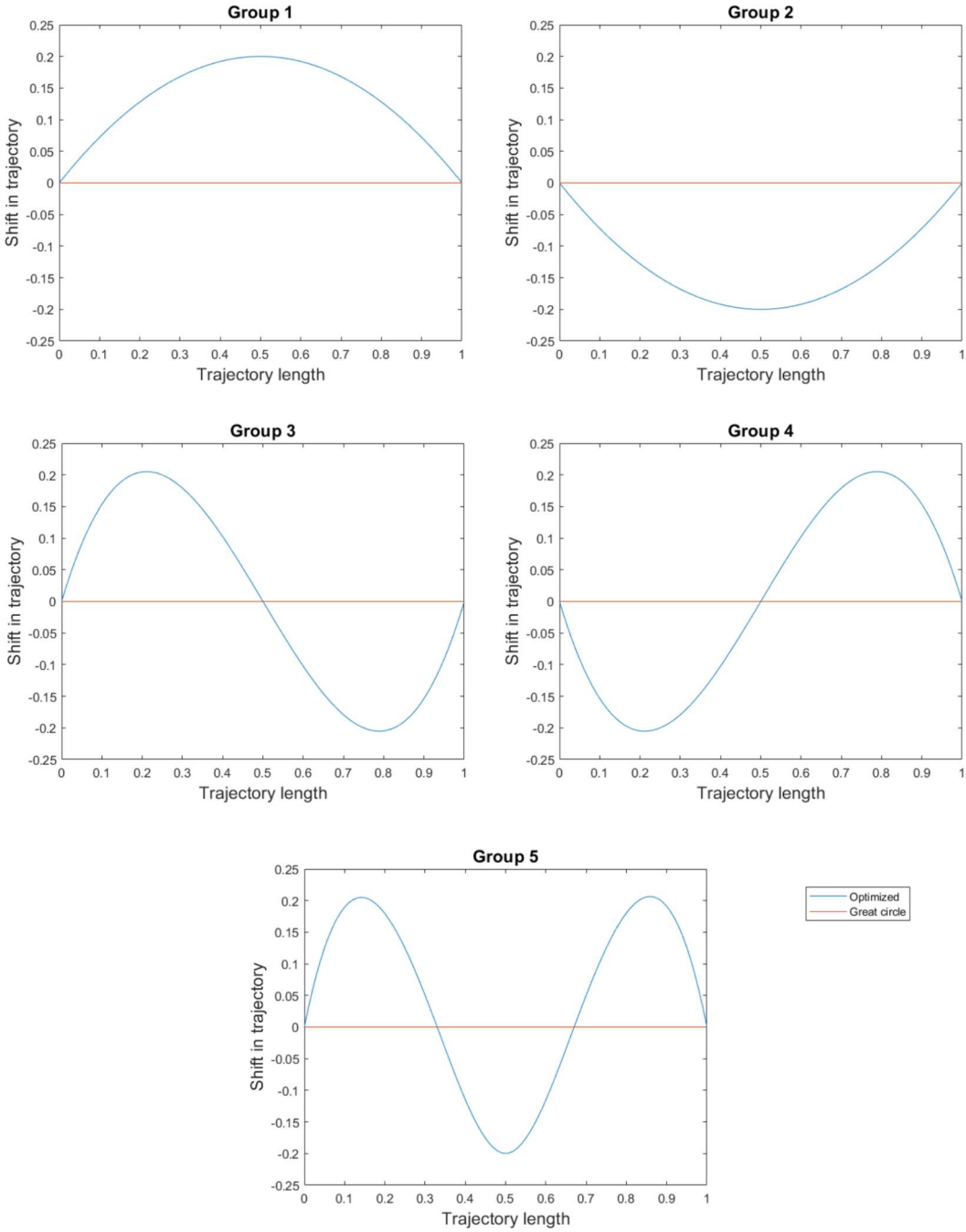

Figure 5.7: Classification of the optimized trajectories into five different groups

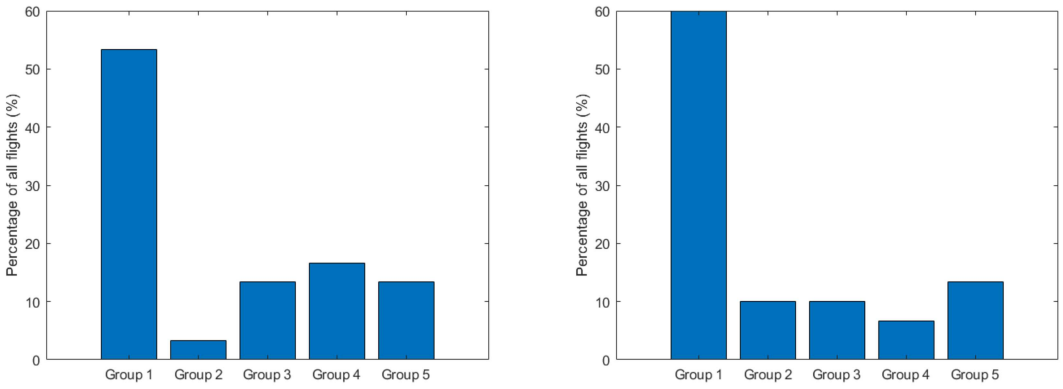

(a) Climate optimized trajectories **(b)** Cost optimized trajectories

Figure 5.8: Analysis of the offset type for 30 days of climate and cost optimized flights between Istanbul and Madrid

The effect that the atmosphere has on the aircraft trajectory and performance of the aircraft will be further discussed in chapter 6.

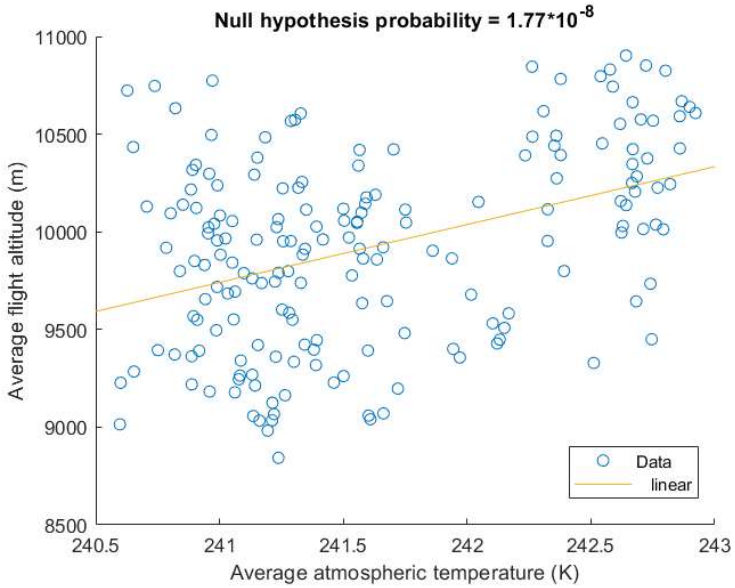

Figure 5.9: Correlation between the average atmospheric temperature and the average flight altitude of the flight between Istanbul and Madrid

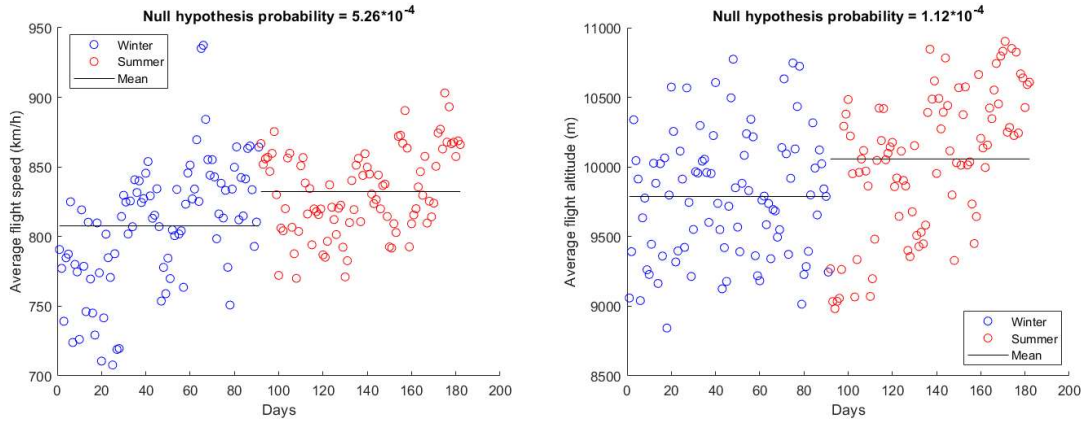

(a) Average flight speed **(b)** Average flight altitude

Figure 5.10: Average flight speed and altitude over a period of six months for a flight between Istanbul and Madrid

5.4 Seasonal Effect

To determine whether the season has any significant impact on the flight trajectory and the climate impact of the European flights, the data of the first three months (January, February, March) of 2016 is compared to the data of the second three months (April, May, June) of the same year. The first three months of the year can be seen as the winter season and the second three months can be seen as the summer season. To determine if there is a significant difference between the seasons, a statistical test can be used called the Wilcoxon rank sum test.

The Wilcoxon rank sum test or also called the Mann-Whitney U-test is a test which determines whether or not two samples of data come from a continuous distribution with the same median. Similar to the Spearman's correlation test, the test is a non parametric test which can be used as an alternative for the student's t-test when the data series is not normally distributed. However, the test is weaker than the student's t-test. The test can be used to examine whether for instance the offset of climate optimized trajectories from the great circle trajectories show a significant difference in offset for different flight directions. The test also indicates a test decision to determine if the null hypothesis is rejected or not. The significance level of the test is 5%, which is often used as the significance level since it is seen as the best trade-off between reducing the type I and type II errors. A type I error indicates the rejection of the null hypothesis while in fact the hypothesis is true and a type II error indicates the failure of rejecting the null hypothesis while in fact the hypothesis is false.

To illustrate what effect a season can have on a flight path and its flight characteristics, the average flight speed and altitude of the trajectory between Istanbul and Madrid are evaluated over a period of 182 days. This includes six months starting from January first until June thirtieth 2016. In this time period, the two seasons are analyzed. The results of this analysis are shown in figure 5.10.

Figure 5.10a shows the average flight speed each time the aircraft flies from Istanbul to Madrid for 182 consecutive days. The first season is shown by the blue circles which is named the winter season and the summer season is displayed by the red circles. A similar graph for the average flight altitude is shown in figure 5.10b. The mean of each season is shown by the black lines and clearly shows a difference between the two seasons. To find out if this difference is significant, the null hypothesis states that the data of both seasons come from a continuous distribution with the same median. The probability of both the flight speed and altitude is below the 5% threshold which means that for both data sets, the null hypothesis is rejected and it is therefore concluded that there is indeed a significant difference between the winter and the summer season. Figures 5.10a and 5.10b seem to be similar to each other and therefore it could be expected that there is correlation between the average flight speed and the altitude. However, using a correlation test explained in 5.1, the probability of no correlation is 38%. This value is higher than the threshold value and therefore the null hypothesis (that there is no correlation) is not rejected.

This chapter has shown the strategy that is used to analyze the flight patterns of the cost and climate optimized trajectories. The effect of the season and the flight direction on the other flights will be discussed in chapter 6.

6 Analysis of the Simulation Results

This chapter discusses the analysis of the EMAC model simulation performed for two different optimization strategies. The optimization strategies optimize towards operating costs and climate impact. The resulting trajectories are compared to the great circle trajectory of each city pair that is analyzed. The analysis is done to find general patterns in the European flight trajectories and to establish the differences between the cost and climate optimized flights.

The great circle trajectories between each city pair can be shown on a map of Europe which is shown by figure 6.1. The red colored line shows the great circle trajectory of every flight that is analyzed. The analysis also includes flights between the same city pairs but in opposite direction and therefore less than 85 lines are shown on the map in figure 6.1.

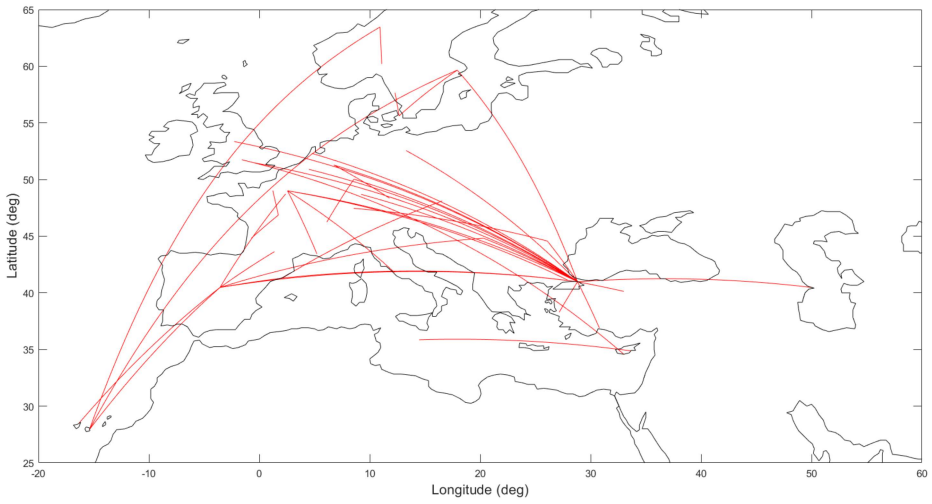

Figure 6.1: Great circle trajectories of 85 flights covering different flight directions and areas of the European airspace

For each of the 85 flights, the great circle trajectory is computed as well as the flight path found when the trajectory is optimized towards reducing the operating costs and climate impact. The operating costs are composed of the fuel costs and the flight time, while the climate impact is measured as the average temperature response after twenty years (ATR20) due to the emission of gasses on the traveled trajectory. Some examples of great circle, climate optimized and cost optimized trajectories are shown for two different days, namely January first and June first of 2016. These trajectories are visualized in figures 6.2 and 6.3 respectively.

Figures 6.2 and 6.3 show that the great circle trajectory is exactly the same for both days while the cost and climate optimized trajectories often show completely different routes. The full set of

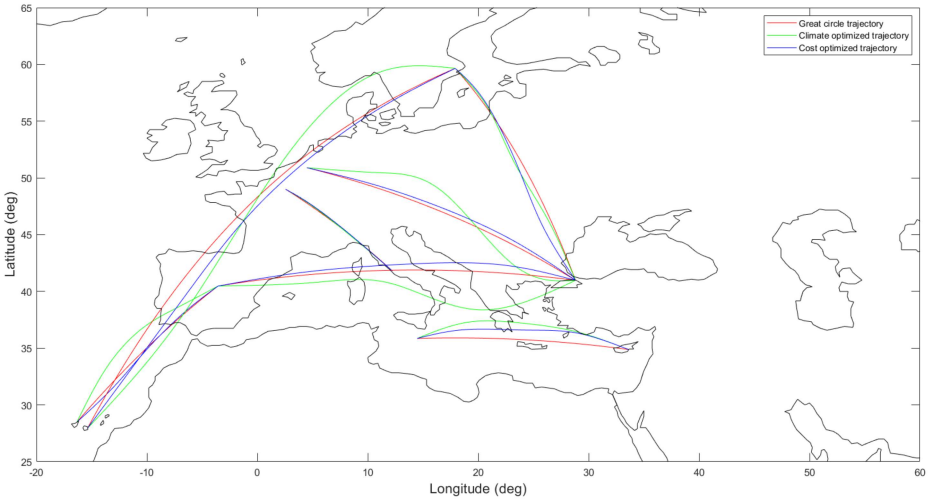

Figure 6.2: Example great circle, climate optimized and cost optimized trajectories on January first 2016

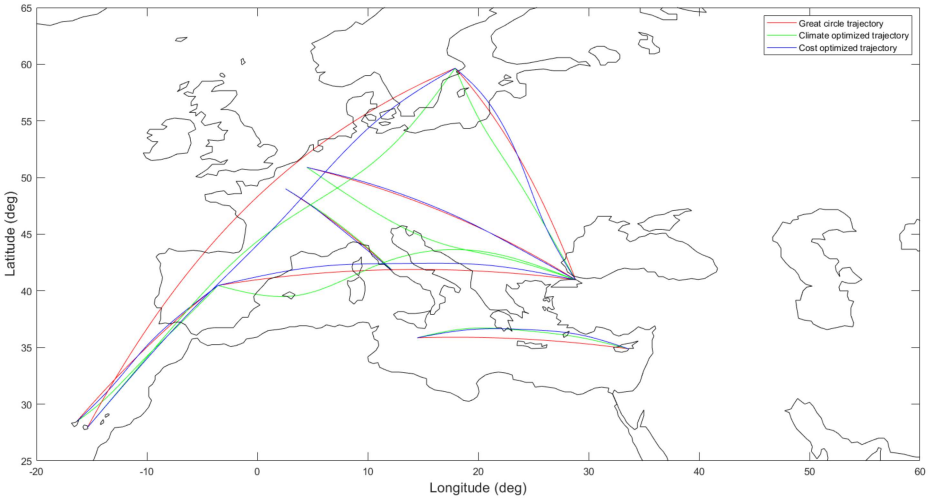

Figure 6.3: Example great circle, climate optimized and cost optimized trajectories on June first 2016

climate optimized flights is shown in figure B.1 and the cost optimized flights are shown in figure

B.2 in Appendix B. To find out if there are trends in the trajectories and emissions, the geographical location, altitude and emissions of the climate and cost optimized trajectories will be compared. Furthermore, the effect of the flight direction and a seasonal effect will be considered. The results of the analysis are discussed in this chapter.

6.1 General Results

Before the direction of flight and seasonal effect are examined, some general patterns of the flights and the atmospheric properties in the European airspace are discussed, where some general characteristics are shown in table 6.1. The table shows trajectory properties for three different flight types which are the great circle, cost optimized and climate optimized flights. Furthermore, the table also shows the atmospheric properties for three different flight altitudes corresponding to the average flight altitudes of the three different flight types.

Table 6.1: General flight and atmospheric properties of the cost and climate optimized, and great circle trajectories

	Great circle	**Climate optimized**	**Cost optimized**
Average flight length (km)	1572	1616	1576
Average altitude(m)	10668	9876	11647
Average flight speed (km/h)	855	863	855
Average flight time (hrs)	1.83	1.86	1.83
Average fuel use (kg)	7792	8540	7179
Total climate impact (K)	$3.63 * 10^{-6}$	$1.26 * 10^{-6}$	$4.74 * 10^{-6}$
Total operating cost ($)	$1.50 * 10^{8}$	$1.57 * 10^{8}$	$1.44 * 10^{8}$
	Flight level 11	**Flight level 12**	**Flight level 10**
Average wind speed (m/s)	21.2	19.8	22.2
Average wind direction (deg)	-1.0	-1.3	-0.45
Average relative humidity (%)	59.9	62.2	55.2
Average temperature (K)	215.5	219.8	212.3
Average CPC (%)	24.9	24.3	23.6

The flight characteristics are often dependent on the atmospheric properties and thus the atmospheric properties will be treated first. The flight level corresponding with the great circle trajectory is flight level 11. The climate optimized trajectories have a lower average flight altitude averaging a flight level of 12. The cost optimized flights have the highest average altitude at a flight level of 10. The corresponding atmospheric properties are elaborated upon in the next paragraphs.

The average wind speed increases with an increasing altitude. The average wind direction is similar for all three flight levels. It has an angle of approximately minus one degree where an angle of zero degrees corresponds to wind in an eastern direction. Wind in a southern direction corresponds to an angle of -90 degrees and wind in a northern direction is represented by a 90 degrees angle. Average wind in an eastern direction can have a direct effect on the required fuel and climate impact of the flights in all directions. This will be evaluated in section 6.5.

The relative humidity decreases with an increasing altitude which is also true for the average temperature of the atmosphere. Relative humidity describes when air is saturated with water, which happens at a relative humidity of 100%. The amount of water that can be held by air is dependent on the temperature and decreases when the temperature decreases. This means that at a higher altitude (where the temperature is lower) the air to water ratio is reduced. The relative humidity and the temperature determine the contrail potential coverage (CPC) at each location. It is expected that the contrail potential coverage, similar to the relative humidity and the temperature, increases with altitude. However, this happens up until a certain flight level after which the probability decreases. This is illustrated by figure 6.4, which shows the average contrail potential coverage for all 31 flight levels. The results are in line with the results found in the article by Frömming et al. (2011). This results in a lower average contrail potential coverage for cost optimized trajectories since the highest contrail potential coverage is reached at an altitude where all great circle flights are operating. However, due to the lack of mixing in the stratospheric region, the impact of the contrail formation may be higher due to an increased period of persisting contrails.

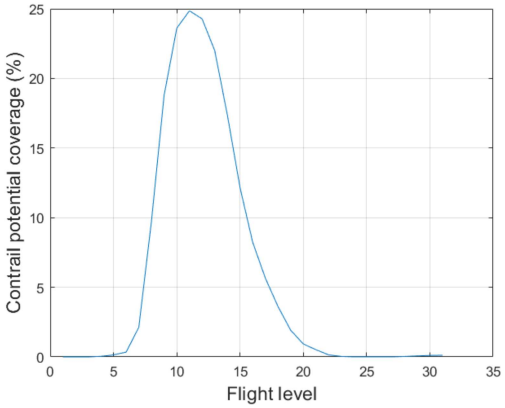

Figure 6.4: Average contrail potential coverage for 31 flight levels where flight level 1 corresponds to an altitude of 32 kilometers and flight level 31 is located at sea level

Table 6.1 shows that the average length of the great circle trajectories is the shortest and the climate optimized trajectories have the longest average travel distance. This is expected because a great circle trajectory is the shortest distance between two points on a sphere and a climate optimized trajectory avoids climate sensitive regions to reduce the climate impact and therefore increases its flight distance. The length of the cost optimized trajectories is 0.3% longer than the great circle trajectories and the climate optimized trajectories are 2.8% longer on average.

The climate optimized trajectories have the lowest average flight altitude while the cost optimized trajectories have the highest average altitude. The great circle trajectories have a constant flight altitude for every flight which is set at the value given in table 6.1. An increased flight altitude results in a more efficient aircraft because the air resistance is less, which allows for an increased flight speed. Increasing the flight speed increases the propulsive efficiency but this also results in a higher threshold

temperature for contrail formation, which means that there is an increased chance of contrail formation (Schumann, 2000). This results in a larger average climate impact at higher altitudes. Therefore, the flight altitude of the climate optimized trajectories is relatively low.

From the previous paragraph, it would be expected that the flight speed is higher as the altitude increases. However, the flight speed of the climate optimized trajectories has the largest magnitude and the average flight speed of the cost optimized and great circle flights have the same flight speed. The Mach number is constant throughout the flight which means that when the altitude increases the flight speed goes down because the speed of sound is lower at higher altitudes.

Chapter 4 describes the failure of the climate optimized trajectories to find a global minimum. An increased propulsive efficiency can be obtained by increasing the flight speed of the aircraft. However, this results in a higher contrail potential coverage probability which may have caused the EMAC model to find an optimum which has a larger climate impact than some of the cost optimized trajectories.

The flight time automatically follows from the combination of flight distance and speed. Even though the average flight speed of the climate optimized trajectories has the largest magnitude, the flight distance is substantially larger, which results in the longest average flight time for the climate optimized flights.

The fuel used during the flight is a function of the propulsive efficiency and the average flight distance. The propulsive efficiency is increased with altitude and flight speed. The climate optimized trajectories have a high average flight speed but also a long flight distance and a low average altitude. Therefore, the climate optimized trajectories have the largest average fuel consumption. The cost optimized trajectories have a high average altitude and a relatively low average flight length, while the flight speed is reduced only slightly compared to the climate optimized trajectories. This results in the lowest average fuel consumption for cost optimized flights. Even if the fuel consumption per kilometer is considered, the average fuel use is substantially larger than the flight distance for the climate optimized flights, which results in a lower fuel consumption for the cost optimized flights.

Finally, the climate impact and the operating costs of the trajectories are the variables that the climate and cost optimized trajectories are optimized for. As expected, the lowest total climate impact is obtained by the climate optimized flights. The climate impact of the climate optimized flights is approximately 73% lower than the climate impact of the cost optimized flights. The climate impact is driven by the impact of contrail potential coverage. Regions with high contrail potential coverage are attempted to be avoided by the climate optimized flights. The total operating costs are a function of the flight time and fuel consumption. These two variables are both minimized for the cost optimized flights and therefore these flights have the lowest operating costs. The total operating costs of the cost optimized flights are approximately 8% lower than the operating costs of the climate optimized trajectories.

6.1.1 Influence of the Latitude on Flights

The geographical location at which species are emitted plays in important role in the magnitude of climate impact. As an example, at flight level ten, the average contrail potential coverage over a

period of six months is given in figure 6.5. It shows that the average contrail potential coverage has an increased potential at higher latitudes. In southern Europe, the average potential contrail coverage is approximately 20%, while in the northern part of Europe, the average potential contrail coverage is around 30-35%. This results in a higher climate impact for flights which fly at the same altitude in the northern part of Europe.

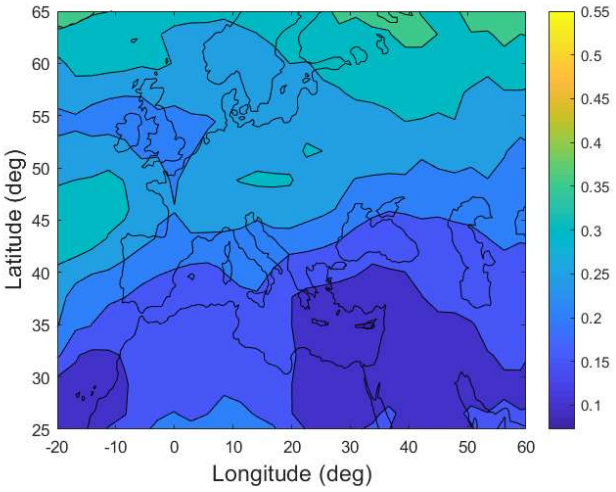

Figure 6.5: Average contrail potential coverage at flight level ten

This is accounted for by the climate optimized flights as the average flight altitude is reduced for higher latitude flights. The cost optimized flights are not affected by the increased contrail potential coverage. This is shown by figure 6.6 where each data point represents the average altitude of a waypoint over a period of six months.

The average altitude of the climate optimized flights is clearly decreasing as the latitude increases. This results in an average flight altitude of 11000 meters at a latitude of 33 degrees while at a latitude of approximately 60 degrees, the average altitude is reduced to about 9500 meters. Figure 6.6 only shows waypoints 20 until 80 of each flight, because the ascend from the initial altitude and descend to the final altitude are not representative of the average maximum altitude.

Because the flights account for the altitude, the climate impact is not affected as much because the contrail potential coverage is similar and the additional climate impact is obtained by the other species which have a lower magnitude.

6.1.2 Effect of the Departure time on the Climate

Studies into contrail formation have shown that depending on the type of contrail and the orientation of the contrails, the time of day affects the radiative forcing induced by these contrails. For instance,

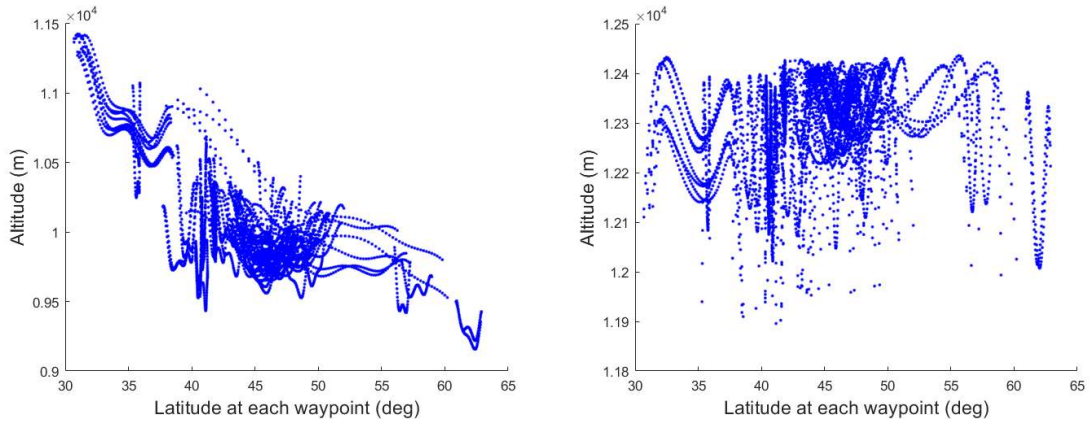

(a) Climate optimized **(b)** Cost optimized

Figure 6.6: Average altitude of each waypoint of the cost and climate optimized trajectories

it was found that persistent contrails always have a warming effect during the night and can have a cooling effect during the day (Rosenow et al., 2017).

The effect of contrail formation during sunrise and sunset depends on several factors. The contrail radiative forcing is determined by the solar zenith angle which results in a larger radiative forcing when the zenith angle increases (Myhre and Storda, 2001) which means that if the sun is on the horizon, the radiative forcing obtains its maximum value. Furthermore, the orientation of the contrails determines the radiative forcing, because contrails which are oriented in an east-west direction induce a higher positive radiative forcing than contrails oriented in a north-south direction. According to Rosenow et al. (2017), during sunrise and sunset, contrails have the highest warming effect on the atmosphere. However, Myhre and Storda (2001) found that contrails have the smallest impact during sunrise and sunset and that any shift of the flights towards sunrise or sunset would reduce the radiative forcing.

The climate impact of contrails can also be evaluated by the EMAC model. The departure and flight time of every flight is known which allows for the evaluation of the climate impact due to contrails at each time during the day. Figure 6.7 shows the climate impact imposed by contrails of the cost and climate optimized flights as a function of the time of day when the flights depart.

Figure 6.7b shows the climate impact due to contrails of the cost optimized flights. The figure shows that the climate impact during sunrise and sunset has the largest impact on the climate. However, during the day, the climate impact can be positive or negative but does not follow a trend. The climate optimized flights shown in figure 6.7a, have a negative climate impact due to contrails at any time of the day and only obtain a positive climate impact during sunrise and sunset. This agrees with the results found by Rosenow et al. (2017). However, the average climate impact due to contrails at night is also negative, which is not possible because at night, contrails only absorb radiation from the earth and do not reflect any radiation coming from the sun.

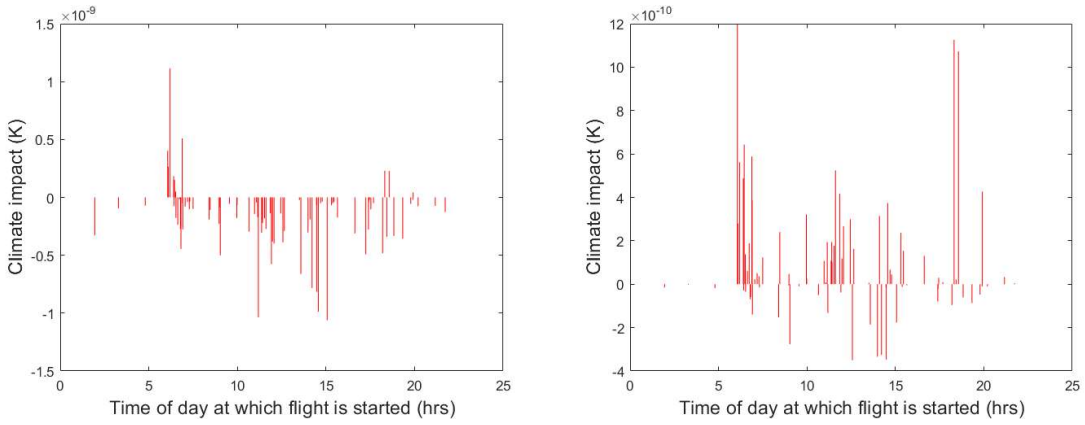

(a) Climate optimized **(b)** Cost optimized

Figure 6.7: Average CPC climate impact of the flights as a function of the departure time of the aircraft

6.1.3 Comparison Between Cost and Climate Optimized Flights

The cost and climate optimized trajectories can be compared to each other by comparing their horizontal offset from the great circle trajectories. The average offset and the standard deviation of the cost and climate optimized trajectories are represented in table 6.2. The mean of both the cost and climate optimized trajectories is close to zero. However, both values are positive which means that the offset towards the north or towards the east is more common than towards the south or west. The standard deviation of the climate optimized trajectories is larger than that of the cost optimized trajectories because the climate optimized trajectories have an increased flight distance to avoid climate sensitive regions.

Table 6.2 also shows the absolute average offset of the cost and climate optimized trajectories from the great circle routes. The absolute average offset is by definition equal or larger than the average offset. The absolute average offset of the climate optimized trajectories has a larger magnitude than that of the cost optimized flights. This shows that climate optimized trajectories fly longer trajectories. The standard deviation of the absolute average offset is smaller than the standard deviation of the average offset since all values are located above zero.

Using both, the average offset as well as the absolute average offset, the cost optimized trajectories show an average offset of almost zero. However, with the relatively high absolute average offset, it shows that the flights do offset from the great circle trajectories, but the offset is located almost equally in a positive as well as a negative direction. The climate optimized trajectories show a larger absolute average offset and the offset is on average more positive than negative. Section 6.5 discusses the offset of the flights in each flight direction which will give a more precise overview of what offset directions are preferred.

Table 6.2: Average offset and standard deviation of the cost and climate optimized trajectories from the great circle trajectories

	Climate optimized (deg)	**Cost optimized (deg)**
Average offset	0.18	0.0043
Standard deviation	1.01	0.49
Absolute average offset	0.74	0.29
Standard deviation	0.21	0.09

There are 15470 cost and climate optimized flights simulated over a period of 182 days. All of these flights induce an impact on the climate and have a positive operating cost. The differences in climate impact and operating costs between each cost and climate optimized flight for the same airport pair at the same day can be visualized by figure 6.8. The x-axis represents the difference in climate impact between the climate and cost optimized trajectories (climate - cost) and the y-axis shows the difference in operating costs between the same types of trajectories (climate - cost).

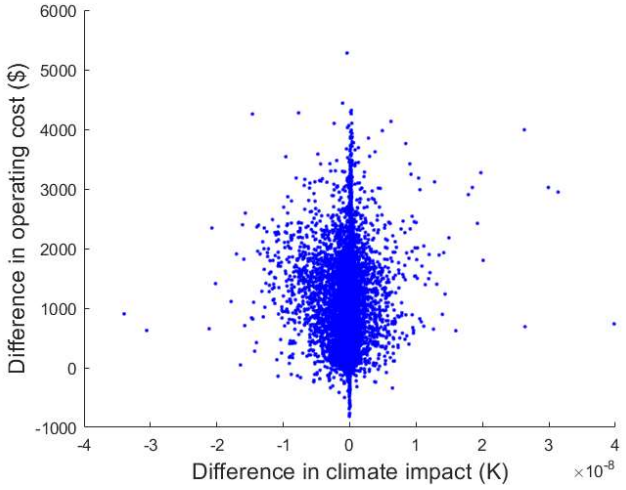

Figure 6.8: Difference in operating costs as a function of the difference in climate impact between all climate and cost optimized trajectories

Figure 6.8 shows that there are climate optimized trajectories which have lower operating costs than their corresponding cost optimized trajectories. A positive difference in climate impact denotes a climate impact of the climate optimized flights which is higher than the equivalent cost optimized flights. Furthermore, it shows that as the difference in operating costs between the flights increases, on average the climate impact change also increases up until a around 1000-1500 dollars. After this point, the increase in operating costs results in an average decrease of the climate impact change, both positive and negative. This can be a result of the lack of flights with a large difference in operating costs.

It is expected that the flights with a longer flight distance have a larger difference in operating costs. This expectation is confirmed by figure 6.9 showing the trajectories with a length of less than 1760 kilometers using the blue dots and the trajectories with a longer flight length using the red dots. The long flights have higher average operating costs but also a larger negative difference in climate impact between the cost and climate optimized trajectories.

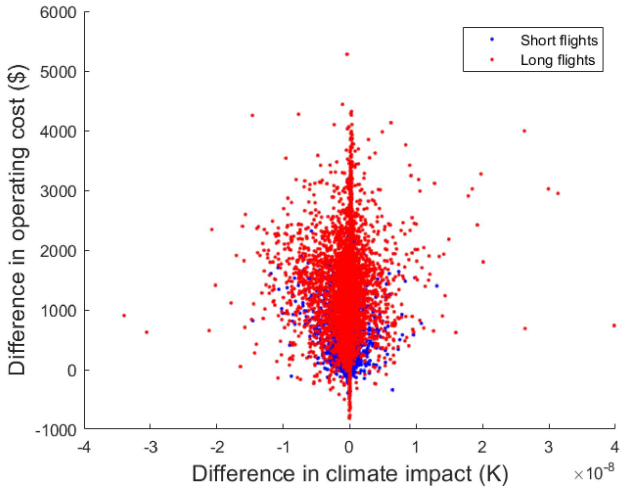

Figure 6.9: Difference in operating costs as a function of the difference in climate impact between all climate and cost optimized trajectories separated for flight distance

6.1.4 Pareto Efficiency

A Pareto efficiency is state where no individual can improve without harming another individual. In terms of trajectory optimization this means that when there is a certain state of operating costs and climate impact, the climate impact can not be reduced without increasing the operating costs. A Pareto optimality is smart way to find solutions to optimization problems which have multiple objectives like the problem concerned in this thesis. It is often used in economics but can also be applied to trajectory optimization (Stanford University, 2012).

A Pareto front can be constructed when objective functions are defined and the feasible boundaries are established. In this case, the objectives are the climate impact in Kelvin and the operating costs in dollars. The objectives are translated into an objective function containing a weighting factor which defines the boundaries of the objective function. The weighting factor can obtain values between zero and one which either results in an optimization towards reducing climate impact, operating costs or a combination of both. During this thesis, only the two bounds are examined and the resulting climate impact and operating costs are shown in figure 6.10.

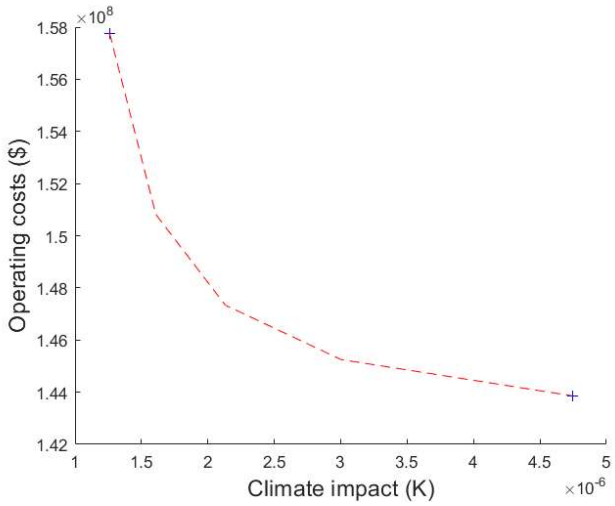

Figure 6.10: Pareto front, which includes the climate impact and operating costs of the fully cost and climate optimized flights

The blue points in figure 6.10 show the operating costs and the climate impact of the fully cost and climate optimized trajectories. Furthermore, figure 6.10 also shows (red dashed line) a possible outline of an entire Pareto front. Fully optimizing towards one objective function usually is accompanied by a large increase in the cost of the other objective function. However, the cost of the secondary objective function can often by decreased by a large amount by only increasing the cost of the primary objective function by a relatively small amount. This is shown by the gradient of the red dashed curve which is close to zero near the cost optimum. Similar results are shown if the climate impact is the primary objective function.

Figure 6.10 shows that the operating costs can be reduced by approximately 8% if the objective function is changed from fully climate optimized to fully cost optimized. However, the climate impact will ensue a 73% temperature increase with respect to a fully climate optimized trajectory. Additional research should be done to determine if optimization towards both objectives using a weighting factor can result in a fairly low climate impact, while keeping the operating costs close to the minimum value.

6.1.5 Offset Type

As was briefly explained in chapter 5, the optimized trajectories are compared to the great circle trajectories and are classified according to their offset from the great circle trajectories. The offset type of each flight over a period of six months is shown in figure 6.11. The total number of flights in the evaluated period is 15470. The figure shows the fraction of the total number of flights in each offset type.

Figure 6.11 shows that there are almost no trajectories which cross the great circle trajectory more

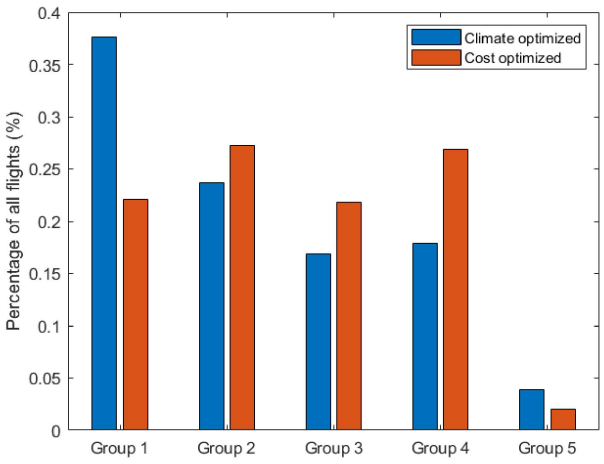

Figure 6.11: Percentage of all flights in each offset type for a period of six months

than once. The cost optimized trajectories tend to be quite evenly distributed over the remaining four groups while there is a clear preference for the climate optimized trajectories. Group 1 represents flights which exclusively have a positive offset. This means that flights which fly in a northern or southern direction have an offset towards the east and aircraft that fly in an eastern or western direction have an offset which is more often directed towards the north.

The percentage of flights in each offset type do not seem to be random, but this can be tested with a two-sample Kolmogorov-Smirnov test. The Kolmogorov-Smirnov test compares if two data sets can come from the same distribution. If the offset type would be random, it would be uniformly distributed. Therefore, the data sets of both the climate and cost optimized flights are compared to random variables drawn from a uniform distribution. Since group 5 is included, it is expected that the test rejects the null hypothesis of the same distribution. However, if group five is excluded from the test, it is interesting to see how the test performs. The test results are shown in table 6.3.

Table 6.3: Probability of having the same distribution utilizing the two-sample Kolmogorov-Smirnov test for the cost and climate optimized trajectories, including and excluding group five

	Including group 5 (%)	**Excluding group 5**
Climate optimized	$2.19 * 10^{-70}$	$1.16 * 10^{-87}$
Cost optimized	$1.29 * 10^{-5}$	0.00372

The probabilities shown in table 6.3 are the average of running the KS test a thousand times, comparing the actual data with the random variables drawn from a uniform distribution. The table shows the probability that the two data sets, (in this case the randomly drawn variables and the number of flights in each group) have the same distribution. All four test statistics show that the null-hypothesis

must be rejected and that the flight trajectories have a preferred offset type or types. It is interesting to see that the exclusion of group 5 results in a stronger test statistic for the climate optimized trajectories while it was expected that the strength of the test would be reduced if group five is excluded. This was indeed the case for the cost optimized trajectories. The null-hypothesis was rejected 995 out of 1000 times for the cost optimized trajectories excluding the data from group 5 and the resulted average probability is 0.37%.

6.1.6 Comparison with Trans-Atlantic Optimization

The thesis written by Verbist (2016) describes a similar optimization of trajectories but for the trans-Atlantic region. It is interesting to compare the general results found in the thesis by Verbist (2016) and results obtained during the optimization of the European trajectories. The fully cost and climate optimized flight results are shown in table 6.4.

Table 6.4: Comparison of the cost and climate optimized trajectories for the trans-Atlantic and European region

	Trans-Atlantic region	**European region**
Mean normalized flight distance shift	3 (%)	2.0 (%)
Mean normalized flight time shift	4.1 (%)	1.2 (%)
Mean latitude shift	2.2 (deg south)	0.23 (deg north)
Mean altitude shift	-1.43 (km)	-1.77 (km)

Table 6.4 shows the mean difference between fully cost optimized trajectories compared to the climate optimized flights (climate - cost). The mean normalized flight distance shift shows the comparison of the climate optimized trajectories compared with the cost optimized trajectories and has resulted in an average increased flight distance of 3% for the climate optimized trajectories. The flight distance shift of the flights in the European region is smaller with an average change of 2.0%. This can be a result of the a reduced average distance between two airports. The European flights have less travel distance to deviate from the cost optimized trajectories. Furthermore, the distance where divergence and convergence from the cost optimized trajectories takes place is relatively longer.

The mean normalized flight time shift for the climate optimized trajectories is 4.1% in the trans-Atlantic region. In the European region, there is a reduced time shift of 1.2%. This is a direct consequence of the reduced flight distance shift of the European flights. However, also the average flight speed plays a role. Where the trans-Atlantic flights tend to fly slower when the emphasis is put on climate impact (Verbist, 2016), the European flights have an increased flight speed of the climate optimized trajectories because the Mach number is fixed. This explains why the flight time shift is positive but of such a small magnitude.

The mean latitude shift of the trans-Atlantic flights is 2.2 degrees in a southern direction. The latitude shift of the trans-Atlantic flights are compared to the mean latitude shift of the European flights heading in a western and eastern direction. This is done because it is difficult and incomparable to include the latitude shift of north- and southbound flights. The mean latitude shift of the European flights is only 0.23 degrees but in opposite direction compared to the lateral shift of the trans-Atlantic

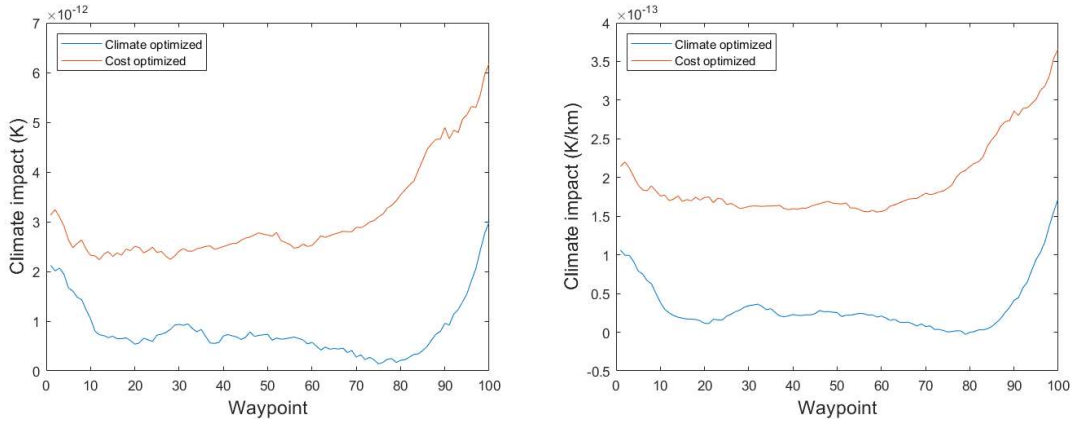

(a) Average climate impact **(b)** Average climate impact per kilometer

Figure 6.12: Average climate impact of the cost and climate optimized trajectories at each waypoint during the flight

region. Latitude shifts will be further elaborated upon in chapter 6.5 for each flight direction.

The mean altitude shift of flights in both the trans-Atlantic and European region show comparable results. It is found that the average flight altitude of the climate optimized flights is substantially lower than the mean altitude of the cost optimized flights. The cause for the altitude shift has been explained in section 6.1.

6.2 Impact of Flight Segments

In order to find out if there is a certain parts of the trajectory which regularly results in a higher climate impact than other parts of the trajectory, all flights are analyzed at each waypoint. The average climate impact at each waypoint of all trajectories combined is shown in figure 6.12. The figure also shows the average climate impact per kilometer as this takes out the dependency of the flight distance. If the flight distance is not considered, the increased flight distance of the longer flight results in a longer distance between two consecutive waypoints. The flights show an initial and final part of the flight where the gradient is large. These sections consist of approximately ten to twenty waypoints which will be referred to as the ascend and descend as these parts of the flight usually contain altitude shifts from and to the initial and final flight location (set by the optimization algorithm).

Figure 6.12a shows that the average climate impact of the climate optimized trajectories is lower at every waypoint. Furthermore, both lines show peaks at the start and end of the trajectories. Because the ascend and descend are usually accompanied by a reduced flight speed and therefore a lower distance traveled per segment, figure 6.12b shows the average climate impact per kilometer. The results are similar and shows that indeed the initial and final sections of the flights are driving the positive climate impact of both the cost and climate optimized trajectories.

It is found for the climate optimized trajectories that on average, 76 out of 85 flights have the largest positive climate impact within the first or last ten waypoints. Similar analysis of the cost optimized flights shows that on average 68 out of 85 flights obtain their largest positive climate impact within the first or last ten waypoints. The climate impact of the trajectories can be decomposed into the climate impact of all individual species which is shown in appendix C in figures C.1 (CPC), C.2 (CO_2), C.3 (H_2O), C.4 (CH_4) and C.5 (O_3).

Besides the impact of the individual species, appendix C shows the fuel consumption (C.6) between each waypoint. The impact of all individual species except for the contrail potential coverage shown in figure C.1 show a similar pattern as the pattern of the fuel consumption. Although, the pattern of the methane impact is flipped upside down, the correlation between the methane impact and the fuel consumption is large. The correlations between the fuel consumption and the impact of the species of the climate optimized flights with corresponding probabilities are shown in table 6.5. The probability shows the likelihood of no correlation where the null hypothesis is rejected for a probability below 0.05.

Table 6.5: Correlation between the fuel consumption and the impact of each individual emitted species

	Correlation coefficient	**Probability**
CPC	-0.12	0.24
CO_2	1.00	$<10^{-99}$
H_2O	0.99	$<10^{-99}$
CH_4	-0.94	$<10^{-99}$
O_3	0.94	$<10^{-99}$

Table 6.5 shows that there is indeed a strong correlation between all species except for the contrail potential coverage. The CO_2 impact is even completely coupled to the fuel consumption which is expected from theory. The contrail potential coverage shows some correlation where depending on the emitted water vapor, more or less contrails are formed. However, the contrail potential coverage is more dependent on the atmospheric properties where the water vapor is emitted and therefore the correlation is not significant.

Appendix C also shows the flight time (C.8), distance (C.7), speed (C.9) and altitude (C.10) of the cost and climate optimized trajectories. The distance traveled during the ascend and descend has a smaller magnitude. Therefore, normalizing for the flight distance is required as is done in figure 6.12b in order to get accurate results. The fuel consumption during the ascend and descend is larger than during the cruise part of the flight. This results in an increased number of emissions during the initial and final flight sections. The fuel consumption is compared to the climate impact of the climate optimized flights. The correlation between the two variables is 83% with a probability of no correlation of $2.1 * 10^{-26}$. The fuel consumption is in its turn a function of the flight altitude. The correlation between the fuel consumption and the flight altitude is -87 and -95% for the climate and cost optimized flights respectively. This means that if the altitude increases, the fuel consumption decreases in approximately the same way.

The distance traveled during the ascend and descend is less than the average distance traveled during

the remaining part of the cruise flight. This is expected since changing the aircraft altitude requires a part of the energy to be transferred into potential energy which is often accompanied by a flight speed reduction. However, figure C.9 shows that the flight speed is higher during the initial and final parts of the flight. This results in a reduced time between two consecutive waypoints.

All figures in appendix C show a certain pattern which can be explained by either the flight speed, fuel consumption or flight altitude. However, the behavior of the flight speed where the initial and final flight speed are higher than during the phase seems counter intuitive.

The wind speed at flight level 12 is shown in figure 6.13. The direction and speed are indicated by the direction and magnitude of the arrows respectively. The average flight speed can be corrected for the wind speed and direction by tracing back the wind speed and direction at every waypoint during the flight.

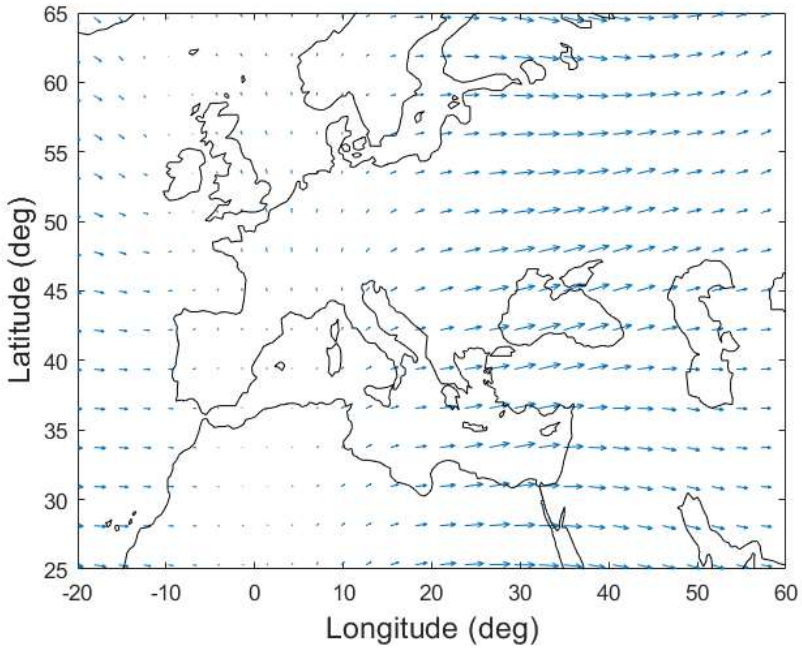

Figure 6.13: Average horizontal wind speed at flight level 12 during a period of six months

However, the wind speed is not causing the increased flight speed, but rather, the Mach number which is kept constant during the entire flight for all three flight types. The Mach number is a function of the speed of sound and since the speed of sound is determined by the temperature which is a function of the altitude, the flight speed must decrease when the altitude increases in order to keep the Mach number constant. This explains the high flight speed during the initial and final sections of the flights.

The climate impact of the cost and climate optimized trajectories can also be compared to each other to establish where there is a large difference in climate impact between cost and climate optimized trajectories. However, in order to be able to accurately compare a cost optimized flight to a climate optimized flight, segments of each trajectory need to be compared. The trajectories will be segmented as shown in figure 5.4 in chapter 5.2. The flight path is divided into 25 equally spaced segments and is calculated by subtracting the climate impact of the cost optimized flights from the climate optimized flights. The result is shown in figure 6.14.

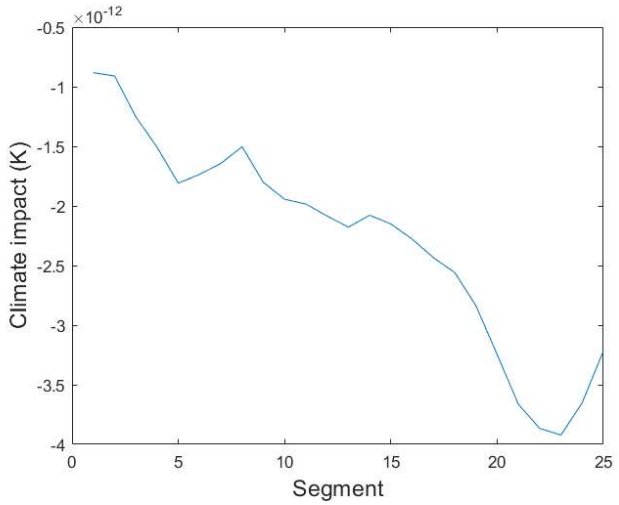

Figure 6.14: Comparison of the climate impact between the cost and climate optimized trajectories

Figure 6.14 shows that the difference in average climate impact is consistently negative throughout the entire flight. However, the magnitude is decreasing as the flight progresses. This means that the difference in impact between the cost and climate optimized trajectories is increasing. This is potentially a result of a climate optimized flight, making a detour at the start of the flight (increasing the climate impact) which reduces the climate impact of this trajectory in a later stage of the flight. Also, due to the additional flight distance, additional fuel is required which is burned up during the flight. The difference in the fuel on board becomes less and therefore the fuel consumption of the climate optimized flights is reduced compared to the cost optimized flights.

6.3 Flight Length

The 85 flights which are evaluated, are not evenly distributed by flight length. There is a large number of trajectories which have a fairly short flight distance while other flights have relatively long flight distances. To address the difference between the flight length, A number of short distance flights will be compared to a number of medium ranged flights. All flights will be normalized in order to be able to compare the flight parameters of the short and long flights.

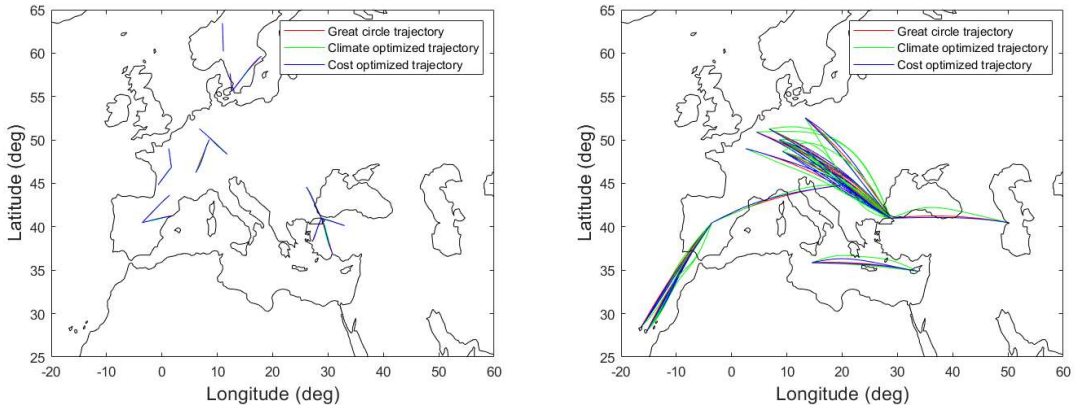

(a) Short range **(b)** Medium range

Figure 6.15: Short and medium range flight paths

The data set containing the short flights will consist of flights with a flight distance between 220 and 490 kilometers and the data set containing the medium range flights consists of flights with a flight length between 1730 and 2350 kilometers. Both data sets contain 27 flights, which are shown in figure 6.15.

Tables 6.6 and 6.7 contain the average flight distance, altitude, speed, and fuel consumption of the climate and cost optimized flights where the average fuel consumption is normalized for flight distance.

Table 6.6: Comparison of the flight characteristics of short and medium ranged climate optimized flights

	Short flights	**Long flights**	**Probability**
Average flight length (km)	408	1901	$3.03 \cdot 10^{-10}$
Average altitude (m)	9766	10035	0.029
Average speed (km/h)	859	865	0.76
Average fuel consumption (kg/km)	6.24	6.37	0.46

Table 6.7: Comparison of the flight characteristics of short and medium ranged cost optimized flights

	Short flights	**Long flights**	**Probability**
Average flight length (km)	406	1857	$3.03 \cdot 10^{-10}$
Average altitude (m)	11623	11644	0.075
Average speed (km/h)	850	857	0.76
Average fuel consumption (kg/km)	5.28	5.42	0.093

The cost and climate optimized flights both show that the average flight altitude of the short flights is

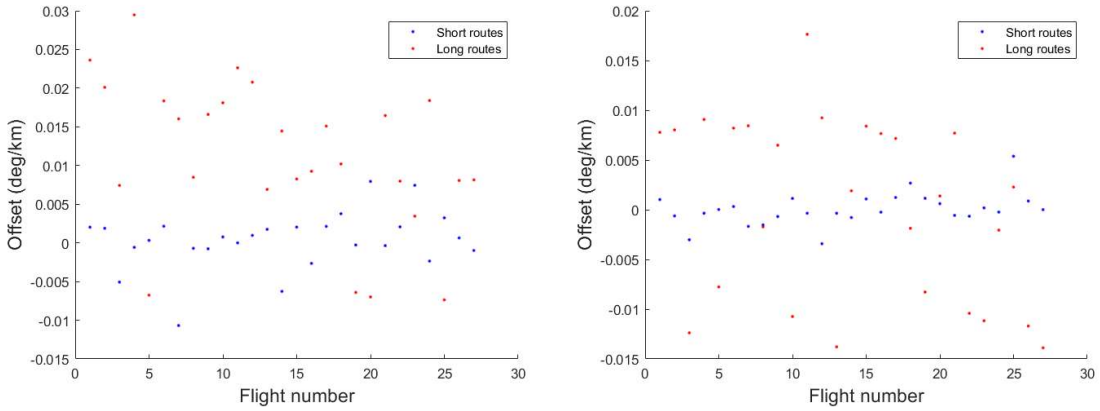

(a) Climate optimized **(b)** Cost optimized

Figure 6.16: Average offset of the short and long, cost and climate optimized trajectories

lower than the altitude of the long flights. This can partly be explained by the fact that the percentage of the flights where the climb and descend takes place is larger for the short flights. However, when the climb and descend part are taken out, the long flights still have an increased flight altitude for the climate optimized trajectories. For a shorter flight, the additional fuel required to reach a certain altitude may be more than the fuel reduction at that altitude, due to the short period where the short flights stay at their maximum altitude. The average altitude of the cost optimized trajectories is similar when the ascend and descend are left out.

The magnitude of the average flight speed of the short flights is also lower than the flight speed of the long flights for both cost and climate optimized trajectories. This can be explained by the increased flight altitude of the long flights, which allows the aircraft to fly faster. However, the results are not significantly different from each other (probability 76%) as also shown in table 6.6

The fuel consumption per kilometer is smaller for the shorter flights for both the cost and climate optimized trajectories. This is an interesting result since it would be expected that an increased flight altitude and speed reduces the average fuel consumption. The increased fuel consumption of the longer flights can be attributed to the additional fuel which is required for longer flights resulting in an increased take-off weight and therefore a less efficient aircraft. Also, the results obtained are not significantly different (probability 46%) which is proven by a Mann-Whitney U test.

The average offset of the cost and climate optimized trajectories from the great circle trajectories are also normalized by dividing by the trajectory length and are shown in figure 6.15a. Each dot represents either a short (blue) or a relatively long (red) flight.

Figures 6.16a and 6.16b show that even when the trajectories are normalized for their length, the offset of the long routes still have a larger magnitude. The normalized offset of the climate optimized trajectories is a factor of ten larger than the offset of the cost optimized routes. Longer

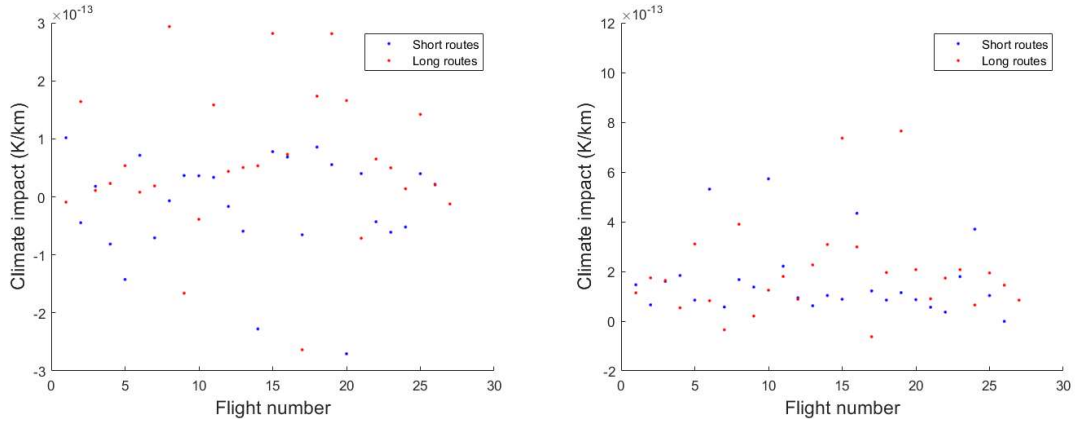

(a) Climate optimized **(b)** Cost optimized

Figure 6.17: Average climate impact of the short and long, cost and climate optimized trajectories

trajectories allow for a larger offset from the great circle trajectory and will therefore also try to avoid climate sensitive regions more often. This results in an increased average offset per kilometer traveled.

If the longer trajectories offset more from the great circle trajectories it would be expected that the climate impact per kilometer is less, especially for the climate optimized trajectories. Figure 6.17a shows the impact of the short and long climate optimized trajectories and figure 6.17b shows the same for the cost optimized flights.

Figure 6.17 shows that the short and long routes of both the cost and climate optimized trajectories have approximately the same spread in the data. The average climate impact of the short and long flights is also similar for the cost optimized trajectories. Using the Mann-Whitney U test, the null hypothesis is not rejected and therefore there is no significant difference found between the mean of the short and long trajectories. The climate impact difference between the short and long routes of the climate optimized trajectories does show a significant difference between the mean of both series. The average climate impact of the short routes has a minor negative climate impact (reduction of the atmospheric temperature) and the average climate impact of the long routes has a small positive impact on the climate. This does not agree with the expected climate impact reduction per kilometer of the long routes compared to the short flights.

A possible explanation for the differences can be attributed to the increased take-off weight of the aircraft, which travel long distances and therefore have an increased fuel consumption. If this is true, the climate impact of the long routes should be similar to the climate impact of the short trajectories towards to the end of the flight. The average climate impact at each waypoint of the short and long optimized trajectories is shown in figure 6.18.

Figure 6.18 shows the impact per kilometer traveled between two consecutive waypoints. It is normalized because the distance between two consecutive waypoints is different for different trajectory

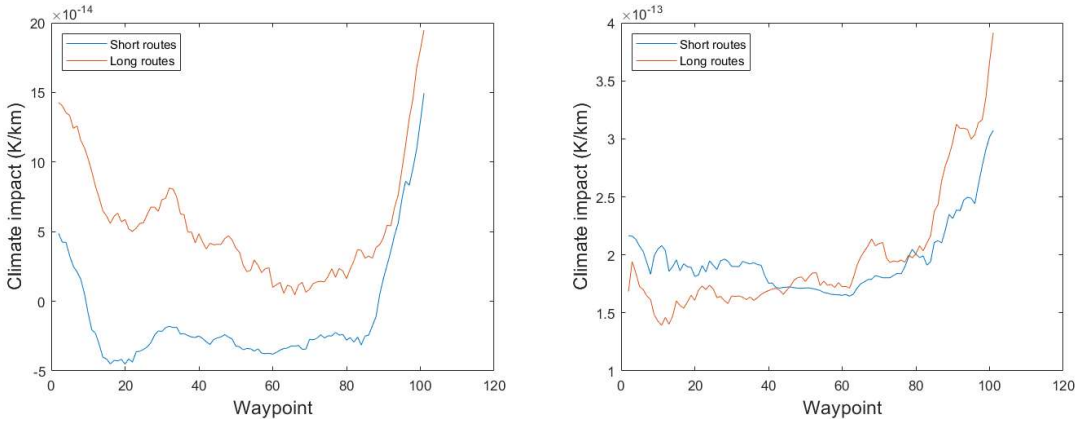

(a) Climate optimized **(b)** Cost optimized

Figure 6.18: Average climate impact per kilometer between two consecutive waypoints of the climate and cost optimized trajectories

lengths. A longer trajectory has increased emissions and that results in an increased average temperature response. The long routes of the climate optimized trajectories have a positive average climate impact throughout the entire flight with peaks around the start and end of the flights. The short routes have a negative average climate impact and only have a positive impact at the first and last ten waypoints.

The cost optimized trajectories show a more similar pattern regarding the short and long routes. The first half of the flights has a fairly constant climate impact, but as the flight progresses, the climate impact increases. A large fraction of the climate impact is obtained in the last phase of the flights. The cost optimized flights have an average climate impact which is positive during the entirety of the flight which is a result of objective function that does not take the climate impact of the cost optimized flights into account.

The impact of the long routes shown in figure 6.18a is decreasing as the flight progresses which can be attributed to the decrease in aircraft weight. This decreases more between two consecutive waypoints because the distance is longer. However, the long routes never obtain a negative average climate impact. Another cause for the positive climate impact of the long trajectories can be the geographical location of these trajectories. As shown in figure 6.15, the longer trajectories are almost all located in the central part Europe, while the short trajectories are spread out more evenly over Europe. In order to find out if the different sized trajectories have a significant difference in climate impact, additional trajectories need to be analyzed flying in different regions.

6.4 Seasonal Effect

To determine if there is a seasonal effect on the flight trajectories and their corresponding cost and climate impact, the six month analysis is split up into two equal parts, which are considered the

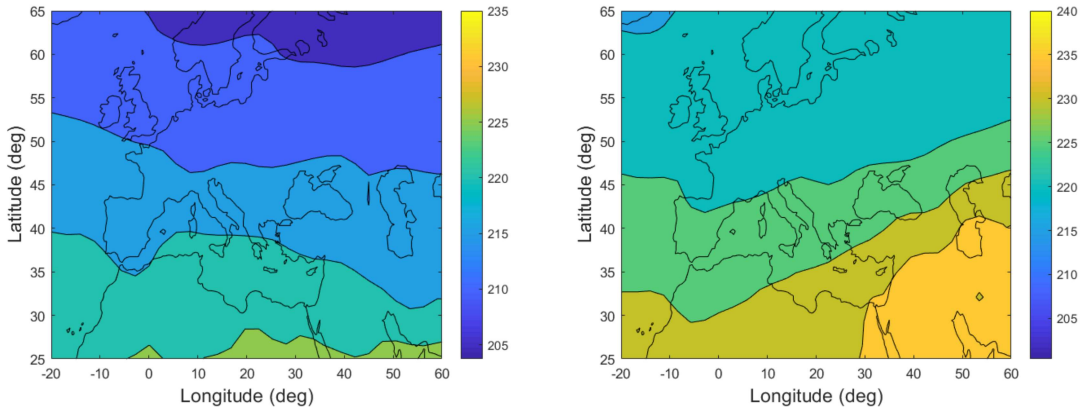

(a) January **(b)** June

Figure 6.19: Average temperature at flight level 12 corresponding to an altitude of approximately ten kilometers

summer and winter season. The winter season starts at January 1^{st} and ends at March 31^{st} 2016 and the summer season starts at April 1^{st} and ends at June 30^{th} 2016. The effect of the season on geographical location, altitude and emissions are considered for the cost and climate optimized trajectories. Occasionally, the cost and climate optimized trajectories will be compared to the great circle flights.

The geographical location or horizontal flight path of the three flight types will be compared to each other to see if there is any change in the offset between the seasons. It will be extensively explained and illustrated in section 6.4.3. The altitude or the vertical flight path of the cost and climate optimized trajectories will be compared while the great circle trajectories will be left out of this comparison since the initial and final altitude of the great circle flights is different compared to the cost and climate optimized flights. This will be explained in section 6.4.4. The emissions and climate impact of the cost and climate optimized trajectories will be evaluated in section 6.4.5. However, first the atmospheric and general flight properties will be evaluated over the entire season which allows for a possible cause of a seasonal effect.

6.4.1 Atmospheric Characteristics

During the year, the temperature at the surface of the earth changes due to the change of the position of the earth with respect to the sun. It would be expected that the atmospheric temperature also changes as the season progresses. Figure 6.19 shows the average temperature for January and June at flight level 12 which is an altitude of approximately ten kilometers. Most climate optimized aircraft fly around this altitude. Figure 6.19 shows that there is a seasonal effect present. The temperature in January shown in figure 6.19a on average is about 12 degrees Kelvin lower than the temperature in June shown in figure 6.19b.

The average temperature can be examined to evaluate if there is statistical evidence for a seasonal effect. The average atmospheric temperature in the European airspace is shown in figure 6.20. The figure shows an increasing trend from approximately day fifty onward, where the average temperature increase is approximately 0.1 degree Kelvin per day. The lowest temperature is reached in February which is expected since February 2016 was the coldest month of the year.

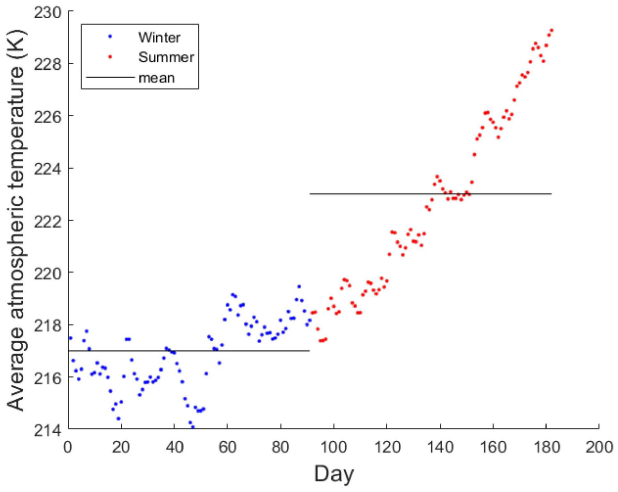

Figure 6.20: Average atmospheric temperature at flight level twelve corresponding to an altitude of approximately ten kilometers during a period of six months

The blue dots in figure 6.20 represent the temperature during the winter season and the red dots represent the temperature during the summer season. The black lines show the average of both the winter and summer season. The difference between winter and summer season is substantial and can deviate trajectories especially in altitude. The null hypothesis of the Mann-Whitney U test is rejected which shows that there is a seasonal trend present in the data (probability <0.05).

The relative humidity of the air determines the potential for clouds to form and is an important atmospheric property that determines the climate impact of a trajectory. Although the humidity is different at every point in the atmosphere, an average humidity inside the European airspace at flight level twelve is calculated and shown in figure 6.21 for six months.

Figure 6.21 shows a decrease in the average relative humidity as the year progresses. However, the variance of the data is large. The relative humidity changes during the day as it is affected by rainfall and the temperature of the atmosphere. In general there is a down going trend and there is a significant difference between the humidity in the winter and summer season (probability <0.05).

The contrail potential coverage is another important variable that defines an aircraft route especially considering climate optimized trajectories. The contrail potential coverage is dependent on several

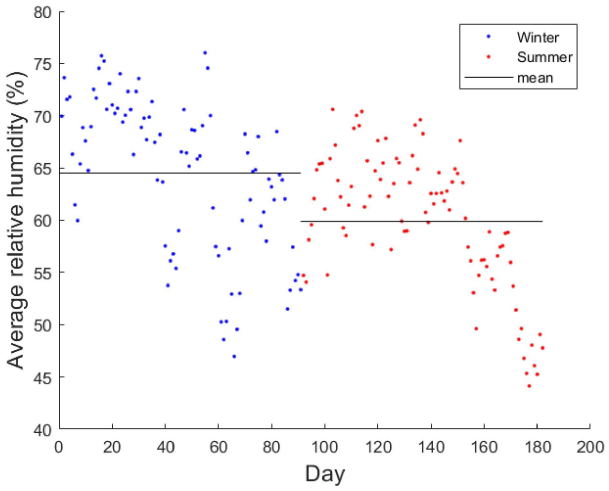

Figure 6.21: Average relative humidity at flight level twelve corresponding to an altitude of approximately ten kilometers during a period of six months

atmospheric properties such as the humidity of the atmosphere as well as the temperature. It is a highly fluctuating variable and it may therefore be difficult to observe a seasonal trend. The average contrail potential coverage over the European airspace at flight level twelve is shown in figure 6.22.

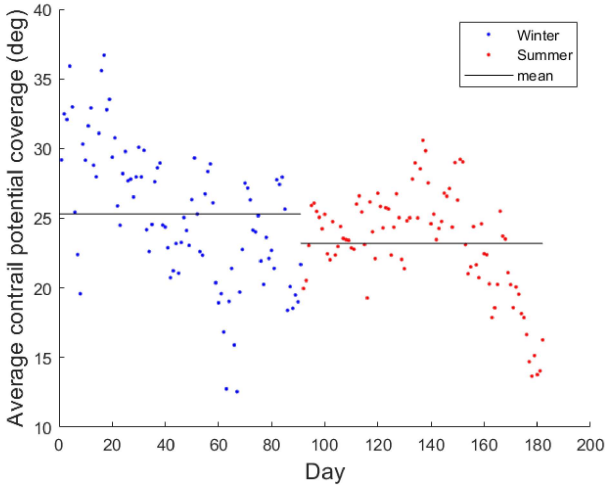

Figure 6.22: Average contrail potential coverage at flight level twelve corresponding to an altitude of approximately ten kilometers during a period of six months

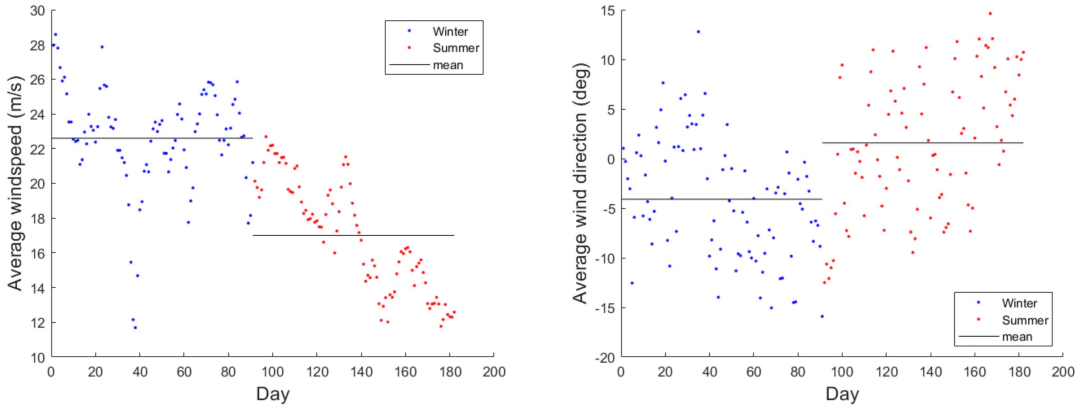

(a) Wind speed **(b)** Wind direction

Figure 6.23: Average wind speed and direction at flight level twelve corresponding to an altitude of approximately ten kilometers during a period of six months

The average contrail potential coverage shows a decreasing trend over time. The figure shows many similarities to the average relative humidity shown in figure 6.21. To find out if there is any relation between the relative humidity and the contrail potential coverage, a correlation test is performed. The correlation test shows an 82% correlation between the two variables and a probability of no correlation of 10^{-44}. This means that there is a powerful relationship between the humidity and the contrail potential coverage. A correlation test between the contrail potential coverage and atmospheric temperature shows a correlation of -48% between the two variables (probability <0.05). This means that there is a negative but nevertheless strong relationship between atmospheric temperature and the contrail potential coverage. This agrees with the Schmidt-Appleman criterion shown in figure 2.4.

Finally, wind plays an important role in the efficiency and climate impact of aviation and is known to play an important role for trans-Atlantic flights. The wind can be decomposed into speed and direction. The average wind is computed taking the average wind in the European airspace at flight level twelve. The average wind speed is shown in figure 6.23a and the average wind direction is shown in figure 6.23b.

The average wind speed in the European airspace has a decreasing trend as can be seen in figure 6.23a. During the first three months of the year, the average wind speed is 22.6 meters per second while during the second three months, the average wind speed is 17.0 meters per second.

The spread of the average wind direction at flight level twelve considering the entire European airspace is limited. Wind in a zero degrees direction is considered eastern wind. This means that the average wind direction remains fairly constant during the year with a maximum offset from the eastern direction of about 15 degrees in a north- and southeastern direction. The average angle of the wind is decreasing during January and February after which it increases up until June.

The decreasing trend in the average wind speed can be proven using a Mann-Whitney U test. The test statistic of the U test is $2.27 * 10^{-21}$. Similarly, the average flight direction shows a test statistic of $1.32 * 10^{-7}$ which is not quite as high, but nevertheless shows that both data sets have a significant offset between the means of each season.

6.4.2 General Flight Characteristics

One of the general flight characteristics which is often determined by the location of the aircraft and often determines the climate impact of the trajectory is the use of fuel over time. The total fuel consumption of the entire set of flights on each day is shown in figure 6.24. What becomes apparent from observing the figure is that the average total fuel consumption is the largest for climate optimized trajectories which is expected because the climate optimized trajectories aim to avoid climate sensitive regions, which induces an increase in fuel consumption. Furthermore, the average flight altitude of the climate optimized trajectories is lower than the average flight altitude of the other two flight types. This also results in an increased fuel consumption because the aircraft is more fuel efficient at higher altitudes due to reduced air resistance. Moreover, the fuel consumption of the cost optimized trajectories has the lowest magnitude, because the cost optimized trajectories are optimized towards reducing the flight time and fuel consumption. To reduce the flight time, the average altitude of the flight is increased because a decreased air resistance allows an aircraft to increase its flight speed and as previously explained, an increased flight altitude reduces the fuel consumption.

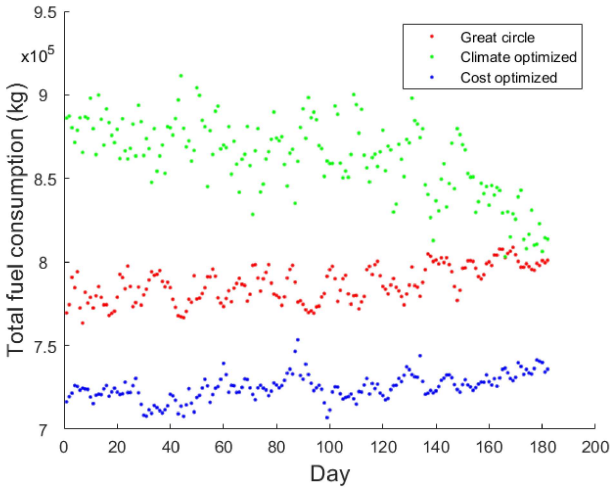

Figure 6.24: Total fuel consumption during a period of six months for three different flight types

Figure 6.24 shows a decreasing trend for the fuel consumption of the climate optimized trajectories and a small increasing trend for the great circle and cost optimized trajectories. To find out if there is a significant trend existing in the data, the data of the first three months will be compared to the data of the second three months. The statistical test which applies to such a data series is the Mann-Whitney U test. The mean of the data sets and the probabilities of the Mann-Whitney U test

are shown in table 6.8.

Table 6.8: Mean fuel consumption and probability of equal mean for three flight types

	Mean Winter (kg)	**Mean Summer (kg)**	**Probability (%)**
Great circle	$7.82 \cdot 10^5$	$7.92 \cdot 10^5$	$2.20 \cdot 10^{-9}$
Climate optimized	$8.72 \cdot 10^5$	$8.52 \cdot 10^5$	$4.82 \cdot 10^{-9}$
Cost optimized	$7.23 \cdot 10^5$	$7.27 \cdot 10^5$	$2.57 \cdot 10^{-6}$

The results show that there is a significant difference between the fuel consumption means of the winter and summer season for all three trajectory types. Interesting to note is that the climate optimized trajectories tend to use less fuel as the year progresses while the great circle and cost optimized trajectories have an increasing fuel consumption during the year. The great circle and cost optimized trajectories also seem to show a sinusoidal trend in the data. This can possibly be explained by the atmospheric properties such as temperature and air pressure which can alter the altitude and the efficiency of an aircraft.

Another flight characteristic which is related to the fuel consumption is the flight speed. The flight speed is determined by the altitude and is expected to be the largest for cost optimized flights and the lowest for climate optimized flights. Figure 5.10a has already shown that there exists a seasonal effect for the flight between Istanbul and Madrid. The flight speed for all three flight types is shown in figure 6.25a. Unexpectedly, the climate optimized trajectories show the largest average flight speed. An explanation for the phenomenon is explained in section 6.2.

The wind speed correction is performed resulting in the actual airspeed which is shown in figure 6.25b. The wind speed correction results in a smaller variability of the average flight speed, as for instance the great circle and cost optimized flights are often negatively affected by the wind speed. The cost optimized trajectories have more days with a higher average flight speed compared to the climate optimized trajectories when the ground speed is corrected for the wind speed. The average airspeed is shown in table 6.10.

The results in figures 6.25a and 6.25b clearly show an increasing trend as the year progresses for all three flight types. This is supported by the results of the Mann-Whitney U test which show an almost zero percent chance that the medians of both seasons can be the same. The test shows even stronger evidence for a seasonal effect than the test for the fuel consumption. From the figure, it seems as if the there is a decreasing trend during the first forty to fifty days after which it changes towards an increasing trend. If this trend is continued for the second six months of the year, it is expected to have a smoothing of the data around day number 200 after which a decreasing trend is expected as towards the autumn and winter the temperature decreases in a similar manner.

Table 6.9 shows the mean flight speed during the winter and the summer season where the difference between the winter and summer of the great circle has the largest magnitude. Therefore, the probability of having the same median for both seasons is the lowest for the great circle trajectories. Table 6.10 shows that the mean flight speed is increased for each flight type during both winter and summer when only the airspeed is considered. This means that on average, the wind speed negatively

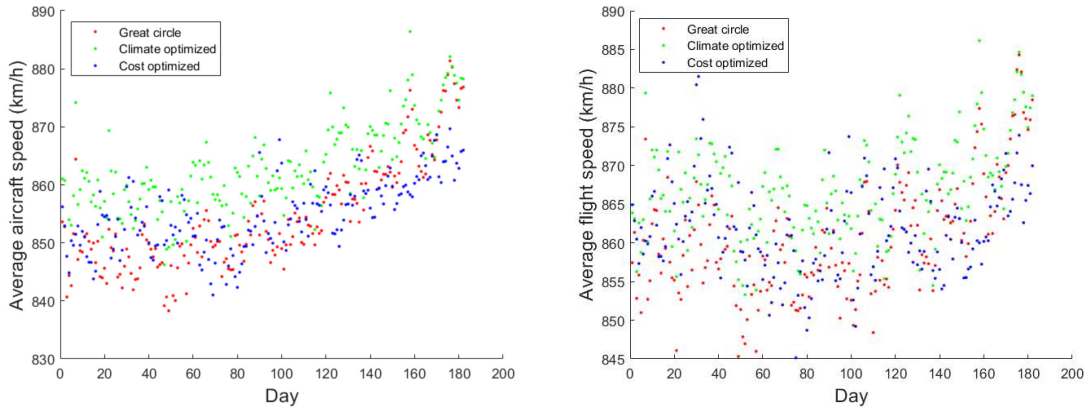

(a) Ground speed including wind speed **(b)** Ground speed corrected for wind speed (airspeed)

Figure 6.25: Average aircraft speed during a period of six months for three different flight types

Table 6.9: Mean flight speed and probability of equal mean for three flight types

	Mean Winter (km/h)	**Mean Summer (km/h)**	**Probability (%)**
Great circle	848.3	860.9	$7.47 \cdot 10^{-20}$
Climate optimized	858.2	867.5	$6.41 \cdot 10^{-16}$
Cost optimized	851.3	858.6	$8.32 \cdot 10^{-15}$

Table 6.10: Mean flight speed corrected for wind speed and probability of equal mean for three flight types

	Mean Winter (km/h)	**Mean Summer (km/h)**	**Probability (%)**
Great circle	857.3	863.6	$3.95 \cdot 10^{-4}$
Climate optimized	864.8	868.8	0.45
Cost optimized	861.2	862.2	13.0

influences the ground speed. Excluding the wind speed also reduces the difference in flight speed between the winter and summer season, where there is no statistical evidence that the cost optimized trajectories contain a seasonal effect. Tables 6.9 and 6.10 show that the flight speed is more negatively affected by the wind speed and direction during the winter season than during the summer season.

Finally, the final flight characteristic which is determined by the flight trajectory and the speed of the aircraft is the flight time. Similar to the fuel consumption, it determines the overall cost of the trajectory. Therefore, it is expected that the flight time of cost optimized trajectories is relatively short, while for the other two trajectories, the flight time is not considered in the optimization process. On the other hand, since the flight time is dependent on the aircraft speed, it is expected that the climate optimized trajectories have a relatively short flight time. However, the possible additional flight length may compensate for this. The average flight time during the two seasons is given in figure 6.26.

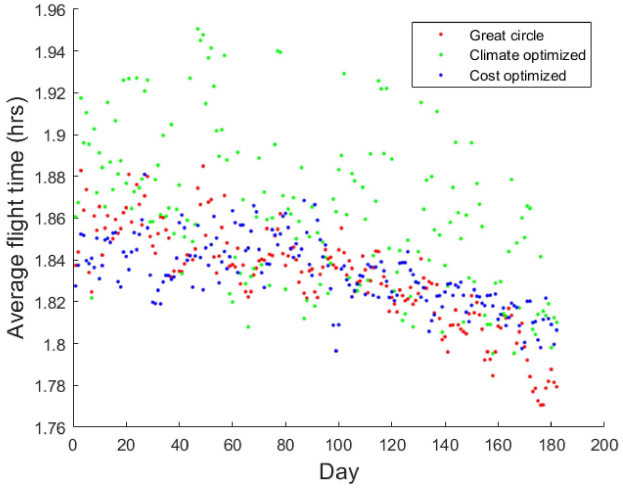

Figure 6.26: Average flight time during a period of six months for three different flight types

Figure 6.26 shows a decreasing trend of the average flight time as function of the day for all three flight types. Similar to the average aircraft speed but in opposite order. Between the first and approximately the fortieth day, the trend is slightly upwards, after which the trend redirects towards a decreasing average flight time. The great circle and cost optimized trajectories are fairly close together while the variance of the climate optimized trajectories is tremendous. The large variance can not be explained by the seasonal change in flight speed as the variance of the flight speed for climate optimized trajectories is rather small. It can possibly be explained by the trajectory length, but this will be evaluated in section 6.4.3.

The seasonal effect seems to be present for all three trajectory types and can be proven by the Mann-Whitney U statistical test. The results of the test are shown below. The results show strong evidence for all three trajectory types but the strength of the climate optimized trajectories is reduced due to the large variance in the data.

Table 6.11: Mean flight time and probability of equal mean for three flight types

	Mean Winter (hrs)	**Mean Summer (hrs)**	**Probability (%)**
Great circle	1.85	1.82	$4.63 \cdot 10^{-22}$
Climate optimized	1.88	1.85	$5.87 \cdot 10^{-8}$
Cost optimized	1.84	1.82	$1.33 \cdot 10^{-20}$

Many of the general flight characteristics either determine or are determined by the actual trajectory that the aircraft follows. This is true for the horizontal as well as the vertical trajectory. Both horizontal and vertical trajectories are treated independently in the next sections.

6.4.3 Horizontal Trajectory

The horizontal trajectory of an aircraft is the trajectory determined by the longitudinal and lateral coordinates of the flight path. The trajectory is determined by the type of optimization. If the trajectory is optimized towards reducing the climate impact of aviation, the trajectory aims at avoiding climate sensitive regions. If the trajectory is optimized to reduce the operational costs, the trajectory tends to reduce the flight time and fuel consumption which can be obtained by for instance following the jet stream. Figures 6.2 and 6.3 show some example trajectories of horizontal great circle, cost and climate optimized flights. The figures show different trajectories for flights in January compared to the same flight in June.

To determine whether or not the horizontal trajectories have a seasonal change in the trajectory, the average trajectory length for 182 days is shown in figure 6.27. The average flight length of the great circle trajectories is constant since the great circle distance between two airports does not change over time. The cost optimized flights travel a slightly longer distance on average, but the flight distance of a single day is relatively close to the mean. The climate optimized trajectories have a mean which is significantly larger than the mean of the great circle and cost optimized trajectories (probability <0.05). Except for the increased mean, the variance of the trajectory length is also quite high. The climate optimized trajectories are trying to avoid climate sensitive regions which sometimes results in a large detour of the trajectory. Although a longer trajectory is usually accompanied with additional fuel burn, the locations at which the combustion products are released, result in a reduced climate impact. For the cost optimized trajectories, the optimization module aims at using or avoiding wind (depending on the flight direction) in order to reduce the fuel consumption and flight time.

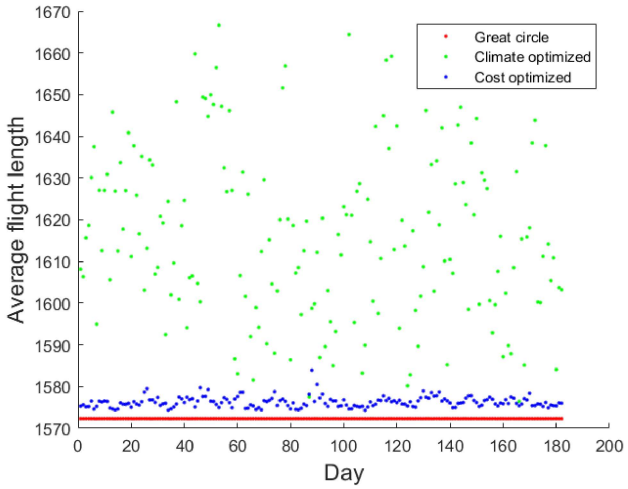

Figure 6.27: Average trajectory length during a period of six months for three different flight types

To give some more insight on the flight length compared the mean of each of the flights, figure 6.28 shows the average flight length compared to the mean over a period of six months. This is done

independently for each trajectory type.

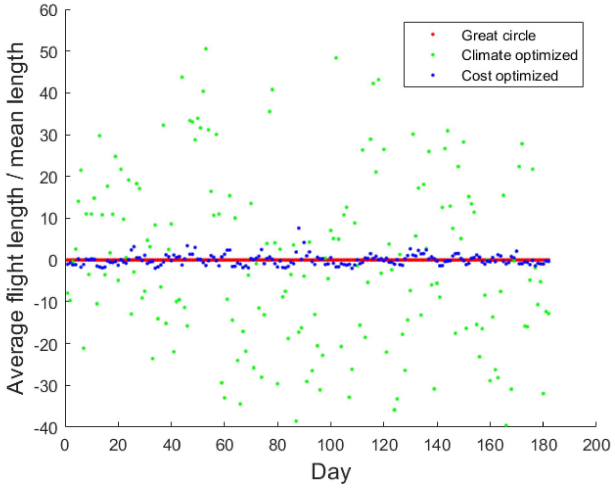

Figure 6.28: Average trajectory length compared to the mean trajectory length during a period of six months for three different flight types

The great circle trajectories have an average flight length compared to the mean length of zero because the flight length is constant over time. The average flight length compared to the mean of the cost optimized trajectories is close to zero with almost every trajectory within five kilometers from the mean flight length. The climate optimized trajectories show a larger deviation from the mean, with flight lengths deviating up to 50 kilometers from the mean. There is no seasonal trend in the length of the trajectories for all three flight types. Therefore, there is no reason to believe that the mean during the first three months is different compared to the mean of the second three months.

Not only is the trajectory length an important parameter to analyze, but the route that the trajectory is taking can also change during the season and therefore contain a seasonal trend. The path of the cost and climate optimized trajectories will be compared to the great circle trajectories. Since the great circle trajectories are the shortest distance between two airports, any deviation from these trajectories results in an increased flight distance.

The mean average and absolute average offset of all 85 trajectories during the winter and the summer season (182 days) are shown in figure 6.29. Figure 6.29a represents the average offset of the climate optimized trajectories with respect to the great circle trajectories and figure 6.29b shows the average absolute offset. Both figures show the offset, the mean during winter and summer, and a linear trend line.

Both, figures 6.29a and 6.29b show a similar trend where the mean of the summer season has a lower magnitude than the mean of the winter season. The magnitude of the average absolute offset is larger

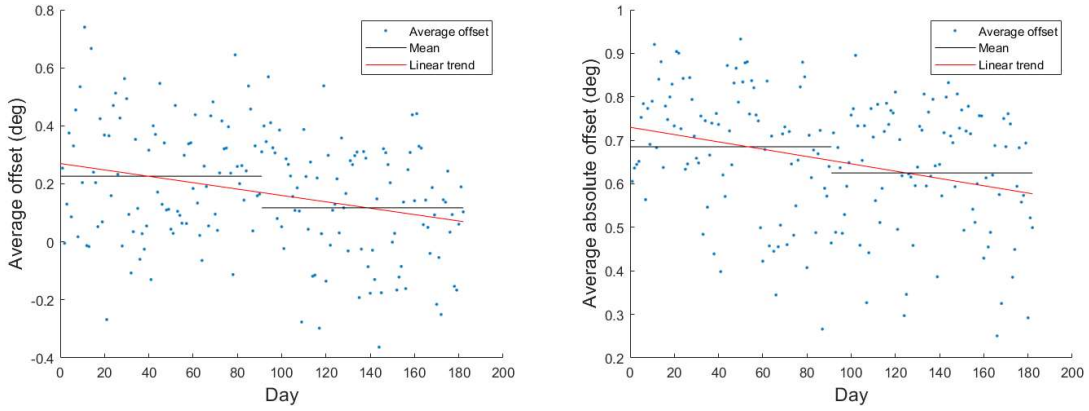

(a) Average offset **(b)** Average absolute offset

Figure 6.29: The average and absolute average offset of the climate optimized trajectories with respect to the great circle trajectories

because it considers all offset as positive offset. The trend line shown in both figures also behaves similarly with a similar gradient. A Mann-Whitney U test provides that both, the average and average absolute offset contain a seasonal trend because null-hypothesis is rejected (probabilities of 0.2% and 0.6%).

The same analysis is done for the cost optimized trajectories comparing them to the great circle trajectories. However, the results are different which is shown in figure 6.30. The magnitude of both the average and the absolute average offset are smaller than the offset of the climate optimized flights. Also, the difference between the mean of the winter and summer season is minimal compared to the variance of both data sets. The trend line almost coincides with means of the seasons and is therefore not shown in the figures.

As was already established earlier in this section, the average flight length of the climate optimized trajectories is longer than the average length of the cost optimized trajectories. This automatically results in a larger absolute offset for the climate optimized trajectories. It was shown that the climate optimized trajectories do not have a seasonal trend. However, figure 6.29 does show a seasonal trend for the offset of the flight trajectories. The cost optimized trajectories do not have a seasonal trend in the trajectory length and also no trend in the average and absolute offset as can be seen in figure 6.30.

What can also be observed from figures 6.29a and 6.30a, is that the climate optimized trajectories tend to have a more positive offset on average, while the cost optimized trajectories have a more equally divided offset (both positive and negative).

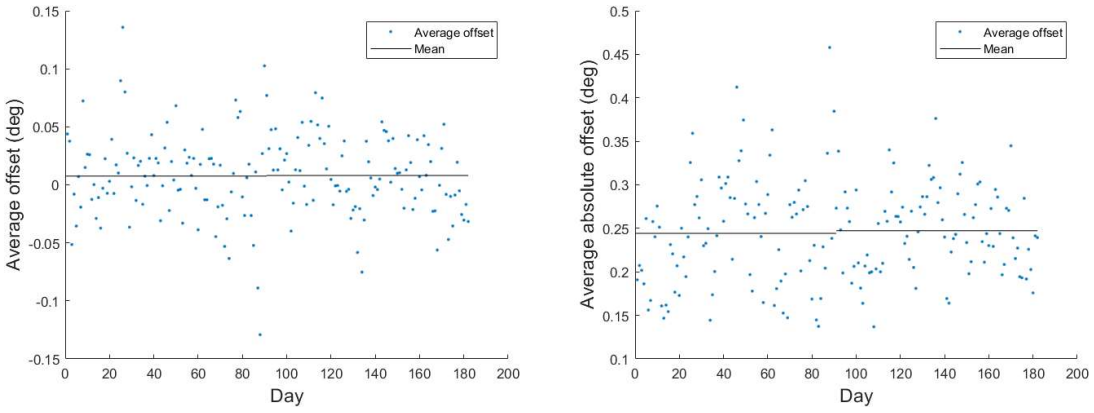

(a) Average offset **(b)** Average absolute offset

Figure 6.30: The average and absolute average offset of the cost optimized trajectories with respect to the great circle trajectories

6.4.4 Vertical Trajectory

Independent of the flight trajectory, the model has a set initial and final altitude. For the cost and climate optimized trajectories this altitude is set to approximately 8840 meters. The great circle trajectories have a constant altitude over the entire flight which is about 10670 meters. Since the starting and final altitude of the great circle flights are different, it is difficult to compare the trajectories so the great circle flights will be left out of the vertical trajectory analysis.

As shown in figure 5.2b, from the starting altitude, the cost optimized trajectories have the tendency to increase their altitude rapidly while the climate optimized trajectories often stay at approximately the same altitude and rise to avoid climate sensitive regions. Figure 6.31 shows the average altitude of the cost and climate optimized flights during the winter and the summer season. The ascend and descend of the flights is incorporated in the average flight altitude and therefore the preferred altitude of a flight is usually higher than depicted in the figure. The terms ascend and descend are used to describe the change in flight altitude from and to the initial and final altitude and not from sea level.

Figure 6.31 shows that the average altitude of the cost optimized trajectories is far above the average altitude of the climate optimized trajectories. It also shows that the variance of the cost optimized trajectories is small and that the climate optimized trajectories have a larger variance. This is also shown in figure 6.32 which shows the average altitude compared to the mean altitude. The cost optimized trajectories are almost all within a hundred meters of their mean altitude, while the climate optimized trajectories deviate up to a thousand meters away from the mean.

Figures 6.31 and 6.32 also show a trend in the data. The climate optimized flights have the tendency to fly higher in the summer season than in the winter season. This is less evident for the cost optimized trajectories but the Mann-Whitney U test will provide a statistical likelihood for a seasonal

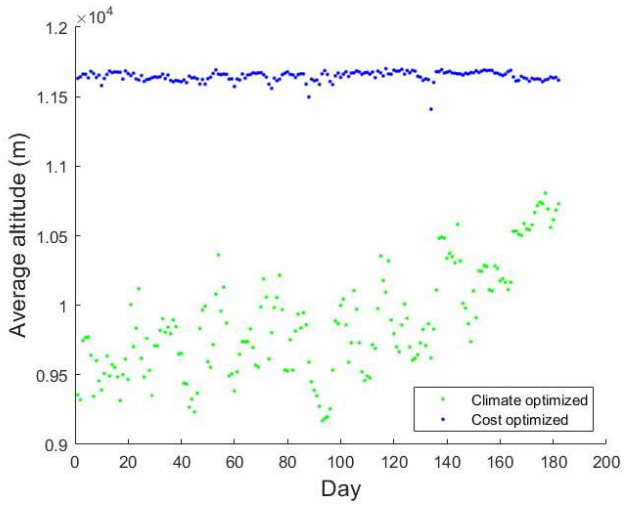

Figure 6.31: Average trajectory altitude during a period of six months showing the cost and climate optimized trajectories

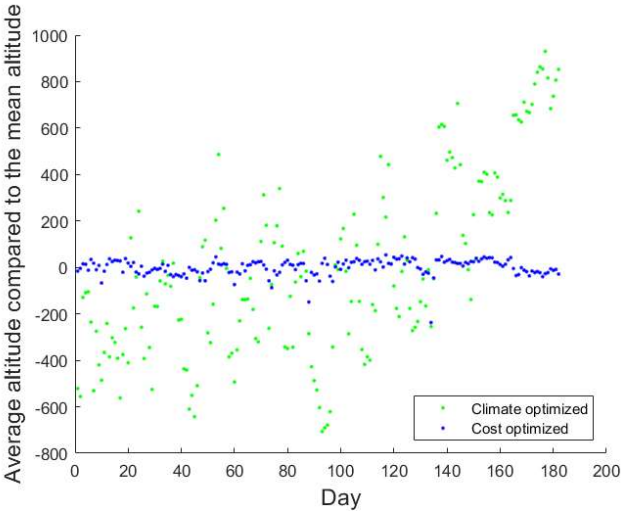

Figure 6.32: Average trajectory altitude compared to the mean trajectory altitude during a period of six months showing the cost and climate optimized trajectories

effect. The U test provides a test statistic for both optimized trajectories and concludes that both cost and climate optimized trajectories reject the null-hypothesis and therefore contain a seasonal trend. Although the magnitude of the difference between winter and summer season is small for the cost optimized trajectories, the difference is large enough to conclude a seasonal trend. The small

variance in the data increases the power of the test.

The difference in altitude between the cost and climate optimized trajectories is shown in figure 6.33. The figure shows a decreasing trend for the difference in altitude and a linear trend line which suits the data relatively well. The Mann-Whitney U test provides a test statistic of $5.67 * 10^{-10}$ which indicates a strong seasonal effect, showing that the difference in flight altitude reduces from January to June.

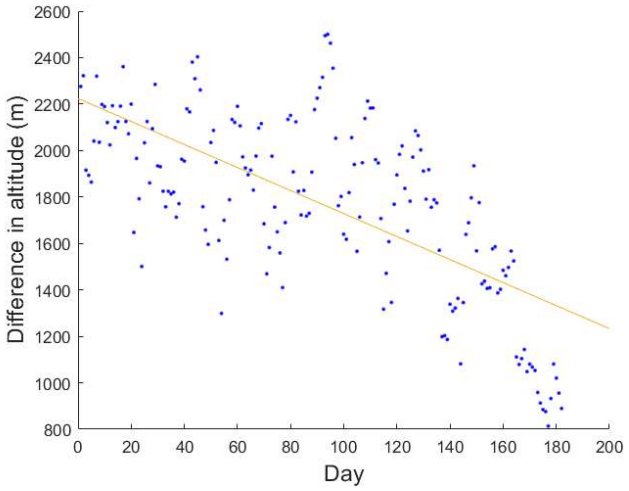

Figure 6.33: Difference between the average cost and climate optimized flight altitude during a period of six months

The difference in flight altitude between the winter and summer season can be explained using figure 6.22. The average contrail potential coverage is reduced during the season allowing aircraft to fly higher without forming sustained contrails. This is not considered for the cost optimized flights so these flights are not affected by the reduced contrail potential coverage.

6.4.5 Emissions

Important parameters which determine the flight trajectories of the climate optimized flights, are the emissions resulting in radiative forcing. As was already established before, the most important source of radiative forcing is the contrail potential coverage, but occasionally when the contrail potential coverage is approximately zero, other species such as carbon dioxide and ozone dominate the total radiative forcing. The ATR20 of the cost and climate optimized trajectories is shown in figure 6.34.

Figure 6.34 shows that the climate impact of the cost optimized flights is positive (temperature increase) for the majority of the days. The climate optimized impact has a larger variance where also a large number of days show a negative climate impact (which results in a temperature decrease of the atmosphere). On average, the climate optimized flights have a lower climate impact. There is no

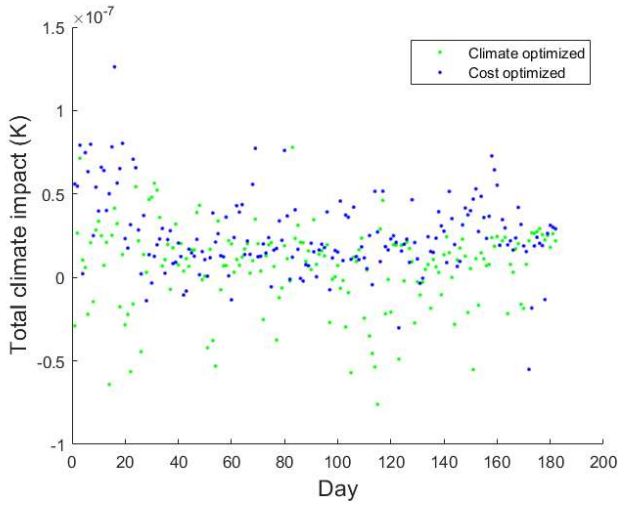

Figure 6.34: Total climate impact of the cost and climate optimized trajectories during a period of six months

direct motivation to believe that the climate nor the cost optimized flights contain a seasonal trend. This is supported by the Mann-Whitney U test which does not reject the null-hypothesis.

6.4.6 Operational Costs

As was shown in the previous section, there is no clear indication of a seasonal effect for the climate impact of the cost and climate optimized flights. A similar analysis can be done to establish whether or not the operating costs change during the year. The operating costs are a function of the flight time and fuel consumption. The total operating costs per day are shown in figure 6.35, where the operating costs of the climate optimized trajectories is represented by the green dots.

Figure 6.35 shows that the operating costs of the climate optimized trajectories are higher during the entire analysis spectrum. However, the climate optimized trajectories seem to show a decreasing trend while the operating costs of the cost optimized trajectories are fairly constant during the year. To find out if these trends show a significant seasonal effect, the Mann-Whitney U test will be used. The test provides a test statistic which rejects the null-hypothesis of both the cost and climate optimized flights which means that the operating costs of both flight types contain a seasonal trend. The cost optimized trajectories have a significant difference in operating costs because the standard deviation is small and the number of days which are analyzed is relatively large, resulting in a large number of data points.

on average, the operating costs have a smaller magnitude in the summer season compared to the winter season. This is a result of the reduced flight time in the summer season (figure 6.26), because the flights have a larger operating speed (figure 6.25a). For the climate optimized flights, the decreased flight time is accompanied by a reduced fuel consumption (figure 6.24) in the summer season, which

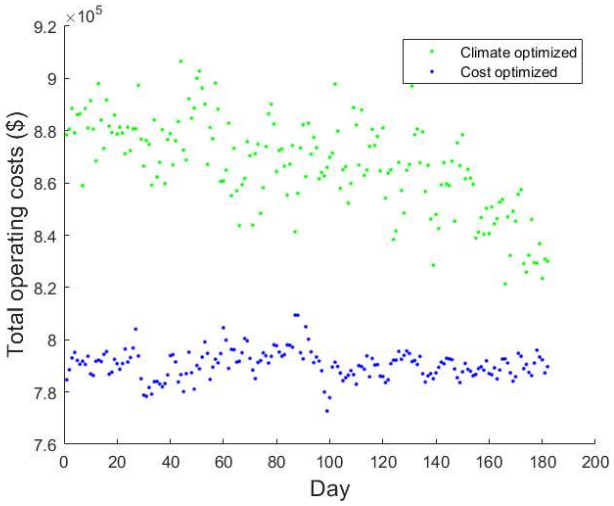

Figure 6.35: Total operating costs of the cost and climate optimized trajectories during a period of six months

amplifies the seasonal effect. The fuel consumption of the cost optimized flights has an increased value during the summer season which almost levels the operating costs during the year. Although, there is a notable difference in the gradient between the cost and climate optimized trajectories, both flight types contain a seasonal trend.

6.4.7 Offset Type

The analysis of the offset type can be used to see if there is a significant difference between the two seasons. Figure 6.36a shows the fraction of the flights in each offset type for the winter season while figure 6.36b shows the same for the summer season.

The KS method provides a statistic about the probability of having the same distribution of the trajectory types during winter and summer season. The distribution of the climate optimized flights has a statistically significant probability ($1.04 * 10^{-31}$) to reject the null-hypothesis and therefore it can be concluded that there is indeed a difference between the offset types of the summer and the winter season. The null-hypothesis of the cost optimized trajectories is not rejected (0.32), meaning that it can not be concluded that there is a significant difference between the cost optimized trajectory types during winter and summer.

6.5 Directional Effect

An important difference between trans-Atlantic and European flights is the fact that trans-Atlantic flights only have two main flight directions (west and east) and European flights, are heading in many different directions. To be able to draw conclusions on the direction of flight for European flights, the

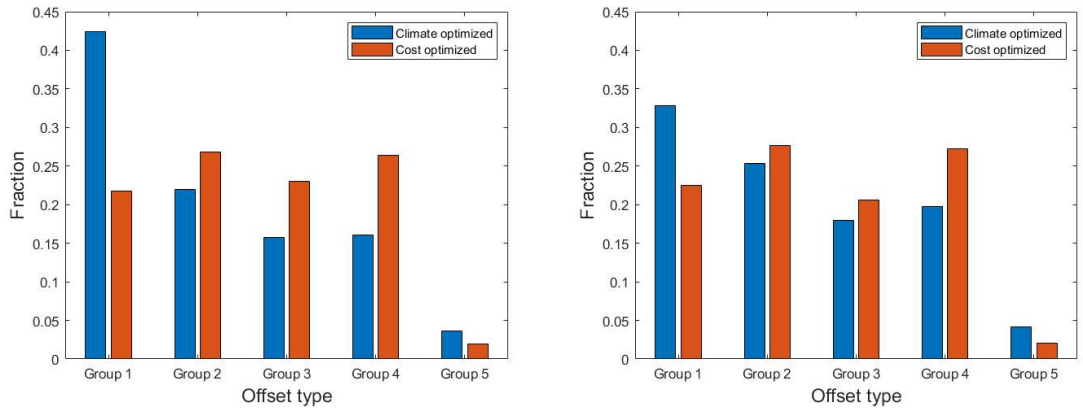

(a) Winter **(b)** Summer

Figure 6.36: Fraction of the flights in each offset type for the winter and the summer season

flights are divided into four flight directions as explained in chapter 5. The variability of the four flight directions will be evaluated by comparing the cost and climate optimized trajectories for geographical location, altitude and emissions. Occasionally, the cost and climate optimized trajectories will be compared to the great circle trajectories.

In contrast to the seasonal analysis, the flights evaluated in each flight direction are different and therefore it is difficult to compare the results of two different flight directions. Furthermore, the number of flights in each flight direction is different. The eastbound direction contains 30 flights, while the northbound flights consist of only 12 flights. There are 32 westbound flights and the southbound direction contains 10 flights. To be able to compare the results more equally, certain results will be normalized by dividing by the flight length, which will be indicated accordingly.

6.5.1 General Atmospheric Characteristics

Atmospheric characteristics play an important role in seasonal analysis as the atmospheric properties change during the year. However, the atmospheric characteristics are also affected by the geographical location as was established in figure 6.5. Each flight direction has its own flights which all fly in a different parts of the European airspace. Table 6.12 shows the average latitude of all flights in a each flight direction.

The average latitude of the flights in each flight direction show a substantial difference. The Mann-Whitney U test provides proof that the north- and southbound flights have a significantly higher average latitude than the east- and westbound flights (probability <0.05).

6.5.2 General Flight Characteristics

General flight characteristics include the fuel consumption, flight speed and time. This is evaluated for the four groups for cost and climate optimized flights. The fuel consumption and flight time are

Table 6.12: Average latitude of the flights in each flight direction

	Average latitude (deg)
Eastbound	43.84
Northbound	45.52
Westbound	43.95
Southbound	44.76

normalized and given per kilometer. This is done to be able to compare the fuel consumption and flight time results of the flights in different directions. The results are shown in tables 6.13 and 6.14 for climate and cost optimized respectively.

Table 6.13: General flight characteristics of the flights in each flight direction for climate optimized flights

	Eastbound	**Northbound**	**Westbound**	**Southbound**
Flight speed (km/h)	912	859	820	862
Fuel consumption (kg/km)	6.01	6.27	6.78	6.22
Flight time (sec/km)	4.02	4.18	4.50	4.16

Table 6.14: General flight characteristics of the flights in each flight direction for cost optimized flights

	Eastbound	**Northbound**	**Westbound**	**Southbound**
Flight speed (km/h)	915	853	802	850
Fuel consumption (kg/km)	4.99	5.33	5.72	5.39
Flight time (sec/km)	3.91	4.20	4.47	4.22

Tables 6.13 and 6.14 show that the average flight speed of both, the cost and climate optimized trajectories have the largest magnitude for eastbound flights and the smallest magnitude for westbound flights. This can be explained by the wind direction which generally has an eastbound direction. This increases the ground speed of eastbound flights and decreases the ground speed of westbound flights. The wind direction also results in lower fuel consumption and flight time for eastbound flights and an opposite effect for westbound flights. North- and southbound flights show similar results as these flights are less, but similarly affected by the wind direction. If the fuel consumption is corrected for the flight speed, the eastbound flights still have the lowest fuel consumption. This occurs because the engine has a higher efficiency when the flight speed is increased.

Comparison of the cost and climate optimized flights shows that indeed the average flight speed of the cost optimized flights is lower than the flight speed of the climate optimized flights. However, the largest differences between cost and climate optimized trajectories is obtained for west- and southbound flights, where the cost optimized eastbound flights, fly faster than the equivalent climate optimized flights.

The fuel consumption of the cost optimized flights is lower for every flight direction compared to the climate optimized flights, which is related to the average altitude and reduced flight distance. This also explains the reduced flight time of the cost optimized flights even though the flight speed of these flights is shorter.

6.5.3 Horizontal Trajectory

The geographical location of each trajectory is given by 101 waypoints where each waypoint includes a lateral and longitudinal coordinate. The horizontal trajectory is composed of these two coordinates. The average flight distance of the cost and climate optimized trajectories sorted by flight direction is shown in table 6.15.

Table 6.15: Average flight distance of the cost and climate optimized trajectories for four different flight directions

	Climate optimized (km)	**Cost optimized (km)**
Eastbound	1718	1669
Northbound	1167	1164
Westbound	1773	1716
Southbound	1333	1331

Table 6.15 shows that the average flight distance of the cost optimized trajectories has a smaller magnitude than the flight distance of the climate optimized trajectories for all flight directions. Furthermore, the average flight distance of the east- and westbound flights have a significantly longer flight distance which is evaluated by Mann-Whitney U test. The table also shows that the difference in flight distance between the cost and climate optimized flights is smaller for shorter flights. The difference in flight distance of the east- and westbound flights is approximately 3% while the difference for the north- and southbound flights is less than 0.3%.

Table 6.15 does not show the spread of the average flight distance during the year. This is visualized in figure 6.37, showing the average flight distance for all four directions of the cost and climate optimized trajectories. Figure 6.37b shows that the spread in the data is relatively small for all flight directions. On the other hand, figure 6.37a shows that the average flight distance of the east- and westbound flights is fluctuating (without a seasonal trend). This can be expressed by the standard deviation of these data series. The standard deviation of the climate optimized east- and westbound flights is ten to twenty times higher than the standard deviation of the other data series.

The results show that there is a notable change in the weather which results in a relatively large change of the average flight distance over time for the east- and westbound flights. The flight distance is changed as such that the climate impact is minimized which sometimes requires additional flight path distance.

The deviation of the cost and climate optimized trajectories can be measured in two ways, which are the average offset and the average absolute offset. This is explained in section 5.2. The two different types of offset allow for general conclusions on the manner in which the cost and climate

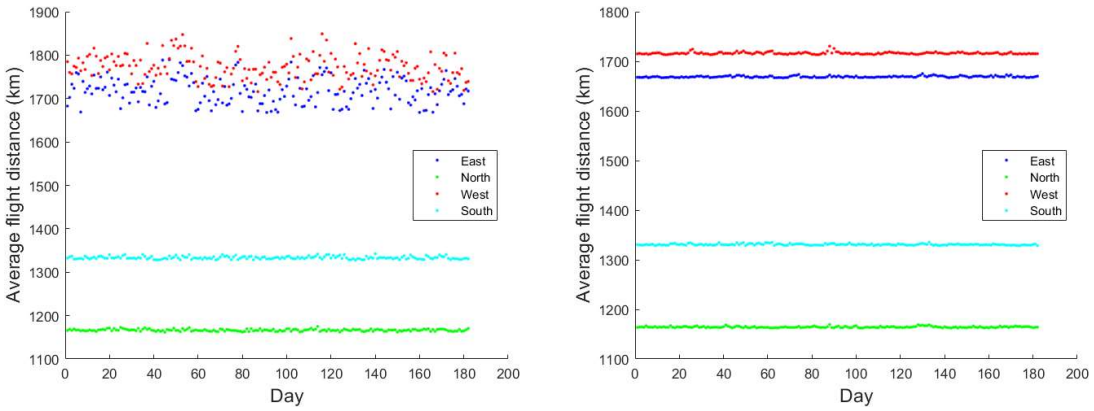

(a) Climate optimized **(b)** Cost optimized

Figure 6.37: Average flight distance of the cost and climate optimized trajectories during the winter and the summer season

optimized flights deviate from the great circle flights. The offset is determined perpendicular to the flight direction which means that for example, the offset of a westbound flight is measured in a lateral direction. For flights in a north- and southbound flight direction, the offset in a longitudinal direction is computed.

Since most flight are not exactly flying in the direction they are appointed to, a correction factor is applied taking the actual flight angle into account. For instance, a flight which has a flight angle of 44.9 degrees is a flight in a northeastern direction. However, it is considered as an eastbound flight. The offset is not only towards the north or south, but also towards the west or east. To compensate for this, the offset towards the north or south is divided by the cosine of the flight angle (represents the correction factor).

The resulting average offset for both the cost and climate optimized flights is shown in figure 6.38 and the absolute offset of both trajectory types is shown in figure 6.39. The four flight directions are all represented by a different color in the figures. The figures show the average offset of each day for a period of six months. The results are also summarized in tables D.1 and D.2 in appendix D.

Figure 6.38a shows the average offset of the climate optimized trajectories. It shows that the north- and southbound flights are located closer to zero with both negative and positive deviations from the great circle trajectories. This is confirmed by figure 6.39a which shows a clear deviation between the offset of the north- and southbound flights, and the east- and westbound flights. The offset is in line with expectations, because an increased trajectory length is accompanied by an increased absolute offset. Figure 6.38a also shows that the average offset is more often positive for the east- and westbound flights meaning that the offset is in a northern direction. Tables D.1 and D.2 reveal that the average offset is positive for all flight directions and that the westbound flights have an offset which is significantly larger than the offset of the other flight directions (probability <0.05). Although, the

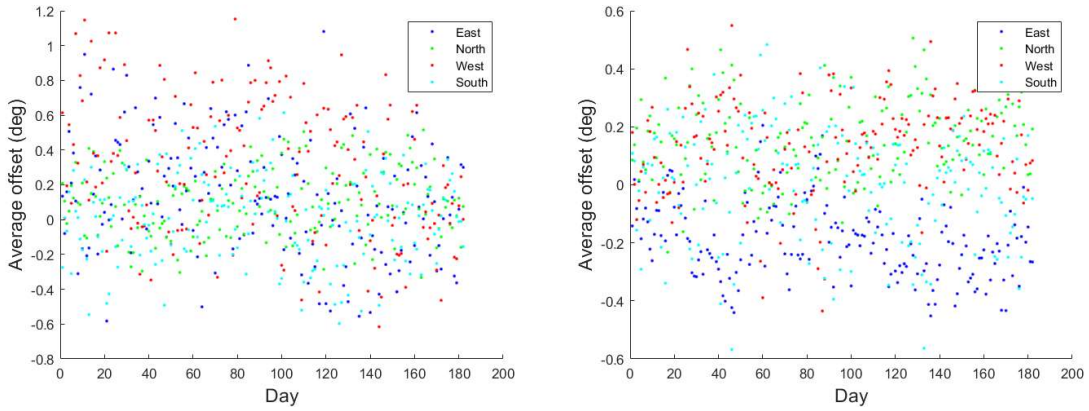

(a) Climate optimized **(b)** Cost optimized

Figure 6.38: Average offset of the cost and climate optimized trajectories from the great circle trajectories during the winter and the summer season

average offset of the eastbound flights is smaller than the average offset of the westbound flights, the absolute offset of the east- and westbound flights are similar. From this, it can be concluded that the eastbound flights have a more even distribution of positive and negative offset, while the westbound flights have a similar magnitude, but are deviating more towards the north.

In section 6.3, it was concluded that if the length of the trajectory is increased, the average offset is increased as well. This is in line with the results found in figure 6.38a. The east- and westbound flights have a longer average flight distance and as a result, the magnitude of the average offset of the flights in these two directions is larger as well.

Figure 6.38b shows that the eastbound flights often have an offset in a negative direction which means that the offset is usually south of the great circle flights. The northbound flights mainly show a positive average offset which denotes an offset towards the west compared to the great circle flights. The westbound flight also have a positive average offset which means that the offset is located north of the great circle trajectory. The southbound flight have and average offset of approximately zero. Even though there is a significant (proven using Mann-Whitney U test) difference in average offset between the four flight directions, the average absolute offset of all directions is similar. This means that for the eastbound flights, the magnitude of the offset is similar to the offset of the flights in the other directions but the average offset is more negative (southwards).

6.5.4 Vertical Trajectory

The altitude of the optimized flights is important as it determines the climate impact but also the fuel consumption and flight time. Table 6.16 shows the average altitude of the cost and climate optimized trajectories for four different flight directions.

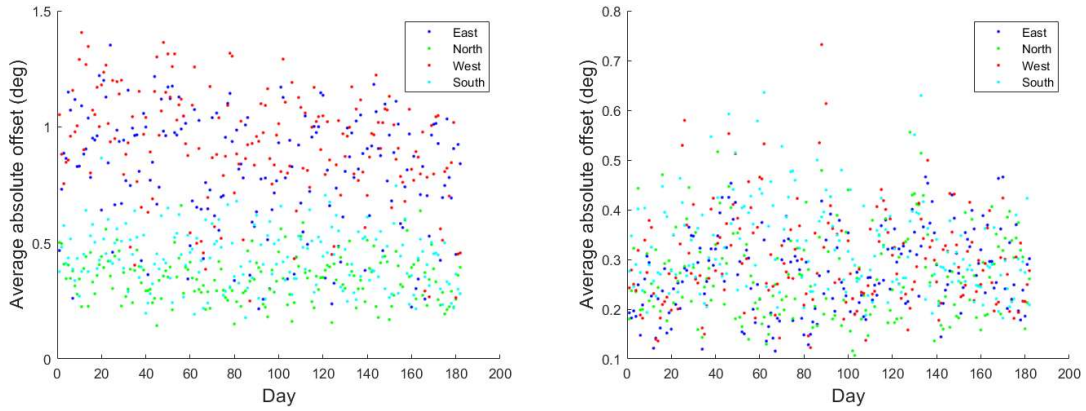

(a) Climate optimized **(b)** Cost optimized

Figure 6.39: Average absolute offset of the cost and climate optimized trajectories from the great circle trajectories during the winter and the summer season

Table 6.16: Average altitude of the cost and climate optimized trajectories for four different flight directions

	Climate optimized (m)	**Cost optimized (m)**
Eastbound	9914	11673
Northbound	9927	11665
Westbound	9812	11619
Southbound	9916	11640

Table 6.16 shows that the climate optimized trajectories have a lower average altitude than the cost optimized trajectories which was already established before. However, the altitude of the flights in the different directions is not similar. The altitude of the westbound flights has the lowest average for both the cost and climate optimized trajectories. The average altitude of the flights during the 182 days which are analyzed, is shown in figure 6.40 for climate (6.40a) and cost (6.40b) optimized trajectories.

Figure 6.40a does not show a clear deviation in altitude between the four directions. The cost optimized trajectories show a more clear deviation between the different flight directions. As can be seen in figure 6.40b, the flights in an eastern direction (blue dots) have the largest average value and the westbound flights (red dots) have the lowest average altitude. This is in line with the results obtained in table 6.16.

In order to find out if the difference in altitude between the different flight directions is significant, the flight directions can be tested using a Mann-Whitney U test to determine whether or not the mean of the data sets is the same. The test rejects the null-hypothesis of all cost optimized flight directions meaning that there is a significant difference in altitude between all four flight directions. Only the

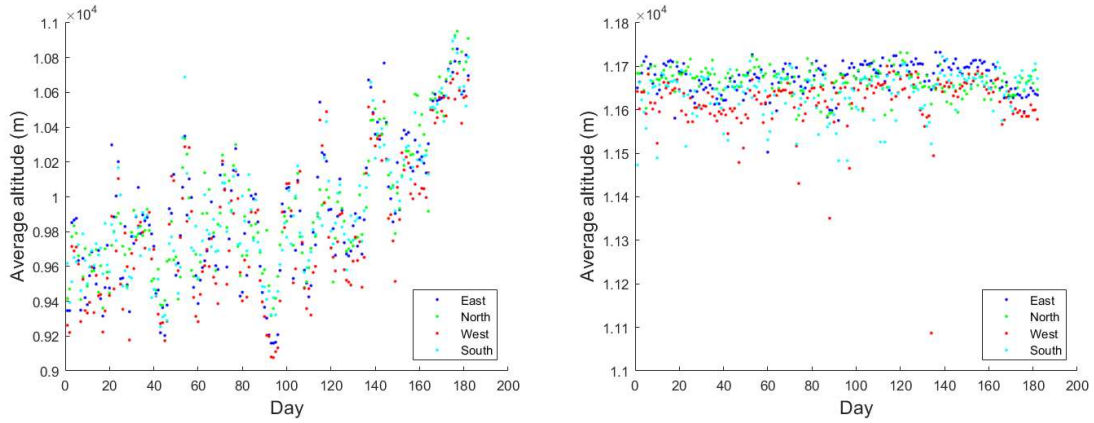

(a) Climate optimized **(b)** Cost optimized

Figure 6.40: Average altitude of the cost and climate optimized trajectories during the winter and the summer season

null-hypothesis of the climate optimized flights heading in a western direction is significantly different from all other directions meaning that the western flights have a significant altitude offset from the other three flight directions.

From table 6.12 it would be expected that since the northbound flights have the highest average latitude, this would result in the lowest average altitude. However, the northbound flights have the highest average altitude for the climate optimized trajectories.

The altitude difference between the cost and climate optimized trajectories is illustrated by figure 6.41. The difference is computed by subtracting the altitude of the climate optimized trajectories from the cost optimized trajectories. The average altitude difference is also numerically evaluated and shown in table 6.17.

Table 6.17: Average altitude difference of the cost and climate optimized trajectories for four different flight directions

	Cost - Climate (m)
Eastbound	1760
Northbound	1738
Westbound	1807
Southbound	1724

The average altitude difference is decreasing for the summer season as was also found in figure 6.33, but figure 6.41 shows that this holds for every individual flight direction. Using table 6.17, the average altitude difference of the east- and westbound flights have the highest magnitude but these flight also

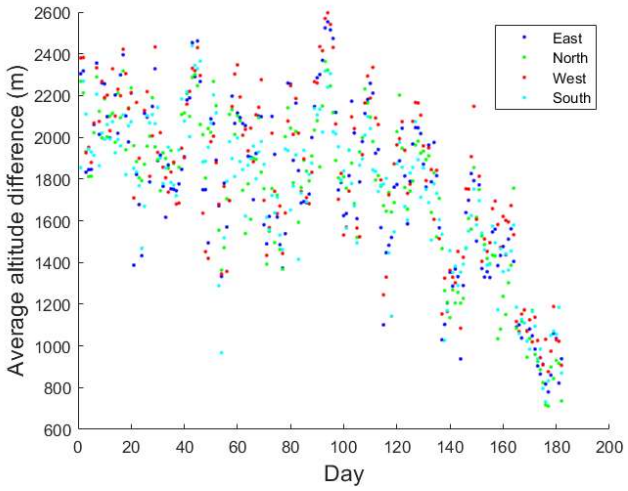

Figure 6.41: Difference in altitude between the cost and climate optimized trajectories for four different flight directions

show the largest fluctuation. While the north- and southbound flights are located closer towards the mean, the east- and westbound flights show more extreme values both positive and negative with respect to the mean. Similar to the average offset of the east- and westbound trajectories, the average flight distance represented in figure 6.37a shows that the east- and westbound flights are trying to avoid climate sensitive regions which occasionally requires more additional flight distance and altitude. The fluctuation is most likely related to the average flight distance, as an increased flight distance allows for more offset from the mean.

6.5.5 Emissions

The emissions and corresponding climate impact of the flights in different directions is expected to be different, because the average flight distance of the flights in four different directions is dissimilar as is shown in table 6.15. The east- and westbound flights have significantly longer flight trajectories than the north- and southbound flights. Therefore, in order to be able to analyze the climate impact of the trajectories, the climate impact is normalized such that the climate impact per kilometer is shown. The results of the average climate impact per kilometer for the cost and climate optimized trajectories is shown in figure 6.42. The means of the flights in each direction for the cost and climate optimized routes are represented in table E.1 in appendix E.

Figure 6.42 shows that the climate optimized trajectories have a lower average climate impact than the cost optimized trajectories. Furthermore, figure 6.42a shows that the south- and westbound flights have a more positive impact during the winter season and moreover, the westbound flights show a more negative climate impact during the summer period. Using a Mann-Whitney U test, it is confirmed that there is a seasonal effect present for the west- and southbound flights. Figure 6.42b shows that the first month of the cost optimized flights in all flight directions results in a relatively high

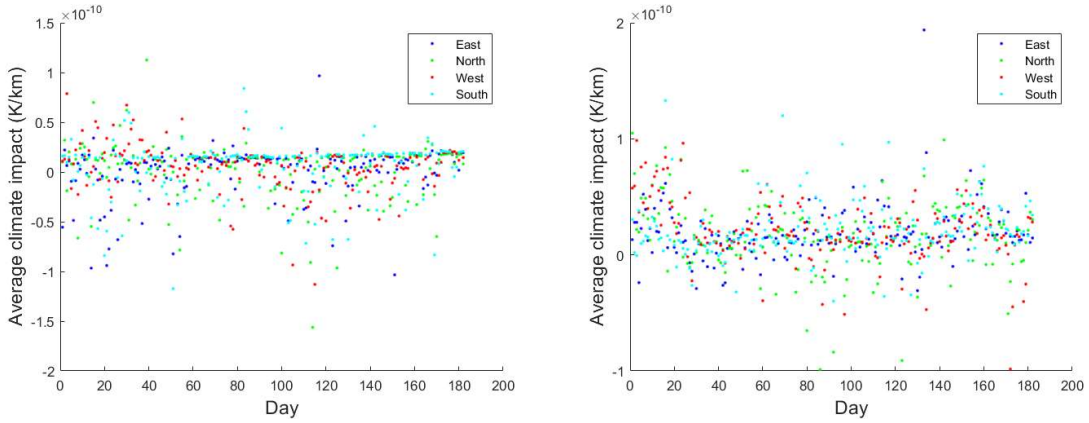

(a) Climate optimized **(b)** Cost optimized

Figure 6.42: Average climate impact per kilometer of the cost and climate optimized trajectories for four different flight directions

positive average impact per kilometer. This is mainly caused by contrail formation during a cold period resulting in a high climate impact.

In section 6.3, it was shown that the average climate impact per kilometer is not affected by the flight distance. So any differences in the average offset between the flights in different directions can not be assigned to the difference in flight distance. During the summer period the trajectories which are climate optimized shows numerous days with negative outliers while during the winter period, the outliers are almost equally divided among positive and negative values. The Mann-Whitney U test shows that the difference in climate impact between all flight directions is insignificant (probability >0.05), except for the difference in climate impact between the east- and southbound climate optimized flights (probability <0.05), where the eastbound flights have a lower average climate impact.

Figure 6.43 shows the average climate impact per kilometer of the cost and climate optimized trajectories where the contrail potential coverage is left out. There is a clear seasonal trend visible for the flights in all flight directions. Furthermore, figures 6.43a and 6.43b show a more clear separation of the climate impact per flight direction. It reveals that the southbound flights have the highest average climate impact when contrail potential coverage is not taken into account. This is not true for the climate impact including contrails.

The climate optimized trajectories have a higher average climate impact without taking contrails into account. This is also amplified by figure 6.43a which only contains positive values, while the climate impact including contrails also often contains days with a negative climate impact (temperature decrease). However, when the contrail potential coverage is included, the standard deviation also increases which means that the data contains more extreme values, both positive and negative. The trajectories which are cost optimized have a larger average climate impact when the contrails are taken into account. This shows that when a trajectory is optimized to reduce the climate impact,

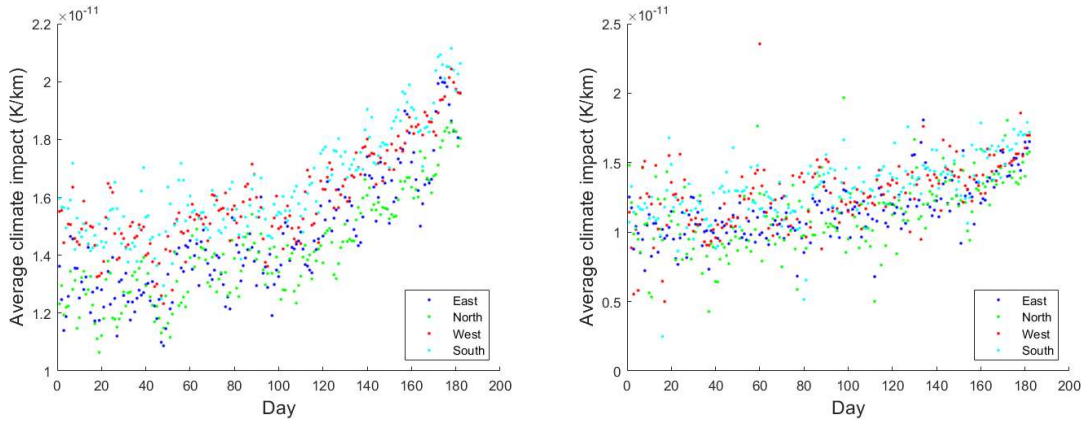

(a) Climate optimized **(b)** Cost optimized

Figure 6.43: Average climate impact per kilometer without the contrail potential coverage of the cost and climate optimized trajectories for four different flight directions

contrail potential coverage can be used if utilized correctly, to decrease the overall climate impact of the flights.

6.5.6 Operational Costs

The total climate impact contains a seasonal trend and although it is not clearly present in the contrail potential coverage, the other species show an increasing trend as the year progresses for all flight directions. The operating costs are also considered for each flight direction and are dependent on the flight time and fuel consumption. Since the flight direction plays an important role in how effectively wind can be used, it is expected that there are differences in operating costs between the various flight directions. The operating costs of the cost and climate optimized trajectories are presented in table 6.18. Since the number of flights in each direction is not the same and the average flight distance is different as well, the operating costs are averaged per flight and kilometer.

Table 6.18: Average operating costs per kilometer of the flights in each flight direction during a period of six months

	Climate optimized ($/km)	**Cost optimized ($/km)**
Eastbound	2.98	2.53
Northbound	3.18	2.70
Westbound	3.34	2.90
Southbound	3.15	2.73

Table 6.18 shows that there is a difference in the operating costs for each flight direction. For both, the cost and climate optimized trajectories, the highest operating costs per kilometer are obtained for westbound flights and the lowest costs are obtained for eastbound flights. This is mainly a result

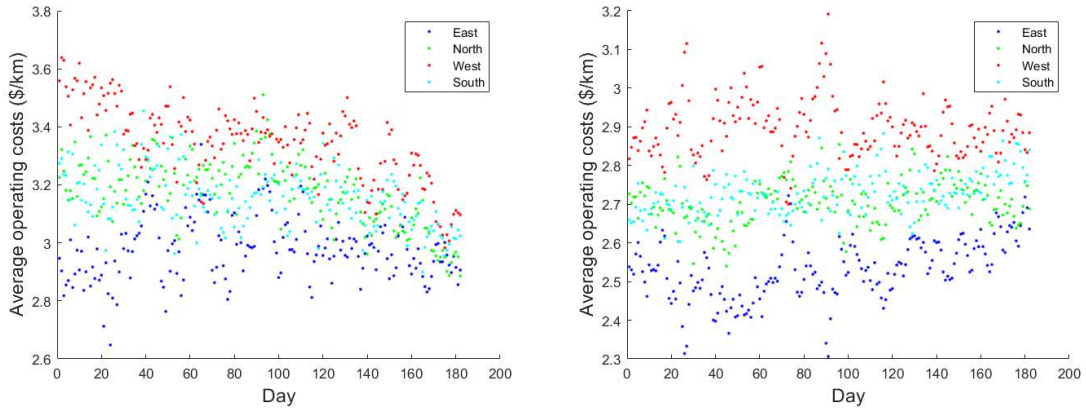

(a) Climate optimized **(b)** Cost optimized

Figure 6.44: Operating costs of the flights in four different flight directions during a period of six months

of the wind direction which is has an eastbound direction. The wind results in additional fuel consumption and an increased flight time for flights in a westbound direction. Furthermore, the climate optimized operating costs have a higher magnitude than the same cost optimized operating costs for all directions.

The operating costs of the flights in each flight direction can also be shown graphically for the entire simulation period. This is shown in figure 6.44 for both, the cost and climate optimized flights. The operating costs are presented per kilometer. Figure 6.44 shows that the operating costs of both, the cost and climate optimized flights are converging as the year progresses. This is a result of the reduction of the wind speed during the year. As table 6.18 already indicated, the average operating costs per kilometer of the north- and southbound flights are really close together.

The difference between each of the flights in various directions is significantly different from the other directions for both, the cost and climate optimized flights even though the operating costs of the north- and southbound flights are close together. This is proven using the Mann-Whitney U test which provides the test statistic for whether or not the data has the same mean. However, the probability of having the same mean is the largest when comparing the north- and southbound flights.

6.5.7 Offset Type

The manner in which the aircraft tend to offset from the great circle trajectory for all different flight directions is captured in figure 6.45. Each flight direction is represented by its own color in the figure and the fraction of all flights in each offset type is shown by the magnitude of each bar.

The offset types of the climate optimized flights differ a lot from the offset types of the cost optimized trajectories. The westbound flights dominantly offset in a northern direction for both the cost and

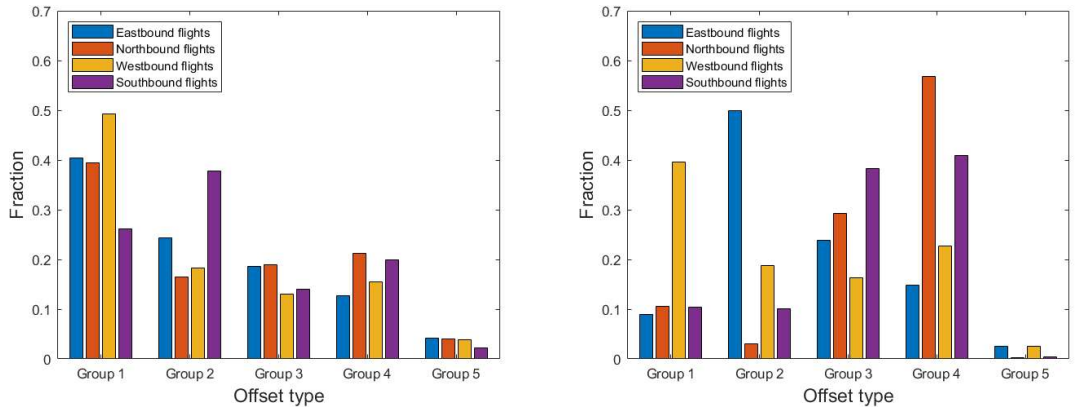

(a) Climate optimized **(b)** Cost optimized

Figure 6.45: Distribution of the flights over five different offset types as established in figure 5.7

climate optimized flights. The climate optimized flights flying in a southern direction, mainly have a negative offset meaning that the trajectories are strictly west of the great circle routes.

Furthermore, most east-, north- and southbound climate optimized flights are located in the first offset type, which means that the offset is positive compared to the great circle path. There is a larger spread for the offset types of the cost optimized trajectories where the maximum fraction of the west- and eastbound flights is located in group one and two respectively. The largest fraction of the north- and southbound flights is located in group four. Finally, the southbound cost optimized flights are predominantly in groups three and four meaning that they consistently cross the great circle trajectories once. The same holds for the northbound flights where approximately 90% of the flights crosses the great circle trajectory once during the flight.

6.6 Summary of the Results

The objective of this thesis was to examine the variability of the trajectories when for instance a cost optimized trajectory is optimized towards reducing the climate impact or vice versa. Furthermore, the trajectories were compared to the great circle trajectories to evaluate the offset from these great circle trajectories. Finally, the flight direction was examined and the existence of a seasonal trend was explored.

From a cost optimized point of view, which are the flight trajectories which are currently exploited by airliners, the climate impact can be reduced by approximately 73% if the flight trajectories are climate optimized. However, this induces a cost increase of about 8%. The cost increase is induced by additional fuel burn and flight time.

The climate impact reduction is not only caused by a reduction of emissions, since the emissions are increased for the climate optimized trajectories. This results in higher climate impact of species such

as carbon dioxide, water vapor and ozone. However, contrail formation is highly location dependent and by optimizing to reduce the climate impact, the trajectories often avoid regions with high contrail potential coverage which results in an overall climate impact reduction.

In order to keep the operating costs low, the cost optimized flights, fly at a flight altitude which is about 18% higher than the flight altitude of the climate optimized flights. In order to avoid climate sensitive regions, the climate optimized flights make more detours which results in higher average offset from the great circle trajectory. As a result, the average length of the cost optimized trajectories is only 0.3% longer than the great circle trajectories, while the flight length climate optimized trajectories is approximately 2.8% longer.

The presence of a seasonal effect is proven by the Mann-Whitney U test, by comparing the first three months to the second three months. Due to a temperature increase in the summer season, contrail potential coverage is reduced which allows for an offset reduction and an altitude increase of the climate optimized flights. The average offset of the climate optimized trajectories is almost halved during the summer season and the altitude of the climate optimized flights during the second three months is increased by 4%. As a result, the operating costs of the climate optimized flights are reduced by 2% but there is no direct reason to believe that the climate impact is different in the winter than during the summer.

The flights grouped in each flight direction have different properties and are therefore more difficult to compare. The operating costs and climate impact of these flights are affected by the wind direction and speed. The dominant wind direction was nearly east and therefore eastbound flights could utilize the wind in order to reduce the fuel consumption or flight time and the westbound flights tried to avoid the jet stream in eastern direction. The jet stream results in a significant difference in flight speed, flight time and fuel consumption of the eastbound flights for both the cost and climate optimized flights and therefore an increase in operating costs.

7 Future of Aviation

Aviation is an important means of transport as it allows people to travel fast between places all over the world. However, as established in this study as well, aviation is also a highly polluting means of transportation. As explained in chapter 1.1, there are several ways in which climate impact from aviation can be mitigated, one of which is examined in this thesis. This thesis shows that with the current technologies, the climate impact of aviation can be reduced by avoiding climate sensitive regions such as regions with high probability of contrail formation. However, flying these trajectories is accompanied with additional operating costs. Therefore, other propulsion types should also be examined to detect other ways to reduce the climate impact of aviation.

An example type of propulsion which could be examined, is electrical flying. This can be done fully electrical or hybrid. Electrically powered aircraft have the advantage of (partially) substituting fossil fuels for renewable energy. Lithium batteries have the potential to function as the energy source for short-haul flights in the upcoming future (H. Kuhn, 2012). However, not only electric flying has to be considered, but alternative fuels can also be utilized.

Two alternative fuels that can be used for the engine combustion are liquid hydrogen (LH2) and liquid natural gas (LNG), which mostly consists of methane. The advantage of these types of fuel is that it omits carbon dioxide as a product of combustion. However, taking into account the calorific values of both kerosene and liquid hydrogen and the amount of water vapor that is released during the combustion process, combustion of liquid hydrogen results in an increase of the emissions of water vapor. This is shown by equation 3.

$$2H_2 + O_2 \rightarrow 2H_2O \tag{3}$$

The higher calorific value of liquid hydrogen is approximately 142 MJ/kg (Engineering Toolbox, 2003) and by burning 1 kilogram of liquid hydrogen, approximately 9 kilograms of water vapor are emitted. The higher calorific value of kerosene is 43 MJ/kg (Engineering Toolbox, 2003) and during the combustion process of kerosene, 1.29 kilogram of water vapor is released by burning 1 kilogram of kerosene. This shows that in order to have the same power coming from the aircraft engine, the water vapor emissions are more than doubled.

The advantage of burning liquid hydrogen as fuel is that there are no carbon products involved in the combustion. A conventional aircraft engine will almost always have an incomplete combustion which results in byproducts such as unburned hydrocarbons and soot particles. There are strong indications that these particles increase the contrail-cirrus formation as ice crystals are more easily formed on these particles. Overall, it is expected that liquid hydrogen as fuel will reduce the radiative forcing due to contrails (Grewe et al., 2016).

Liquid hydrogen can be implemented in the model as fuel for simulating air traffic. This will require a modification of the EMAC model. Analysis of the climate optimized trajectories should eventually show if liquid hydrogen indeed results in a lower average temperature response in twenty years. Since the model focuses on the reduction of contrail potential coverage, the results immediately reveal the impact of liquid hydrogen on contrail formation and how the contrails sustain. Finally, it is required

to also analyze the operating costs accompanied with liquid hydrogen. In this analysis, parameters such as the production costs and the required fuel volume/weight need to be evaluated as well.

The flight planning that is done in this model is planned on previously known weather situations, which is useful to get a general idea about flight patterns that on average avoid climate sensitive regions or flight paths that on average result in low operating costs. Eventually however, it would be ideal to accommodate aircraft with live flight planning, where flights are planned according to the current weather situation. This requires a computationally heavy software which is capable of doing real time flight planning.

Overall, future technologies are required to reduce the fuel consumption of air traffic. Burning sustainable types of fuel and flight planning can be used now and in the future to reduce the climate impact of aviation even more. Reduction of climate impact is often accompanied with additional operating costs which is a trade-off and a Pareto front can be used which is created using a weighted optimization to find a balance between operating costs and climate impact.

8 Discussion & Conclusion

The aim of this research was to identify how trajectory optimization affects the direct operating costs and the climate impact of flights in the European airspace and to evaluate the variability of these trajectories. Furthermore, during the project, the effect of the season and the flight direction were evaluated. The model that was used to analyze these flight trajectories is the EMAC model which includes an earth atmospheric model as well as a sub-model to simulate and optimize air traffic.

The analysis was done simulating an Airbus A330 using two General Electric CF6 engines. The simulation time period was chosen between January 1^{st} and June 30^{th} of the year 2016 which allowed for the comparison between two seasons which are named the winter and summer season. Furthermore, a six month period allows for a data set with a large number of data points which increases the strength of the statistical analysis done for general results as well as the comparison between flight directions.

The results that were obtained from the simulation of the EMAC model show that there were days in which the climate impact of the climate optimized flights is higher than the climate impact of the same cost optimized flights. This shows that the model is not performing as intended. Similarly, there are flights which are climate optimized which have lower operating costs than their equivalent cost optimized flights. However, this does not result in daily averages with higher operating costs for the cost optimized flights.

Research has revealed that on average, each day, 53 out of 85 flights have a climate impact which is larger for the climate optimized flights than for the cost optimized flights. Out of these 53 flights, most flights have no difference in the radiative forcing due to contrails but rather had a larger climate impact due to CO_2 and NO_x emissions. However, during days in which the difference between the climate impact of the cost and climate optimized trajectories is relatively large, both positive and negative, this is caused by the difference in the contrail potential coverage. This shows that the optimization model aims at optimizing towards reduction of the impact of contrails.

The model also shows that there are regions in Europe where the simulation concludes more extreme results, both for a positive and a negative climate impact. It shows that the trajectory which on average has the highest positive difference in climate impact between the cost and climate optimized route is originated from the same airport (and arrives at an airport close to) as the trajectory with the highest negative difference in climate impact between the cost and climate optimized route. The region between Gran Canaria and Portugal has shown to be a volatile region where the optimization has trouble to converge to a global minimum. Finally, the central European region where many flights are located also leads to a large number of trajectories where the optimum is not found, especially for the climate optimized trajectories. The difference in climate impact between the cost and climate optimized trajectories is dominated by the difference in contrail potential coverage. This shows that the central European region is a region with a large potential to form contrails which can be utilized both in a positive and a negative manner. The genetic algorithm is often unable to find a global optimum due to the complexity of contrail formation in the atmosphere.

The results of the cost and climate optimized flights can be compared to the great circle trajectories, showing that by definition, both flight types have a longer average flight length but, the cost optimized

routes have a distance which is fairly close to the great circle distance to reduce the flight time and fuel consumption. The climate optimized trajectories have an increased average flight length which results in additional fuel burn and flight time. Furthermore, the average flight altitude of the cost optimized trajectories is significantly higher than the altitude of the climate optimized trajectories. A higher altitude results in less emissions as the fuel consumption is reduced, but the impact of the emitted species is higher which makes it efficient for the climate optimized routes to fly lower. As a result, the climate optimized routes have the lowest total climate impact, but this leads to the highest total operating costs.

The latitude also plays an important role in the climate impact of aviation. In order to reduce the climate impact of the climate optimized flights, the average flight altitude is reduced as the latitude increases. Furthermore, the manner in which the climate and cost optimized flights offset from the great circle trajectories is different. The cost optimized trajectories are almost equally divided over the first four groups while the climate optimized flights are clearly more present in the first group meaning that for east- and westbound flights, the offset is more north than south and for the north- and southbound flights, the offset is more often towards the east.

If the results of the simulation for Europe are compared to a similar simulation for the trans-Atlantic region, it shows that although the flight patterns are different since the flights are not dominantly flying east or west, the results are still similar. For both, the trans-Atlantic and the European region, the normalized flight distance and time are longer for the climate optimized trajectories and the altitude is lower compared to the cost optimized trajectories. However, the mean latitude shift of the trans-Atlantic flights is south while the analysis of the European flights shows an average shift towards the north.

After the analysis of the flight segments it was found that the initial and final segments of the flight where often a change of altitude takes place shows an increase in the fuel consumption and therefore an increase in the climate impact during these phases of the flights. This is also a result of the flight altitude where the efficiency of the aircraft is increased as the altitude increases. Furthermore, an average increased flight speed was found during the initial and final sections of the flight, which happens because the Mach number is constant during the flight and the speed of sound is dependent on the flight altitude. Interesting to see is that the difference in climate impact between the cost and climate optimized trajectories reduces as the flight progresses but is always negative on average (temperature decrease).

The flight length plays an important role in the climate impact imposed by the flights. An increased flight length does not only show an increased total fuel consumption and climate impact, but the values also have a higher standard deviation (sometimes positive and sometimes negative) if the analysis is performed per kilometer. While, it would be expected that the longer routes are able to avoid more climate sensitive regions and therefore have a smaller climate impact per kilometer, the opposite happens and the longer routes have a slightly (although not significantly) higher climate impact per kilometer.

A seasonal effect is felt at sea level as the temperature increases during the summer season and often the humidity (rainfall) and other atmospheric parameters change. A seasonal effect is also present in the higher layers of the troposphere and lower parts of the stratosphere. Due to the increased atmo-

spheric temperature and reduced relative humidity, contrail and cirrus cloud formation are reduced leading to an increased average flight altitude in the summer season.

While, the climate impact of both the cost and climate optimized flights is not seasonally dependent, the operating costs of the climate optimized flights are significantly reduced during the summer season. This is a result of the increased flight speed and reduced fuel consumption (due to increased altitude). There is also a significant difference between the way the climate optimized flights offset from the great circle trajectory in winter and summer which is not the case for the cost optimized flights.

The flights are divided into four flight directions to be able to better compare similar flights. For instance, the wind direction and wind speed play a role in the flight speed and therefore the fuel consumption and flight time of the flights. The wind is most commonly directed towards the east which increases the flight efficiency of the eastbound flights. The wind results in a higher fuel consumption of the westbound flights as well as an increased flight time.

The average flight distance of the north- and southbound flights is significantly shorter than the flight length of the east- and westbound flights. Furthermore, the east- and westbound flights are represented by approximately 30 flights each while the north- and southbound flights contain only 12 and 10 flights respectively.

The offset of the east- and westbound climate optimized flights is positive and larger than the offset of the north- and southbound flights on average. The magnitude of the offset is shown in absolute sense, which shows a large difference between east/west and north/south. This is mainly a result of the larger flight length of the east- and westbound flights. The westbound flights have the lowest average altitude for both the cost and climate optimized trajectories. This is possibly a result of the wind speed which increases with altitude and has a negative impact on the westbound flights. The eastbound flights have a high average altitude which is a result of the positive impact of the wind speed.

The average climate impact of the northbound flights is smaller than the climate impact of the other flights, whereas the climate impact of the southbound flights is the highest on average. Furthermore, when contrails are not taken into account, the average climate impact is increased as contrails increase the variance of the results but more often lead to a negative climate impact (reducing atmospheric temperature). Due to wind, the westbound flights have the highest average operating costs while the eastbound flights have the lowest average operating costs. This is a result of increased flight speed and reduced fuel consumption of the eastbound flights.

The east- and westbound climate optimized flights dominantly fly north of the great circle trajectory. The northbound climate optimized flights most often fly east of the great circle trajectory while the southbound flights more often fly west of the original trajectory. The cost optimized flights seem to be distributed more evenly, although the westbound flights still dominantly fly north of the great circle trajectory. The north- and southbound cost optimized flights most often cross the great circle trajectory once during the flight.

The results presented in this study do not always lead to perfectly optimized results. The optimization module often fails to find a global minimum which affects the strength of the conclusions drawn.

However, the results found are definitely useful. For instance, the general trend in the data does show that the optimization results in an optimum on a daily average. The algorithm used in this research is the most advanced algorithm that is currently available allowing for daily weather data quickly generated using algorithmic climate change functions. Since it was established that the trajectory optimization module is not performing optimally and it was also shown where the shortcomings of the EMAC model are located, it can be further examined and improved in order to create a better performing algorithm in the future.

The future of aviation is dependent on finding sustainable solutions as fossil fuels will possibly be running out within the next century. In order to reduce the fuel consumption but also reduce the climate impact due to aviation, flight planning regarding the climate impact can help as is shown in this thesis. The results presented in this thesis show some promising alternative routes that reduce the climate impact of aircraft which will invoke additional costs compared to the cost optimized flights. However, a Pareto front is still required to be able to compare how the reduction of the climate impact, increases the operating costs of the flights. Finally, this research poses a first step in the potential of climate impact reduction for the European region, but the simulation model and the scope of this thesis are not yet able to fully define optimal trajectories and will require additional research within the coming years to further improve an accurate trade-off between operating costs and climate impact.

9 Recommendations

The results presented in this study already show promising results which allow for more cost or climate efficient trajectories depending on the intentions of the user. However, in order to get better results, the analysis done within the scope of this thesis requires additional simulation days. The simulation domain should be extended from a six month simulation period towards a full year simulation period. This allows for a better understanding and visualization of the seasonal trend present in the simulation data.

The flights that were analyzed during this thesis were not distributed evenly among the European airspace since 48 out of 85 flights are either headed towards or coming from Istanbul airport in Turkey. The routes were chosen such that the flights present actual Airbus A330 trajectories. In a follow up research, the European airspace could be employed using an evenly spread out distribution of the flights and also the total number of flights should be increased to equalize the flights in each flight direction. Additional flights in different regions are also required to do a proper analysis of the differences between long and short trajectories.

Since the optimization process is not working as intended, it is required to find out the exact reason for the failure of the EMAC model to find a global minimum. This can happen due to the low number of iterations to keep the computational effort reasonable or possibly an error in the model. To be able to analyze the results obtained in this thesis, it is required that all results represent a global minimum, otherwise, the strength of the conclusions drawn is reduced.

The initial and final altitude of the great circle flights is not located at the same height as the altitude of the cost and climate optimized trajectories. This results in some discrepancies as for instance the cost optimized trajectories have a lower initial and final altitude while the average altitude is higher than for the great circle flights. For this reason, the altitude of the cost and climate optimized flights is not compared to the great circle trajectories.

The model seems to overevaluate the impact of contrails and therefore not consider (or consider less) the other species which are emitted by the aircraft engine. This has resulted in a large number of days where the difference in climate impact due contrails between the cost and climate optimized flights is zero while the other species show a larger impact of the climate optimized flights. In order to solve this problem, it is required to verify the EMAC model.

This research has resulted in a better understanding of how the atmospheric properties play a role in the determination of aircraft trajectories for both the cost and climate optimized flights. However, in this study, only the cruise part of the flights is analyzed and in order to use the results for actual flight planning, the take-off and landing parts of the flights should also be considered.

Finally, in this research, aircraft collisions are not considered which need to be considered for actual flight planning. If there is a climate sensitive region which is avoided by many aircraft, this means that another part of the European airspace may be clogged with flights which may result in aircraft collisions. In order to avoid this, certain flights may have to fly through climate sensitive regions reducing the effectiveness of the optimization.

References

Berntsen, T. K. and Isaken, I. S. A. (2016). *Effects of lightning and convection on changes in tropospheric ozone due to NO_x emissions from aircraft.* Tellus B: Chemical and Physical Meteorology, 51:4, 766-788, DOI: 10.3402/tellusb.v51i4.16484.

Burkhardt, U. and Kärcher, B. (2011). *Global radiative forcing from contrail-induced cloudiness.* SPIE, DOI: 10.1117/2.1201110.003764.

Dupré, S., Thomö, J., Dejonckheere, S., Fischer, R., Weber, C., Cummis, C., and Srivastava, A. (2016). *Climate Strategies and Metrics.* WRI, UNEP-FI and 2° Investing Initiative Portfolio Carbon Initiative.

Engineering Toolbox (2003). *Fuels - Higher and Lower Calorific Values.* `https://www.engineeringtoolbox.com/fuels-higher-calorific-values-d_169.html` [Online; accessed 17-08-2018].

Frömming, C., Ponater, M., Burkhardt, U., Stenke, A., Pechtl, S., and Sausen, R. (2011). *Sensitivity of contrail coverage and contrail radiative forcing to selected key parameters.* Atmospheric Environment 45 (2011) 1483e1490.

Frömming, C., Ponater, M., Dahlmann, K., Grewe, V., Lee, D. S., , and Sausen, R. (2012). *Aviation-induced radiative forcing and surface temperature change in dependency of the emission altitude.* Journal of Geophysical Research, Vol. 117, D19104, doi:10.1029/2012JD018204.

Gardi, A., Sabatini, R., and Ramasamy, S. (2016). *Multi-objective optimisation of aircraft flight trajectories in the ATM and avionics context.* Progress in Aerospace Sciences, 83, 1–36.

Gierens, K. M., Lim, L. L., and Eleftheratos, K. (2008). *A Review of Various Strategies for Contrail Avoidance.* The Open Atmospheric Science Journal 2(2008-01):1-7 DOI: 10.2174/1874282300802010001.

Graham, S. (1999). *Clouds and Radiation.* `https://earthobservatory.nasa.gov/Features/Clouds/` [Online; accessed 17-01-2018].

Grewe, V. (2015). *Internal Lecture Slides TU Delft: Climate Impact of Air Traffic.* Course AE4462, period 2.

Grewe, V. (2018). *Internal Lecture Slides TU Delft: Climate Impact of Air Traffic.* Course AE4462-17, period 3.

Grewe, V., Bock, L., Burkhardt, U., Dahlmann, K., Gierens, K., Hüttenhofer, L., Unterstrasser, S., Rao, A. G., Bhat, A., Yin, F., Reichel, T. G., Paschereit, O., and Levy, Y. (2016). *Meteorologische Zeitschrift, PrePub DOI 10.1127/metz/2016/0758.* Deutscher Luft- und Raumfahrtkongress 2012 DocumentID: 281440.

Grewe, V., Dahlmann, K., Flink, J., Frömming, C., Ghosh, R., Gierens, K., Heller, R., Hendricks, J., Jöckel, P., Kaufmann, S., Kölker, K., Linke, F., Luchkova, T., Lührs, B., van Manen, J., Matthes, S., Minikin, A., Niklaß, M., Plohr, M., Righi, M., Rosanka, S., Schmitt, A., Schumann, U., Terekhov,

I., Unterstrasser, S., Vázquez-Navarro, M., Voigt, C., Wicke, K., Yamashita, H., Zahn, A., and Ziereis, H. (2017). *Mitigating the Climate Impact from Aviation: Achievements and Results of the DLR WeCare Project.* Aerospace 4, 34; DOI:10.3390.

H. Kuhn, A. S. (2012). *Fundamental Prerequisites For Electric Flying.* Deutscher Luft- und Raumfahrtkongress 2012 DocumentID: 281440.

Haby, J. (2001). *Vorticity Basics.* `http://www.weather.gov/source/zhu/ZHU_Training_Page/Miscellaneous/vorticity/vorticity.html` [Online; accessed 14-02-2018].

Houghton, J. (1994). *Global Warming The Complete Briefing.* Cambridge Univeristy Press, ISBN 978-0-521-88256-9.

Irvine, E. A., Hoskins, B. J., Shine, K. P., Lunnon, R. W., and Froemming, C. (2013). *Characterizing North Atlantic weather patterns for climate-optimal aircraft routing.* Meteorol. Appl. 20: 80–93.

Jain, S. (2017). *Introduction to Genetic Algorithm & their application in data science.* `https://www.analyticsvidhya.com/blog/2017/07/introduction-to-genetic-algorithm/` [Online; accessed 11-07-2018].

Joeckel, P. (2018). *The highly structured Modular Earth Submodel System (MESSy).* `http://www.messy-interface.org/` [Online; accessed 13-03-2018].

Lee, D. S., Fahey, D. W., Forster, P. M., Newton, P. J., Wit, R. C., Lim, L. L., Owen, B., and Sausen, R. (2009). *Aviation and global climate change in the 21st century.* Atmospheric Environment 43, 3520-3537.

Lim, Y., Gardi, A., and Sabatini, R. (2017). *Optimal aircraft trajectories to minimize the radiative impact of contrails and CO2.* Energy Procedia 110 446 – 452.

Lu, J., Vecchi, G. A., and Reichler, T. (2007). *Expansion of the Hadley cell under global warming.* Geophysical Research Letters, Vol. 34, L06805, DOI:10.1029/2006GL028443.

Matthes, S. (2016-b). *Environmentally optimized trajectories - Air Traffic Management for Environment ATM4E.* EASN Conference, PowerPoint presentation.

Matthes, S., Grewe, V., Lee, D., Linke, F., Shine, K., and Stromatas, S. (2016-a). *ATM4E: A concept for environmentally-optimized aircraft trajectories.* In Proceedings of the 2nd Greener Aviation 2016 Conference, Brussels, Belgium.

Matthes, S., Grewe, V., Lührs, B., Linke, F., and Irvine, E. (2017). *Climate optimised aircraft trajectories based on advanced MET service for sustainable aviation.* Aeronautical Meteorology Scientific Conference.

Meerkötter, R., Schumann, U., Doelling, D. R., Minnis, P., Nakajima, T., and Tsushima, Y. (1998). *Radiative forcing by contrails.* Ann. Geophysicae 17, 1080-1094.

Mitas, C. M. and Clement, A. (2005). *Has the Hadley cell been strengthening in recent decades?* Geophysical Research Letters, Vol. 32, L03809, DOI:10.1029/2004GL021765.

Mulder, T. J. (2015). *Internal Lecture Slides TU Delft: Aircraft Emissions and Climate Effects.* Course AE4462, period 2.

Myhre, G. and Storda, E. (2001). *On the tradeoff of the solar and thermal infrared radiative impact of contrails.* Geophysical Research Letters,Vol. 28, No. 16, Pages 3119-3122.

Penner, J. E., Lister, D. H., Griggs, D. J., Dokken, D. J., and McFarland, M. (1999). *Aviation and the Global Atmosphere: A special report of IPCC working groups I and III.* Cambridge University Press ISBN: 0 521 66300 8.

Rosanka, S. H. (2017). *Weather influence on aviation NO_x climate impacts via ozone and methane.* Internal TU Delft Thesis: http://repository.tudelft.nl/.

Rosenow, J., Förster, S., Lindner, M., and Fricke, H. (2017). *Impact of Multi-critica Optimized Trajectories on European Air Traffic Density, Efficiency and the Environment.* Twelfth USA/Europe Air Traffic Management Research and Development Seminar (ATM2017).

Schumann, U. (2000). *Influence of propulsion efficiency on contrail formation.* Aerospace Science and Technology 4 (2000) 391–401, S1270-9638.

SESAR Joint Undertaking (2017). *Project ATM4E.* `http://www.atm4e.eu/` [Online; accessed 30-01-2018].

Simons, D. (2015). *Internal Lecture Slides TU Delft: Aircraft Emissions and Climate Effects.* Course AE4462, period 2.

Stanford University (2012). *Pareto Optimality.* `https://web.stanford.edu/group/sisl/k12/optimization/MO-unit5-pdfs/5.8Pareto.pdf` [Online; accessed 13-08-2018].

Søvde, O. A., Matthes, S., Skowron, A., Iachetti, D., Lim, L., Owen, B., Øivind Hodnebrog, Genova, G. D., Pitari, G., Lee, D. S., Myhre, G., and Isaksen, I. S. (2014). *Aircraft emission mitigation by changing route altitude: A multimodel estimate of aircraft NO_x emission impact on O_3 photochemistry.* Atmospheric Environment 95, 468-479.

United States Environmental Protection Agency (2014). *Report on the Environment.* https://www.epa.gov/roe/.

Verbist, P. (2016). *Green Flight Trajectories: A REACT4C data analysis.* Internal TU Delft Thesis: http://repository.tudelft.nl/.

Yamashita, H., Grewe, V., Jöckel, P., Linke, F., Schaefer, M., and Sasaki, D. (2016). *Climate Assessment Platform of Different Aircraft Routing Strategies in the Chemistry-Climate Model EMAC 2.41: AirTraf 1.0.* Geoscientific Model Develepment Discussions, doi:10.5194/gmd-2015-272.

Yamashita, H., Grewe, V., Jöckel, P., Linke, F., Schaefer, M., and Sasaki, D. (2015). *Towards Climate Optimized Flight Trajectories in a Climate Model: AirTraf.* Eleventh USA/Europe Air Traffic Management Research and Development Seminar (ATM2015).

A Climate Impact of Impactful Trajectories

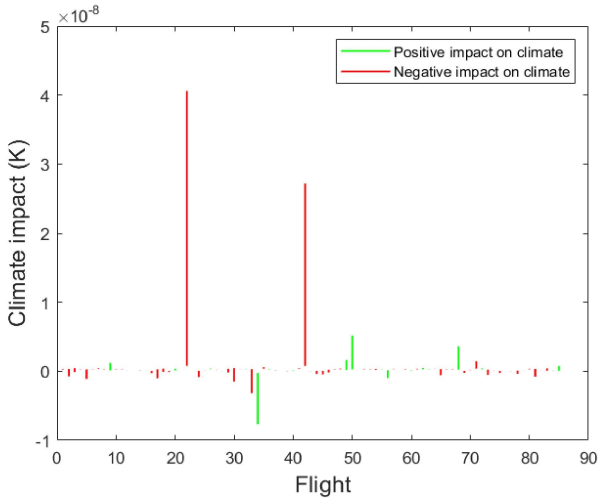

Figure A.1: Difference in climate impact between each cost and climate optimized trajectory on March 23^{th}

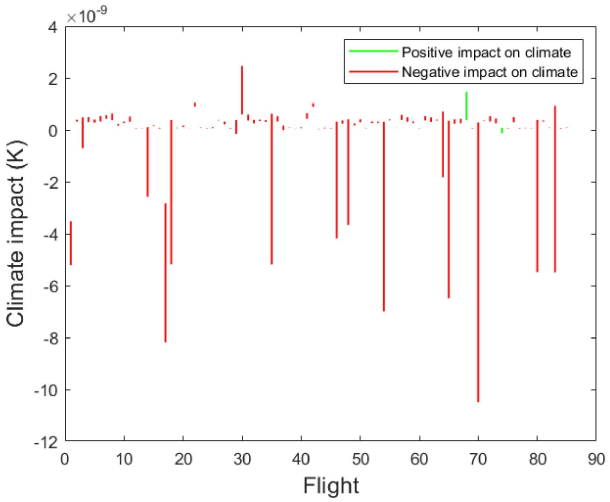

Figure A.2: Difference in climate impact between each cost and climate optimized trajectory on June 20^{th}

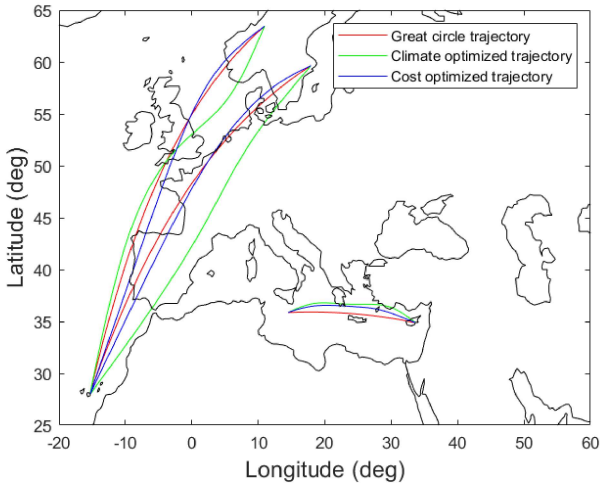

Figure A.3: Trajectories of the three most impactful climate optimized flights on March 23^{th}

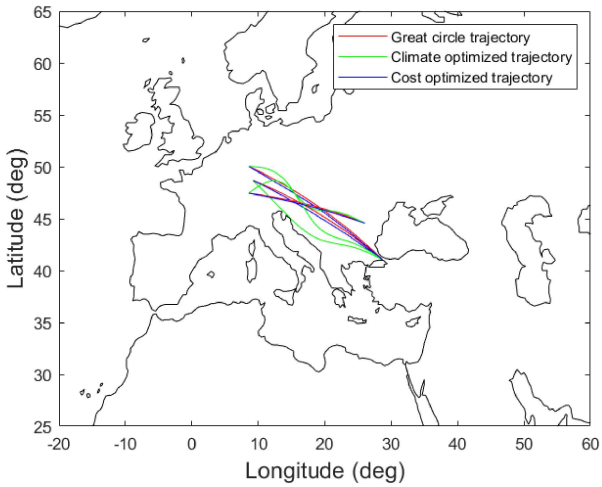

Figure A.4: Trajectories of the three worst optimized climate optimized flights on June 20^{th}

B Location of All Trajectories Analyzed in the European Airspace

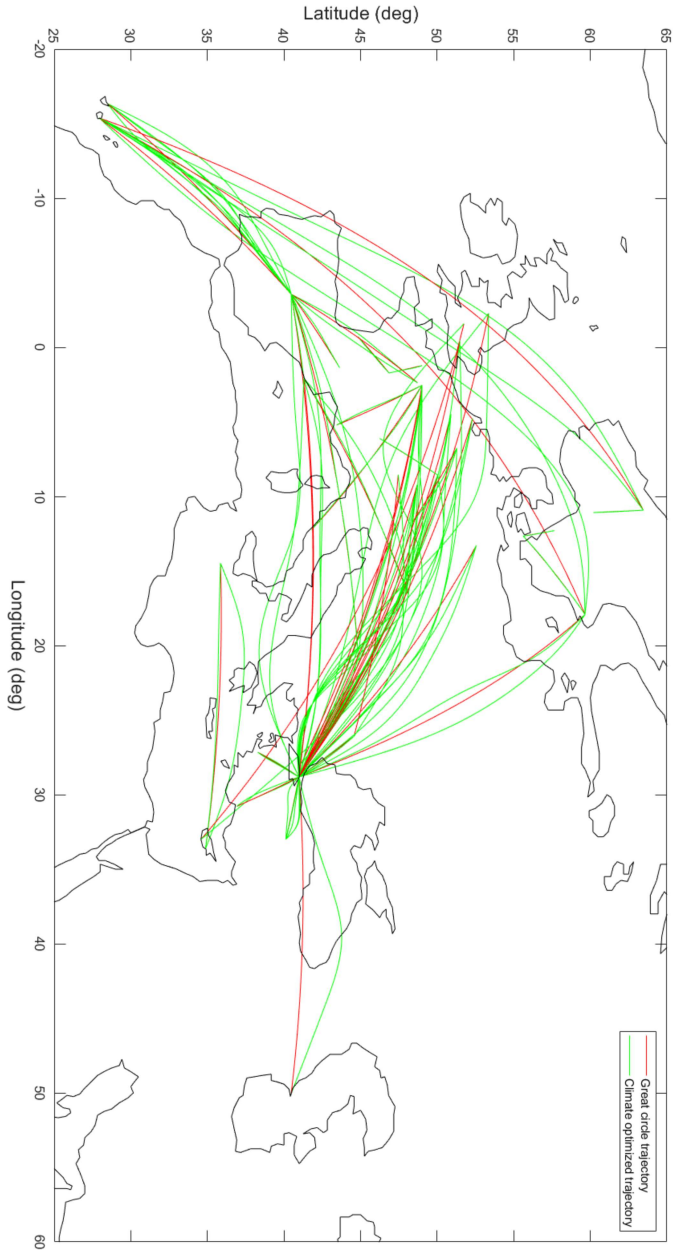

Figure B.1: All climate optimized and great circle trajectories on January first 2016

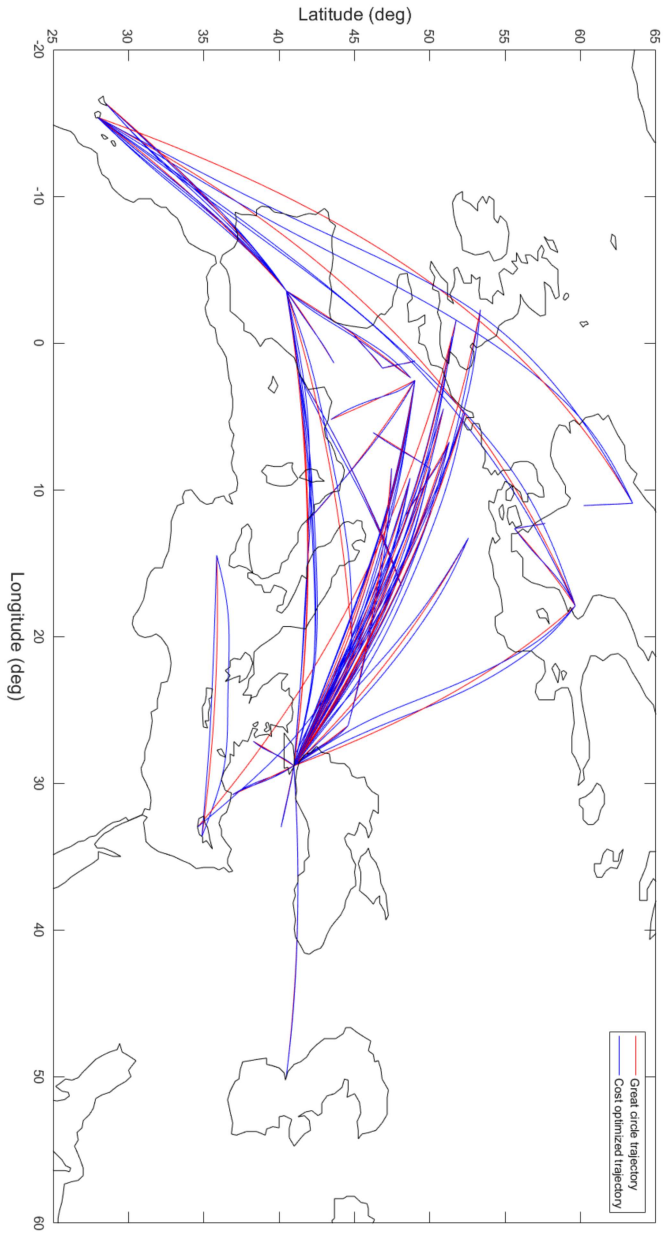

Figure B.2: All cost optimized and great circle trajectories on January first 2016

C Flight Characteristics Measured for Each Waypoint

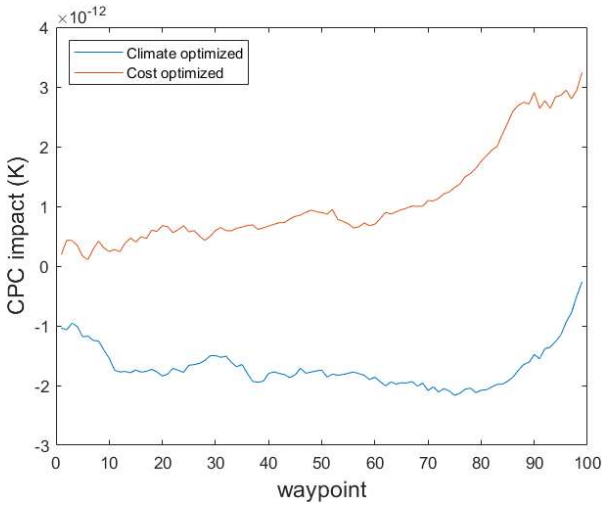

Figure C.1: Climate impact of CPC between two consecutive waypoints for cost and climate optimized flights

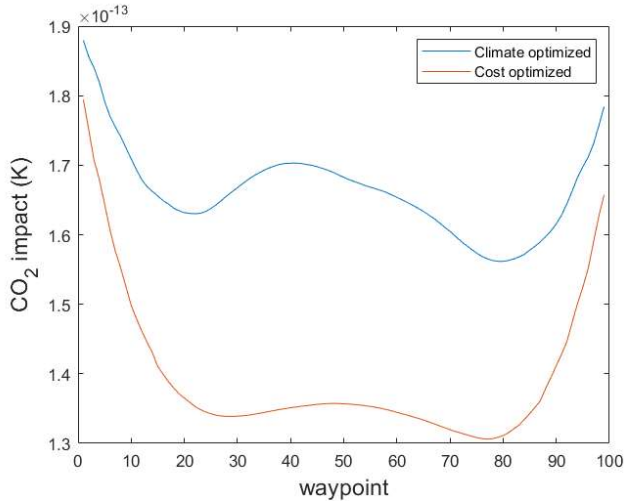

Figure C.2: Climate impact of CO_2 between two consecutive waypoints for cost and climate optimized flights

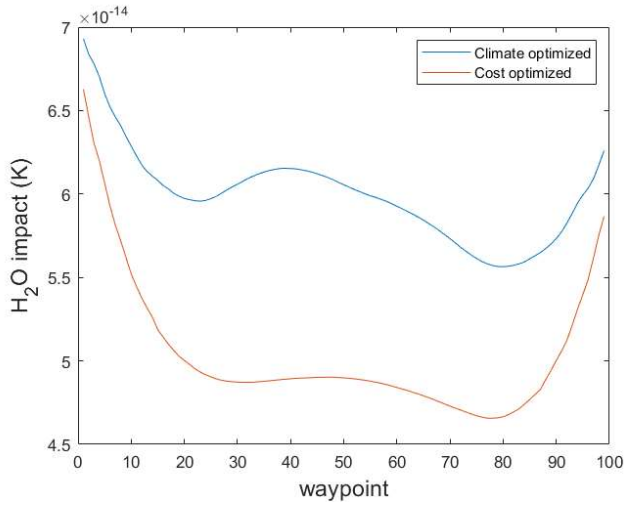

Figure C.3: Climate impact of H_2O between two consecutive waypoints for cost and climate optimized flights

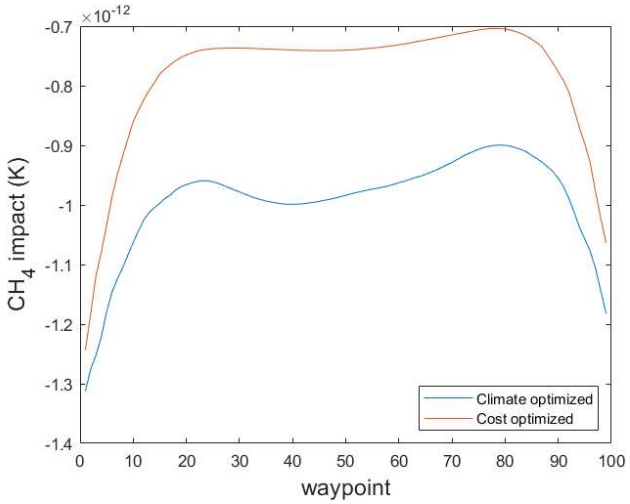

Figure C.4: Climate impact of CH_4 between two consecutive waypoints for cost and climate optimized flights

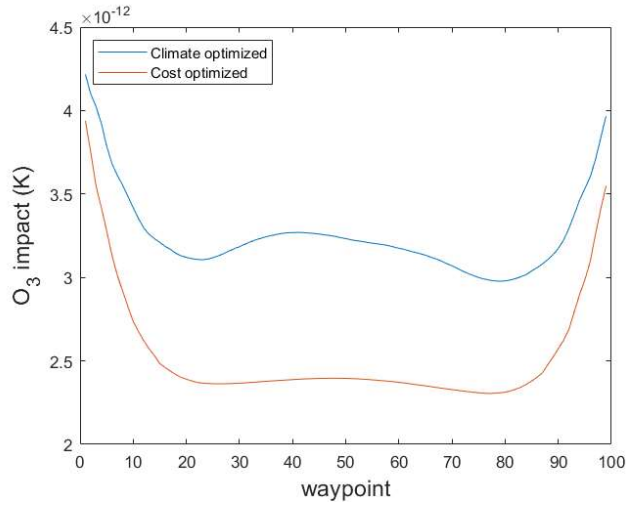

Figure C.5: Climate impact of O_3 between two consecutive waypoints for cost and climate optimized flights

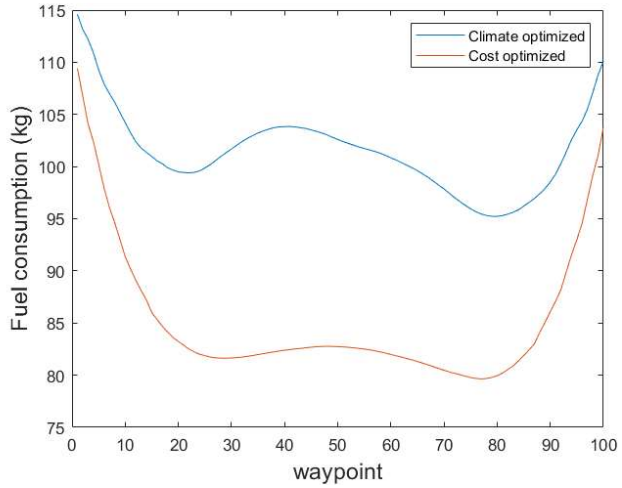

Figure C.6: Average fuel consumption between two consecutive waypoints for cost and climate optimized flights

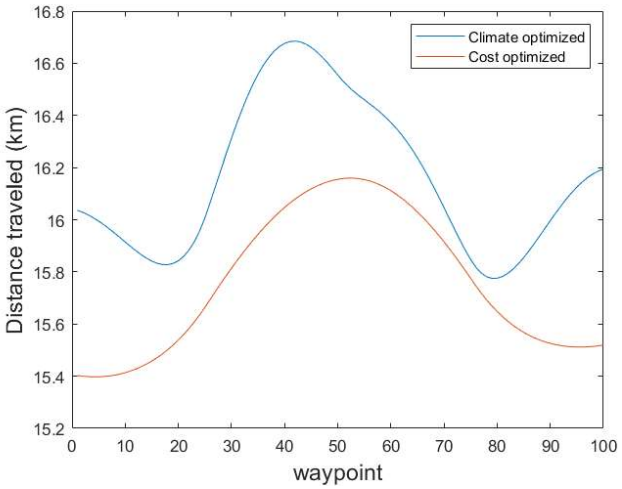

Figure C.7: Average flight distance between two consecutive waypoints for cost and climate optimized flights

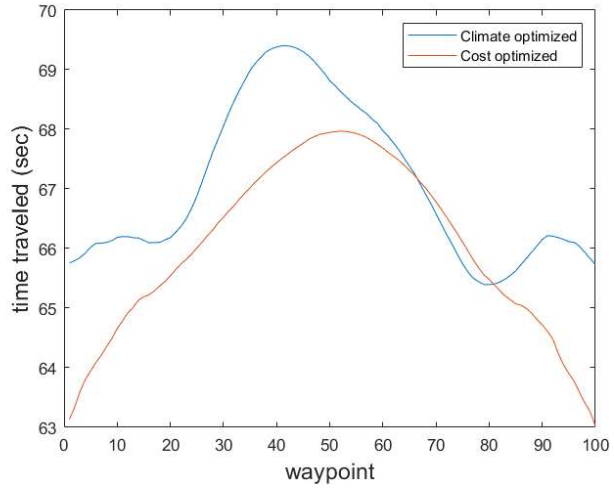

Figure C.8: Average flight time between two consecutive waypoints for cost and climate optimized flights

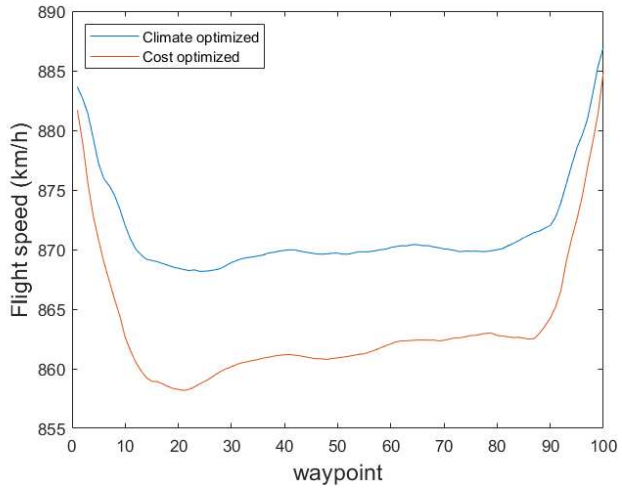

Figure C.9: Average flight speed between two consecutive waypoints for cost and climate optimized flights

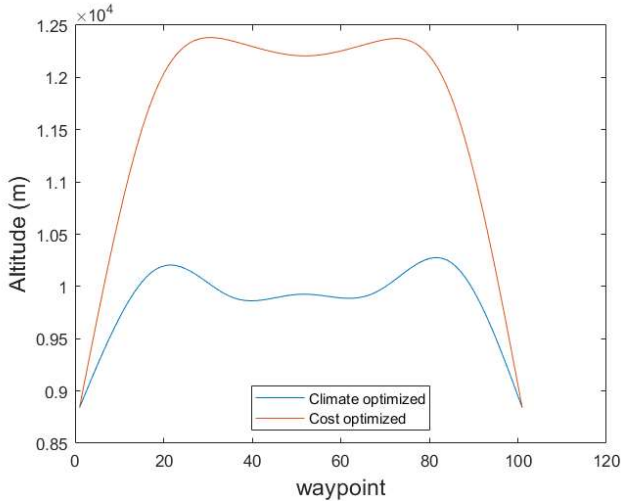

Figure C.10: Average altitude between two consecutive waypoints for cost and climate optimized flights

D Average and Average Absolute Offset of the Cost and Climate Optimized Trajectories

Table D.1: Average offset of the cost and climate optimized trajectories from the great circle trajectories for four different flight directions

	Climate optimized (deg)	**Cost optimized (deg)**
Eastbound	0.133	-0.194
Northbound	0.100	0.151
Westbound	0.303	0.132
Southbound	0.011	0.002

Table D.2: Average absolute offset of the cost and climate optimized trajectories from the great circle trajectories for four different flight directions

	Climate optimized (deg)	**Cost optimized (deg)**
Eastbound	0.804	0.273
Northbound	0.350	0.271
Westbound	0.915	0.300
Southbound	0.432	0.323

E Average Climate Impact of the Cost and Climate Optimized Trajectories

Table E.1: Average climate impact per kilometer of the cost and climate optimized trajectories for four different flight directions

	Climate optimized (K/km)	**Cost optimized (K/km)**
Eastbound	$1.24 * 10^{-12}$	$1.87 * 10^{-11}$
Northbound	$7.25 * 10^{-13}$	$1.69 * 10^{-11}$
Westbound	$5.47 * 10^{-12}$	$2.07 * 10^{-11}$
Southbound	$4.97 * 10^{-12}$	$2.08 * 10^{-11}$

Table E.2: Average climate impact per kilometer without contrail potential coverage of the cost and climate optimized trajectories for four different flight directions

	Climate optimized (K/km)	**Cost optimized (K/km)**
Eastbound	$1.46 * 10^{-11}$	$1.15 * 10^{-11}$
Northbound	$1.41 * 10^{-11}$	$1.13 * 10^{-11}$
Westbound	$1.59 * 10^{-11}$	$1.27 * 10^{-11}$
Southbound	$1.64 * 10^{-11}$	$1.32 * 10^{-11}$